EVOLUTIONARY IMPLICATIONS OF THE STANDING GENETIC VARIATION IN NATURAL POPULATIONS OF MIMULUS GUTTATUS

BY

PATRICK J MONNAHAN

Submitted to the graduate degree program in Ecology and Evolutionary Biology and the Graduate Faculty of the University of Kansas in partial fulfillment of the requirements for the degree of Doctor of Philosophy.

_____

Chair: John K. Kelly

_____

Maria E. Orive

_____

Lena C. Hileman

_____

Mark T. Holder

_____

Stuart J. MacDonald

Date Defended: 21 March 2016

The dissertation committee for PATRICK J MONNAHAN certifies that this is the approved version of the following dissertation:

EVOLUTIONARY IMPLICATIONS OF THE STANDING GENETIC VARIATION IN NATURAL POPULATIONS OF MIMULUS GUTTATUS

_____

Chair: John K. Kelly

Date Approved: 25 March 2016

Abstract

The standing genetic variation present in a population is the raw material on which natural selection can act. The study of the architecture of this variation indicates how evolution might proceed. In this dissertation, I perform a detailed survey of this architecture both within and across natural populations of *Mimulus guttatus.* In the first two chapters, I focus on a single, natural population to demonstrate the role that interactions between genes (epistasis) affecting floral and developmental traits can have on the response to selection. More specifically, the first chapter takes greenhouse estimates of floral and developmental epistasis and demonstrates their contribution to the components of genetic variation. Contrary to popular belief, we find that epistasis largely determines the additive genetic variance in these traits, which directly controls the ability of a population to respond to selection. Moreover, this work suggests that the rate of change at individual loci and the ultimate fate of fixation depends on the frequency of alleles at all other interacting loci. In the second chapter, I demonstrate the natural relevance of the preceding chapter by showing that the epistasis observed in the greenhouse generates epistasis in fitness in a natural setting. In the final chapter, I develop a method to survey the segregating variation in flowering time across multiple populations. The minimal evidence of commonality in genetic architecture even among closely neighboring populations is a possible implication of epistasis (in addition other phenomena such as Genotype-by-Environment interaction). Overall, these observations of the standing genetic variation in natural populations imply a high degree of idiosyncrasy of evolution, in that different populations possess a unique set of variants with which to respond to selection, and even if variants were entirely shared, the genetic trajectory of evolution would depend on the unique set of starting allele frequencies in each population.

Acknowledgements

First and foremost, I'd like to thank my adviser, Dr. John Kelly, whose friendship and guidance was indispensable for the completion of this dissertation. Success in graduate school is very dependent on finding a good fit between student and adviser, and I don't think I could have landed in a better situation. What I valued most was the access that he provides his students to inquire about virtually anything, regardless of whether it had to do with their thesis or not. Some of the biggest developments in my understanding of evolutionary biology were the result of casual conversations around the lab. Looking back, I realize how ideal of a work environment that the Kelly lab is for me, and I will consider myself lucky if I find myself in a similar situation in the future.

I would also like to thank the other members of my committee, each of whom has contributed to my success here at KU. Dr. Lena Hileman provided space and assistance for molecular work and gave helpful guidance on grant applications. Dr. Mark Holder advised on best practices for constructing software to estimate mating system parameters, which ended up being my first authorship as a graduate student. Dr. Maria Orive and I collaborated on a computer model to understand evolutionary dynamics of host-endosymbiont relationships. Dr. Stuart MacDonald has shared resources and expertise that facilitated the adoption of Next-Generation sequencing methods in the Kelly lab. I am grateful to each of these individuals for the generosity and guidance over the years.

Lastly, I'd like to thank my friends at KU and elsewhere, my girlfriend, and my family whose support helped me through difficult times in graduate school and joined me in celebrating the good times of which there were plenty. There are too many individuals to name, so I'll simply leave it by saying you know who you are.

Table of Contents

List of Figures

List of Tables

List of Appendices

Introduction

Long before the advent of modern genetics allowed us to identify and characterize the genes underlying genetic variation, it was well understood that the "architecture" of variation (i.e. the number, effect sizes, and interactions of genes) has important implications for the evolution of populations. The Fisher-Wright debates of the early 20th century, which embodied two alternative visions for the primary mode of evolution, invoked very different assumptions regarding genetic architecture. In Fishers landmark paper (FISHER 1919), he implicitly introduced what would become known as the infinitesimal model of evolution, which assumed that, in conjunction with large, well-mixed populations, traits were based on large number of genes each with an additive, infinitesimal effect (WALSH 2004). However, Wright's 'Shifting Balance Theory' of evolution invoked smaller, fragmented populations where epistasis, or genetic interactions, were a major determinant of traits. In Fisher's view, the fixation of beneficial alleles would be largely deterministic and therefore repeatable, if the allele escapes initial loss. Wright envisioned evolution as more stochastic across populations resulting in a pattern of fixation contingent on starting conditions. In this dissertation, I take a detailed look at genetic architecture within and across populations to bear on the stochastic or idiosyncratic nature of evolution.

Modern genetics now recognizes that epistasis is, in fact, a fundamental component of the mapping between the genotype of an organism and its observed phenotype (CARLBORG and HALEY 2004). This can be understood as a natural consequence of genes existing within the highly complex and interconnected biochemical pathways underlying phenotypes. The effect of a single mutation on the flux through these pathways is expected

to change depending on the existence of additional mutations in the same or related pathways (GIBSON 1996). The importance of epistasis has also been repeatedly demonstrated empirically (LI *et al.* 1997; MOORE 2003; KELLY and MOJICA 2011; HUANG *et al.* 2012). However, the source of the alleles utilized in the vast majority of observations of epistasis calls into question their relevance for understanding the impact on evolution in nature. These studies often utilize artificial, lab-engineered (knockout) mutations or alleles mapped from crosses between divergent populations or species. In both cases, it is not clear that the effects of these alleles and/or their interactions should be expected to resemble those of naturally segregating variation.

The first two chapters of this dissertation are intended to fill this gap, surveying epistasis between naturally segregating alleles to understand its implications for evolution. Towards this end, I utilize novel, inbred lines developed in the model plant species *Mimulus guttatus* (yellow monkeyflower). *M. guttatus* is ideal for this dissertation not only because its fast generation time and self-compatibility allow for efficient controlled breeding necessary for the creation of inbred lines, but also because this species is characteristic of many annual, alpine plant species. The novel, inbred lines (DNIL or Double-NIL lines) employed herein are ideal because they afford maximal power to detect and characterize epistasis. Each line (or rather line-set) contains a pair of loci segregating in an otherwise completely uniform genetic background. Barring environmental effects, any differences among genotypes should be due to the effects of either locus and/or their interactions.

In the first chapter, I synthesize information across all of the DNIL lines to predict how epistasis will contribute to genetic variance components for a number of traits. Over ten thousand plants were grown and measured over the course of 5 years, and the

resulting data were combined with novel theory to show that epistasis is a major determinant of the additive genetic variance, V_A, which determines the rate at which populations change in response to selection. This result is in stark contrast to a widely held assumption that only additive, and therefore not epistatic, effects contribute to the additive genetic variance. The other major result that speaks to the theme of this dissertation is that, with epistasis, the rate and direction of allele frequency change, and therefore ultimate fate of fixation, strongly depends on the frequency of all other interacting, segregating variants in a population. Even if two populations share the same segregating variation, the genetic trajectory of each population will likely be idiosyncratic due to differences in starting conditions (i.e. allele frequencies).

The second chapter establishes the relevance of the first chapter to evolution in natural populations by transplanting one of the DNIL lines in a natural setting to see if epistasis in floral and developmental traits would result in epistasis for fitness components. In the summers of 2012 and 2014, I transplanted thousands of individuals corresponding to the 9 two-locus genotypes to a natural field site located nearby the source population from which the lines were derived. I observed strong epistasis for developmental time, which consequently resulted in epistasis for viability (i.e. the probability that an individual would survive to reproduce). Genotypes that took longer to reach reproductive maturity were less likely to flower and set seed prior to death due to a lack of water availability. Most importantly, the pattern of epistasis was that of sign epistasis, such that an allele has a positive effect on viability in one genetic background, but a negative effect in a different genetic background. This suggests that selection will favor or disfavor an allele depending on which genetic background is at higher frequency in the population. Although we do not

yet know allele frequencies at these loci in nature, this chapter further supports the idiosyncratic, context-dependent nature of evolution in natural populations.

The last chapter maintains the theme of using observations of genetic architecture to bear on the issue of repeatability versus idiosyncrasy of evolution in natural populations, but, instead, looks across populations to determine the degree to which neighboring populations share genetic architecture. A number of factors, including epistasis via differences in allele frequency across populations, could determine whether or not alleles exhibit consistent effects across populations; however, simply observing whether the same genomic sites or loci affect a trait in multiple populations informs the scale at which we might expect parallel evolution to occur. In each of three populations and across two years, I sample plants that flower early in the season and, separately, those that flower late in the season. By sequencing a pooled DNA sample of each sampling event, I am able to identify sites exhibiting significant allele frequency divergence between early and late flowering plants within each population/year. The results of the analysis suggest that populations differ greatly in the number of sites/regions that exhibit divergence in flowering time and that these sites/regions are largely non-overlapping across populations. This observation reinforces the prediction of idiosyncrasy with regard to the genetic trajectory of these populations were they to experience a uniform selection pressure.

Overall, the observations presented in this dissertation would seem to suggest that parallel or repeated evolution based on standing variation of quantitative traits is unlikely at the genetic level. Rather, as Wright envisioned, each population is a unique evolutionary experiment that is highly contingent on the starting conditions, both in terms of the variants present as well as their frequency.

CHAPTER 1*

Epistasis Is a Major Determinant of the Additive Genetic Variance in *Mimulus guttatus*

*Monnahan, P. J. and J. K. Kelly (2015). "Epistasis Is a Major Determinant of the Additive Genetic Variance in *Mimulus guttatus.*" PLoS Genetics **11**(5): e1005201.

Abstract:

The influence of genetic interactions (epistasis) on the genetic variance of quantitative traits is a major unresolved problem relevant to medical, agricultural, and evolutionary genetics. The additive genetic component is typically a high proportion of the total genetic variance in quantitative traits, despite that underlying genes must interact to determine phenotype. This study estimates direct and interaction effects for 11 pairs of Quantitative Trait Loci (QTLs) affecting floral traits within a single population of *Mimulus guttatus*. With estimates of all 9 genotypes for each QTL pair, we are able to map from QTL effects to variance components as a function of population allele frequencies, and thus predict changes in variance components as allele frequencies change. This mapping requires an analytical framework that properly accounts for bias introduced by estimation errors. We find that, even with abundant interactions between QTLs, most of the genetic variance is likely to be additive. However, the strong dependency of allelic average effects on genetic background implies that epistasis is a major determinant of the additive genetic variance, and thus, the population's ability to respond to selection.

Introduction:

Epistasis, the interactions between genetic loci, is an important determinant of phenotypes across a large number of taxa (LI *et al.* 1997; SHIMOMURA *et al.* 2001; CARLBORG *et al.* 2003; MOORE 2003; KELLY and MOJICA 2011; HUANG *et al.* 2012; ZUK *et al.* 2012; BLOOM *et al.* 2013). Yet for quantitative (complex) traits, the net effect of epistasis on the components of variation, specifically the additive genetic variance (V_A) that determines the response to natural or artificial selection, remains polemical. This is evidenced by a renewed debate over the evolutionary relevance of epistasis as exemplified by Crow (CROW 2010) and Hansen (HANSEN 2013). An unfortunate source of confusion sustaining this debate is the simultaneous use of terms to describe both the effects of individual genes as well as the genetic variance components of populations (additive, dominance, and epistatic). It has long been known that high additive genetic variance does not imply additive gene action (FALCONER *et al.* 1996), a conclusion reiterated by the theoretical demonstration in Hill *et al.* (HILL *et al.* 2008) (see also (MÄKI-TANILA and HILL 2014)). However, there is little empirical evidence regarding the extent to which gene interactions determine the additive genetic variance, (GOODNIGHT 1987; CHEVERUD and ROUTMAN 1995; WADE and GOODNIGHT 1998; CARTER *et al.* 2005), which leaves several important questions unanswered. For instance, do interactions among genes tend to increase or decrease V_A of traits, on average? As allele frequencies change in response to selection, does epistasis accelerate or dampen the corresponding change in V_A?

For a particular locus, the contribution to V_A depends on the average effect of substitution at the locus and on the frequencies of the different alleles in the population

(FALCONER *et al.* 1996). The total V_A is a simple sum over all loci affecting the trait. With epistasis, the average effect of a locus will change as the frequency of its epistatic partners in the population change (WADE and GOODNIGHT 1998). Thus, the contribution of a locus to V_A depends simultaneously on its own allele frequencies as well as the allele frequencies of all other segregating loci. Association mapping studies can estimate the V_A contributed by a locus (e.g (ZUK *et al.* 2012)), but this estimate is an average over the genetic backgrounds in the population. The extent to which locus-specific V_A is determined by interactions with other loci remains unknown. An alternative to association mapping is to estimate genetic effects from genotypes produced from experimental crosses, with the remainder of the genetic background held constant. These genetic effects, often termed functional effects (ÁLVAREZ-CASTRO and CARLBORG 2007), can be defined as deviations from a reference genotype, and therefore, do not depend on an unknown distribution of genetic backgrounds. Given allele frequencies in a population, it is straightforward to calculate total and locus-specific variances based on these genetic effects. One can also calculate these variances under the assumption of additivity of loci (i.e. no epistasis). Contrasting these variances to those calculated from genetic effects based on multi-locus measurements provides a simple, direct demonstration of the effect of epistasis on V_A (CHEVERUD and ROUTMAN 1995). Further, one can observe how this contrast changes as population allele frequencies change.

Standard equations used to calculate V_A from genetic effects (FALCONER *et al.* 1996) assume that effects are estimated without error. Estimation error in genetic effects is often substantial even with large sample sizes, and failing to account for this error will result in

an upward bias in variance predictions (LUO *et al.* 2003). This is because genetic effects are squared and different effects are multiplied together when variances are calculated. As the true value for a genetic effect is the estimate minus a residual (the estimation error), treating the genetic effect estimates as the truth results in the inclusion of squared residual terms thus biasing variance components upwards. Luo *et al*. (LUO *et al.* 2003) derived a correction that incorporates the variance-covariance matrix of the genetic effect estimates for the case of a single locus. Here, we extend the bias-correction to multiple loci, accommodating epistatic terms, and demonstrate its validity using parametric bootstrapping. Then, we use the corrected variances to explore the effects of epistasis on the total and additive genetic variances under different models of allele frequency.

We consider loci affecting floral morphology and development rate that are polymorphic within a single population of *Mimulus guttatus* (yellow monkeyflower). *Mimulus guttatus* is an emerging model in evolutionary genetics; notable for its high degree of phenotypic and genetic variation within and between populations as well as its ability to adapt to novel environments (WU *et al.* 2007). The species is broadly distributed across western North America and ranges from high alpine to low-elevation coastal environments. In *Mimulus guttatus*, multiple studies have shown that epistasis contributes to within-population variation in floral morphology, development time, and fitness components (KELLY 2005; KELLY and MOJICA 2011). Interaction effects are routinely of the same magnitude as single-locus effects, although the magnitude and direction of epistasis between loci is highly variable.

In this study, we maximize statistical power to estimate direct and epistatic effects between QTL using Double-NIL lines (DNILs, hereafter), in which two loci segregate in an otherwise isogenic genetic background. We confirm the finding of important but highly variable epistasis between these QTL, but also quantify the contribution of epistasis to population genetic variance using the genetic effect estimates and a model of allele frequency. We find that the average effect, which determines the locus-specific response to selection, depends heavily on genetic background or rather the frequency of different genetic backgrounds in the population (i.e. the genotypes at all other loci). For some traits, this leads to an average increase in genetic variance components, whereas in others, the effect is opposite albeit minimally. Overall, it is clear that epistasis is an important determinant of both individual phenotype as well as the genetic variance components, which govern the ability of a population to respond to natural or artificial selection.

Materials and Methods:

Genetic lines

The DNILs were derived from a previous study by Kelly and Mojica (KELLY and MOJICA 2011). The process of mapping the original QTL began with a large-scale artificial selection experiment on a collection of lines derived from a single natural population at Iron Mountain in Central Oregon. This resulted in populations with highly divergent floral traits (KELLY 2008). Individuals from the tails of the distribution were randomly selected and crossed to produce three F1 populations and each of these populations were backcrossed for six generations to IM767, a commonly used inbred line with medium floral trait values derived from the same natural population (WILLIS 1999). This resulted in 3

panels of Nearly Isogenic Lines (NILs; 493 NILs in total), with each NIL containing a random segment of donor genome from one of the three F1 populations. NILs were measured for corolla width, and selective genotyping of NILs from the tails of the distribution identified 7 QTLs affecting corolla width. Three rounds of background-cleaning were performed for each of the 7 NILs, using a combination of selfing and backcrossing to IM767 to eliminate segments of donor, non-IM767 genome from other parts of the genome.

The seven NILs containing the QTL were crossed in each possible pairing to produce 21 F1's each of which contained solely the double-heterozygote for the donor alleles present in their parents. A single individual from each F1 was self-fertilized, and the resulting F2's were genotyped at the relevant loci (see Appendix 1 for the list of diagnostic markers for the 7 QTL). The four true-breeding (double-homozygous) genotypes from each F2 were set aside and self-fertilized, in order to serve as the parents of a single Double-NIL line set. Each DNIL is essentially a collection of nine genotypes corresponding to two biallelic QTL segregating in an otherwise uniform genetic background. For a single DNIL, we create these nine genotypes by selfing the true-breeders as well as crossing them in all possible directions to produce the five heterozygous genotypes. With seven QTL, there are 21 possible pairs of loci; however, this study examines only 11 of the DNILs owing to loss of several lines used in Kelly and Mojica (KELLY and MOJICA 2011).

Phenotype Data

Plants were grown in the University of Kansas greenhouse in five large cohorts. All nine two-locus genotypes for a particular Double-NIL were included in a cohort, which meant that only a subset of Double-NILs could be included in any one cohort. Within a cohort, multiple seed families from each genotype were sprinkled into unique 2x2 in. pots and watered generously. After approximately 10 days, individual plants were transplanted to their own 2x2 in pot. The pot locations were randomized initially and rotated regularly to avoid effects of inconsistent conditions within the greenhouse. Plants were watered every other day following transplant and fertilized once a week.

Upon flowering, plants were measured for several traits: corolla width (CW), distance between stigma and anther (SA separation), pistil length, and the number of days until first flower (DTF). Measurements were taken on all open flowers present at time first flower, which was typically only one or two. The corolla width is the widest distance of the flattened width of the lower lip of the corolla, while the rest of the measurements are self-explanatory. Kelly and Mojica (KELLY and MOJICA 2011) measured the double-homozygotes for 17 of the 21 DNILs. For this study, we elaborated measurements to include all nine two-locus genotypes for 11 of the 21 DNILs. As there is significant overlap between individuals in this and the aforementioned study, we combined the relevant data from Kelly and Mojica (KELLY and MOJICA 2011), which included plants grown in seven distinct cohorts. This resulted in a highly unbalanced dataset, but provided greater accuracy for estimating particular genotypic means. All individuals were grown at the KU greenhouse under the same watering and fertilizer regiment.

Confirmation Genotyping

Crossing two of the true-breeding genotypes within a DNIL will necessarily result in genetically identical heterozygous offspring; however, we genotyped a subset of individuals from each cohort via touch-down PCR at gene-based markers diagnostic of particular QTL (Appendix 1) in order to confirm that progeny genotypes were as expected (incorrect genotypes occasionally result from mislabeling or accidental pollen transfer during selfing/crossing). The few individuals with incorrect genotypes that were identified (typically < 5% per cohort) were removed from the analysis along with all of their siblings. PCR fragments were analyzed on ABI 3130 BioAnalyzer, and genotype calls were made using GeneMapper (Applied Biosystems, Foster City, CA, USA).

The overall test for epistasis

We performed a likelihood ratio test to compare a full and reduced model for each trait corresponding to models with and without epistatic parameters, respectively. In R, we fit each model using REML as implemented in the "lme4" package followed by a call to the "anova.merMod()" function (BATES *et al.* 2014). This produces a likelihood for each model from which a likelihood ratio is calculated and compared to a Chi-squared distribution with degrees of freedom equal to the difference in the number of parameters between the full and reduced model. There were 60 degrees of freedom in the full model and 16 in the reduced model, which corresponds to the number of genetic effects plus the cohort and family effect. The difference, 44, is the degrees of freedom for each of the likelihood ratio tests.

Linear Model for Estimation of genetic effects

We estimated the single-locus and epistatic genetic effects using the NOIA *functional* genetic effect model (ÁLVAREZ-CASTRO and CARLBORG 2007):

$$Z_{ijklmn} = \mu + a_i X_{a_i} + d_i X_{d_i} + a_j X_{a_j} + d_j X_{d_j} + aa_{ij} X_{a_i} X_{a_j} + ad_{ij} X_{a_i} X_{d_j} + da_{ij} X_{d_i} X_{a_j} + dd_{ij} X_{d_i} X_{d_j} + C_k + F_l[G_m] + \varepsilon_{ijklmn} \quad \text{(eqn. 1)}$$

where

$$X_{a_x} \begin{cases} 2, \text{ if } i = WW \\ 1, \text{ if } i = Ww \\ 0, \text{ if } i = ww \end{cases} \quad \text{and,} \quad X_{d_x} \begin{cases} 0, \text{ if } i = WW \\ 1, \text{ if } i = Ww \\ 0, \text{ if } i = ww \end{cases}$$

Here, *Z* is the trait value, C_k is the random effect due to cohort, F_l is the effect of seed family (environmental maternal effect), which is nested within genotype; *a* and *d* are the single-locus effects, and *aa*, *ad*, *da*, and *dd* are the epistatic effects. The residual variance applies to variance within families. The X_a and X_d variables (corresponding to the design matrix in (ÁLVAREZ-CASTRO and CARLBORG 2007)) are numerical values that, together, specify an individuals diploid genotype at a locus. In this case, *W* is the donor allele and *w* is the reference IM767 allele at a QTL. For a pair of loci, the four pairwise products of these variables provide contrasts by which the four analogous epistatic parameters are estimated. For a completely homozygous IM767 individual (*ww* at all loci), all X_a and X_d terms are 0, and therefore, the standard inbred IM767 line serves as the reference point in the *functional* NOIA model by which all genetic effects are defined as deviations from. These genetic effects can then be used (as described in the proceeding section) to generate predicted genotypic values for multi-locus genotypes. To determine the predicted

genotypic values in the absence of epistasis (non-epistatic values), we fit separate models to estimate single-locus effects using only data corresponding to single-locus genotypes (essentially, the NIL genotype data that forms a subset of the DNIL data). Again, we use the *functional* NOIA parameterization (eqn. 1 without epistatic terms), specifying the homozygous IM767 genotype as the reference point. By this method, we define the non-epistatic value as the predicted multi-locus genotypic value given only information from individual loci in an isogenic background.

It should be noted that the NOIA model has both a *statistical* formulation and a *functional* formulation, which is used here. Effectively, equation 1 is the traditional animal model of genetic effects, and the *functional* NOIA (referred to as NOIA, hereafter) simply refers to the index variables used to specify an individual's genotype. Here, we require functional genetic effects, in order to predict variances for any set of population allele frequencies. We investigated alternative, functional parameterizations for the index variables including the F_∞ model (VAN DER VEEN 1959) and the unweighted-regression (UWR) of Cheverud and Routman (CHEVERUD and ROUTMAN 1995), but these models use a different reference point and the parameters have a different quantitative interpretation. F_∞ and UWR yield the same predicted genotype values as NOIA (the models are inter-covertable), but we prefer the NOIA because parameters are defined as deviations from a reference genotype and, therefore, are more clearly interpretable between the full model (eqn. 1) and the reduced (non-epistatic) model (fit to the reduced dataset). As a result, we find that the non-epistatic coefficients of NOIA (*a* and *d* terms of eqn. 1) are "stable." If we fit the full NOIA model (all terms) to the full dataset (all genotypic combinations included)

we get estimates for the *a* and *d* terms that are nearly equivalent to what we get when we fit the reduced NOIA model (no interactions terms) to the reduced dataset (plants of the reference genotype plus those that differ from the reference genotype at only one QTL). This is not true of analogous estimates from the F_∞ or UWR models, which do not use a common reference genotype as the reference point. While this consistency is convenient for the interpretation of genetic effects, it is not crucial to the results. It is the genotypic values predicted with and without epistasis that serve as the basis for determining the effect of epistasis on genetic variance, and as stated previously, the multiple parameterizations that we investigated all provide the same predicted values.

We used REML (implemented in JMP, Version *11*. SAS Institute Inc., Cary, NC, 1989-2014) to estimate the fixed genetic effects as well as accommodate random effects (cohort and family) in the model. While equation 1 is specified for only 2 loci, all relevant genetic effects were included in the linear model and fit to the entire DNIL (full model) or NIL data (reduced model). Fitting this larger model accommodated the fact that many DNILs have overlapping genotypes. Models were fit separately for each trait. In total, there were 14 single-locus effects (seven '*a*' terms and seven '*d*' terms) as well as 44 epistatic terms (four epistatic terms per DNIL x 11 DNILs). Model fits were based on 4263 measurements carried forward from Kelly and Mojica (KELLY and MOJICA 2011) plus 6234 measurements from the five additional grow-ups.

From effects to variances

Estimation error in genetic effect estimates must be properly accommodated because genetic effect estimates are squared and different effects are multiplied together, when calculating variances. This can introduce bias with or without epistasis. Consider the single locus, 2-allele model (FALCONER *et al.* 1996), where the additive genetic variance (V_A) is

$$V_A = 2pq[a + d(q - p)]^2 \qquad \text{(eqn. 2)}$$

Here, a and d are the additive effect and dominance deviation, respectively, and p and q are the frequencies of alternative alleles. An experimental study will yield estimates for the genetic effects, $\hat{a}$ and $\hat{d}$, but even if unbiased, these estimates will be encumbered with estimation error:

$$\hat{a} = a + \gamma_a \qquad \text{(eqn. 3a)}$$

$$\hat{d} = d + \gamma_d \qquad \text{(eqn. 3b)}$$

Here, the γ are residuals; random variables with mean 0 and a variance contingent on experimental design (e.g. sample sizes). If direct substitution is used to estimate V_A, i.e. $\hat{V}_A = 2pq[\hat{a} + \hat{d}(q - p)]^2$, bias is introduced:

$$E[\hat{V}_A] = 2pq[a + d(q - p)]^2 + 2pq(Var[\gamma_a] + 2(q - p)Cov[\gamma_a, \gamma_d] + (q - p)^2 Var[\gamma_d]) \qquad \text{(eqn. 4)}$$

The second term of the sum, involving the estimation variances ($Var[\gamma_a], Var[\gamma_d]$) and the covariance of errors ($Cov[\gamma_a, \gamma_d]$), is the bias. A bias corrected estimate, denoted V_A^*, can be derived using standard dispersion statistics:

$$V_A^* = \hat{V}_A - 2pq(s_a^2 + 2(q - p)s_{ad} + (q - p)^2 s_d^2) \qquad \text{(eqn. 5)}$$

where s_a^2 is the estimated variance of γ_a (the squared standard error of $\hat{a}$), s_d^2 is the estimated variance of γ_d and s_{ad} is the sampling co-variance. This statistical issue has been addressed for a single locus (LUO *et al.* 2003), and we here generalize bias-correction for genetic variance predictions when there are interactions among loci. We extend the logic of equation 5 to all eight genetic effect estimates associated with each QTL pair (see **Linear Model for Estimation of genetic effects** section above).

Prediction of variance components

The genetic variance of a trait for a particular population is a function of the individual genotypic values and their frequency in the population. For a particular multi-locus genotype (*u*), we can calculate the predicted genotypic value using the genetic effect estimates from the linear model fit as follows,

$$\hat{Z}_{G,u} = \sum_{i=1}^{B} \hat{b}_i X_{i,u} \qquad \text{(eqn. 6)}$$

where $\hat{b}_i$ is the estimate for the i'th effect (*B* is the total number of effects), and $X_{i,u}$ is the relevant indicator variable from equation 1 for genotype *u*. If we let Z_G represent the genotypic value of an individual drawn randomly from a population, then the total genetic variance, V_G, is simply the variance of Z_G, which can be found by,

$$\hat{V}_G = Var[\hat{Z}_G] = E[\hat{Z}_G^2] - E[\hat{Z}_G]^2 \qquad \text{(eqn. 7)}$$

These expected values are functions of the genotypic values and the multi-locus genotype frequencies. For example,

$$E[\hat{Z}_G^2] = \sum_{u \in \Omega} F_u \hat{Z}_{G,u}^2 \qquad \text{(eqn. 8)}$$

where Ω is the set of all possible multi-locus genotypes and F_u is the population frequency of the multi-locus genotype, *u*. Expanding $\hat{Z}_G^2$ (temporarily suppressing the u subscript), we see that

$$\hat{Z}_G^2 = (X_1\hat{b}_1 + X_2\hat{b}_2 \ldots)(X_1\hat{b}_1 + X_2\hat{b}_2 \ldots) = X_1^2\hat{b}_1^2 + X_1X_2\hat{b}_1\hat{b}_2 + \ldots \quad \text{(eqn. 9)}$$

We see that $\hat{Z}_G^2$ is biased because $E[\hat{b}_i^2] > b_i^2$ and $E[\hat{b}_i\hat{b}_j] \neq b_ib_j$, essentially the same reason evident in equation 4. We correct for this upward bias by subtracting off the relevant sampling variance/covariance term, such that the corrected value is,

$$Z_G^{2*} = X_1^2b_1^2 + X_1X_2b_1b_2 + \ldots = X_1^2(\hat{b}_1^2 - s_{\hat{b}_1}^2) + X_1X_2(\hat{b}_1\hat{b}_2 - s_{\hat{b}_1\hat{b}_2}) + \ldots \text{ (eqn. 10)}$$

More generally,

$$Z_G^{2*} = \sum_{i=1}^{B}\sum_{k=1}^{B} X_iX_k(\hat{b}_i\hat{b}_k - s_{\hat{b}_i\hat{b}_k}) \qquad \text{(eqn. 11)}$$

noting that $s_{\hat{b}_i\hat{b}_k}$ is equal to $s_{\hat{b}_i}^2$. Thus, the expected value for equation 11 is

$$E[Z_G^{2*}] = \sum_{u \in \Omega} F_u \sum_{i=1}^{B}\sum_{k=1}^{B} X_{u,i}X_{u,k}b_ib_k \qquad \text{(eqn. 12)}$$

Correcting the estimate for $E[Z_G]^2$ is slightly more involved because the full expansion (substituting eqn. 6 for Z_G) produces terms of squares and cross-products within and across multi-locus genotypes. The bias corrected estimator for $E[Z_G]^2$ is

$$\sum_{u\in\Omega}\sum_{v\in\Omega}F_uF_v\sum_{i=1}^{B}\sum_{k=1}^{B}X_{u,i}X_{v,k}(b_ib_k-s_{\hat{b}_i}s_{\hat{b}_k}) \qquad \text{(eqn. 13)}$$

The additive genetic variance, V_A, due to a set of L bi-allelic loci is

$$V_A=\sum_{k=1}^{L}2p_kq_k\alpha_k^2 \qquad \text{(eqn. 14)}$$

where α_k is the average effect of the allele with frquency p_k at locus *k*. The average effect is $\alpha_k=\alpha_{k,1}-\alpha_{k,2}$, where

$$\alpha_{k,1}=p_kE[Z\,|\,W_kW_k]+q_kE[Z\,|\,W_kw_k] \qquad \text{(eqn. 15)}$$

and

$$\alpha_{k,2}=p_kE[Z\,|\,W_kw_k]+q_kE[Z\,|\,w_kw_k] \qquad \text{(eqn. 16)}$$

Here, $E[Z\,|\,W_kW_k]$ is the mean phenotype across all multi-locus genotypes that are homozygous for allele 1 at locus k, $E[Z\,|\,W_kw_k]$ is the corresponding conditional mean for heterozygotes, and $E[Z\,|\,w_kw_k]$ is the mean for allele 2 homozygotes. Equations 14-16 assume Hardy-Weinberg genotype proportions. We focus on the Hardy-Weinberg case, because without random mating, the additive genetic variance is not a sufficient statistic to predict response to selection (WEIR and COCKERHAM 1977; KELLY 1999; KELLY and WILLIAMSON 2000).

The average effect is a linear function of genetic effects, and as a consequence, direct substitution of effect estimates into equations 15-16 yields unbiased estimates. However, when α_k is squared (eqn. 14), upward bias is introduced by estimation error. Computation of bias-corrected estimates α_k^2 follows the same method of equations 7-13, although the relevant sums are over all loci except *k* (code to implement these calculations was written in C; available upon request). Importantly, in these calculations, we assume that epistasis is absent for pairs of QTL corresponding to DNILs for which we have no measurements. We also assume no higher-order interactions. All parameter estimates from the linear model fit were incorporated regardless of their statistical significance. Our method accounts for uncertainty in parameter estimates by directly incorporating the sampling variance/covariance of estimates into the calculation of variance components. Predictions of V_G, V_A, and locus specific α_k were generated for each set of simulated allele frequencies.

Allele frequency model

We investigated the distributions of genetic variance components under two differing allele frequency models, a uniform distribution and a U-shaped distribution as in Hill *et al.* (HILL *et al.* 2008). Allele frequencies were sampled independently for each locus to create a set of 7 frequencies per set. We drew 200 sets of frequencies from each distribution. For each set of allele frequencies and for each trait, we calculated the corrected and uncorrected genetic variance components variance (eqn.'s 6 -16). We performed this operation, first, using the entire suite of single-locus and epistatic genetic effects to predict genotypic values, and then a second time, using only the single-locus genetic effects estimated from the reduced data set consisting only of single-locus

genotypic data. This allows us to observe the effect of epistasis on the total and locus-specific genetic variance components.

A Simulation Test of the Bias-Correction Procedure

The bias-correction procedure will produce unbiased estimates of variance components if the estimated sampling (co)variances ($s_{\hat{b}_i\hat{b}_j}$) are unbiased estimates of the true sampling (co)variances. However, precision of bias-corrected estimates may be reduced, as including $s_{\hat{b}_i\hat{b}_j}$ in the calculations could increase sampling variance of bias-corrected estimates, particularly if $s_{\hat{b}_i\hat{b}_j}$ terms are large. We performed parametric bootstrapping to determine the effect of our procedure on the precision of estimates as well as to confirm its efficacy in eliminating bias. Using the estimated genetic effects as well as the within-group variance estimated from the linear model fits, we simulated trait values for individuals of particular genotypes producing 500 replicate data sets. Each simulated dataset for each trait was the same size and structure as the original dataset. We then estimated the genetic effects and sampling (co)variance matrices for each replicate dataset and calculated the corrected and uncorrected genetic variance components for two sets of allele frequencies. For the first set, the reference allele frequency was set equal to 0.5 for all loci. For the second set, the reference allele frequency was set equal to 0.05, and thus, the donor allele frequency was set to 0.95 (see **Linear Model for Estimation of genetic effects** section above for definition of reference vs. donor). To determine the bias exhibited by each variance calculation, we calculated the true variances given the genetic effects that we specified to simulate the data. We calculated the mean square error for each

distribution of variance calculations by dividing the sum of squared deviations from the true value by the number of replicates (500). To standardize the mean square error, we divided the sum by the square of the true variance. In addition, we calculated the standardized bias as $\frac{x^* - x}{x}$, where x^* is the average of estimates and x is the true value.

Results:

Prevalence and patterns of epistasis between QTL

There is strong evidence for epistasis for all of the traits (Table 1.1), consistent with the prior study of these loci based solely on homozygous genotypes (KELLY and MOJICA 2011). Concerning the individual terms of the models, we find that epistatic genetic effects are occasionally significant and typically of the same order as single-locus effects (Appendix 2 and 3). There was no clear trend towards positive or negative epistasis, although additive-by-additive interactions are more frequently observed to be significant than other forms. Particular types of epistasis are illustrated by example in Fig. 1.1 (see Appendix 4 for the full collection of graphs), which contrast the predicted genotypic value with epistasis (the bars) to the corresponding non-epistatic value (the 'X'). The non-epistatic value is the genotypic value predicted using only the relevant single-locus effects (*a* and *d* terms) estimated from a linear model fit based on single-locus genotype data (essentially, NILs). The epistatic genotypic value is based on all genetic effects (single-locus and epistatic) estimated from the full linear model fit to the DNIL data. The deviation between these values is the contribution of epistasis to the observed genotypic value. Fig. 1.1-E provides an example of sign epistasis, wherein the positive effect of the donor allele at QTL *x8* in the

QTL *x10a* AA background exhibits a negative effect in the Aa background. Fig. 1.1 A-C demonstrate the potential for consistent epistatic deviations for certain genotypes across multiple traits; particularly, the AABb genotype exhibits striking positive epistasis for all morphological traits. Conversely, some genetic backgrounds have variable effects when combined with other loci. For instance, positive synergism is observed for QTL *x1* in the QTL *x9* AA background (Fig. 1.1-D), whereas negative diminishing returns epistasis is observed for QTL *x5a* in the same AA background of QTL *x9*. Lastly, Figs. 1.1 A-C also provides evidence of the potential of epistasis to modify dominance relationships. In the AA background, overdominance emerges for all traits, despite single-locus predictions of partial dominance (Figs. 1.1-A and 1.1-B) and underdominance (Fig. 1.1-C).

Table 1.1 Model comparison for models with (Full) and without (Reduced) epistasis terms included. The degrees of freedom for each test was 44.

Trait	Model	AIC	LogLike	X^2	P-value
Pist	Reduced	31463	-15713	87.433	0.0002
Pist	Full	31464	-15669		
SA	Reduced	20613	-10288	146.3	<0.0001
SA	Full	20555	-10215		
CW	Reduced	42092	-21027	80.123	0.0007
CW	Full	42099	-20987		
DTF	Reduced	52782	-26372	65.823	0.0182
DTF	Full	52804	-26339		

Figure 1.1. Trait values (in mm's) for selected DNILs as deviations from the reference genotype (IM767) estimated by the linear model. Genotypic mean values are given by bars, whereas non-epistatic values are given by the X's. A.) Corolla Width for DNIL x10a – x5a; B.) Stigma-Anther (SA) Separation for DNIL x10a – x5a; C.) Pistil Length for DNIL x10a – x5a; D.) SA Separation for DNIL x9 – x1; E.) Days to Flower for DNIL x10a – x8; F.) SA Separation for DNIL x9 – x5a.

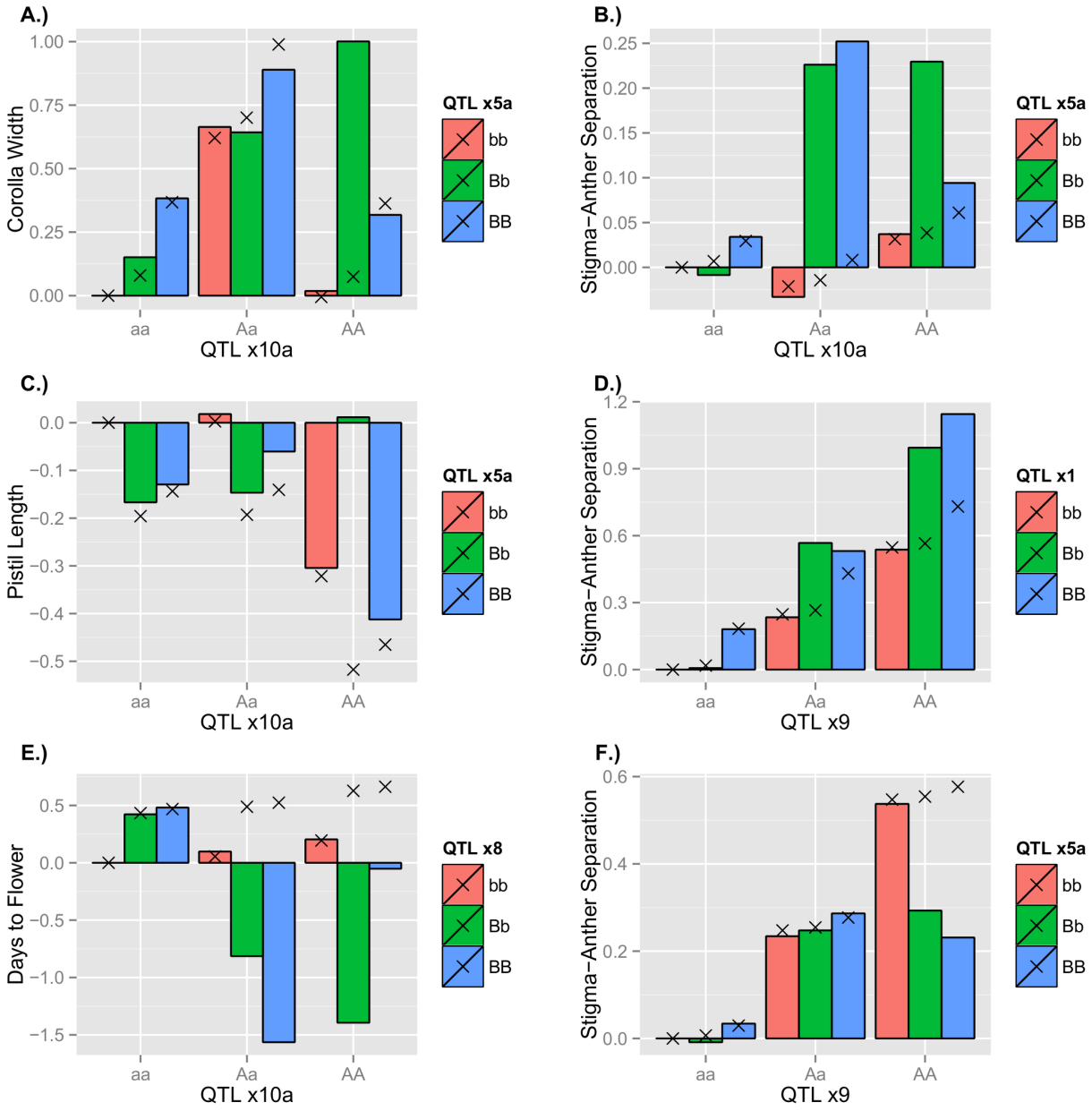

When considered together, the epistatic deviations (deviation between the 'X's and bars in Fig. 1.1) illustrate the pattern of epistasis. Focusing on only the genotypes unobserved in the single-locus NIL model fit (AABB, AaBB, AABb, and AaBb), we find that the average epistatic deviation is near zero for corolla width, SA separation, and pistil length (-0.04, 0.01, and 0.06 respectively), but is more appreciable for days to flower (-0.49). This indicates that plants tended to flower earlier than expected based on non-epistatic predictions. The standard deviations of the epistatic deviations speaks to the variability of epistatic effects and are 0.43, 0.20, 0.30, and 0.68 for corolla width, SA separation, pistil length, and days to flower, respectively. Comparing the sum of absolute deviations from the reference genotype for non-epistatic versus epistatic values provides additional information on the pattern of epistasis. If we subtract the sum of epistasis values from the sum of non-epistatic values, a negative difference would indicate synergism (sometimes called positive epistasis), wherein epistasis gives rise to greater deviations from the reference point, on average. The converse would indicate a diminishing effect of mutations under epistasis. For corolla width, days to flower, pistil length, and SA separation, the percent difference between the sum of absolute deviations for no-epistasis vs. epistasis was 0.04, 0.02, -0.11, and 0.01, respectively. Evidence for cumulative synergism or diminishing returns is rather weak for all cases.

Pleiotropy and correlation among traits

Pleiotropy is common for both single-locus and epistatic effects (Appendix 5 and 6). Effects were typically significant for between two and three traits. Pleiotropy seems to be modular in the sense that QTL/DNILs with a significant effect on one floral trait tends to

also affect other floral traits, in contrast to the day of flowering. Effects were significantly correlated between pistil length and corolla width (r=0.47; p=0.0002), between pistil length and days to flower (r=-0.28, p=0.0305), and between pistil length and stigma-anther separation (r=0.29, p=0.0292; Appendix 5 for full list of values). The traits themselves were also strongly correlated (Appendix 6). While some of the effects are in line with the correlational structure of the data (e.g. single-locus additive effect of QTL *x10b*), this was not a consistent pattern (e.g. single-locus additive effect of QTL *x5a*).

Extension of genetic effects to genetic variance predictions

Density plots of V_A across the 200 simulated allele frequency sets (uniform distribution) calculated from the single-locus (termed "No Epistasis") and DNIL ("Epistasis") data are depicted in Fig. 1.2 (the corresponding densities for the U-shaped allele frequency distribution are given as Appendix 9). With the exception of Corolla Width, epistasis produced an increase in the average of both V_A and V_G for all traits (Table 1.2) regardless of the allele frequency distribution. As expected, average V_A and V_G are always larger for Uniform distribution compared to the U-shaped distribution, whereas the proportion of variance that is additive is greater for the U-shaped distribution. Notably, the genetic variance is mostly additive even in the presence of substantial epistatic interactions. Epistasis also significantly affected the shape (variance) of the distributions of genetic variance estimates in addition to the location (mean). This is evident in Fig. 1.2 as well as Appendices 9-17. Epistasis tended to increase the variance, oftentimes producing long tails representing the observance of more extreme values.

Table 1.2. Mean and standard deviation (in parentheses) for additive and total genetic variance calculated with and without bias-correction (above and below the line, respectively), as well as with and without epistasis for both of the allele frequency distributions.

		Uniform distribution		U-Shaped distribution	
		Epistasis	No Epistasis	Epistasis	No Epistasis
DTF	Va	0.62 (0.57)	0.11 (0.07)	0.38 (0.51)	0.04 (0.07)
	Vg	0.99 (0.68)	0.01 (0.05)	0.67 (0.73)	-0.01 (0.06)
	Va/Vg	0.6	--	0.57	--
CW	Va	0.23 (0.14)	0.29 (0.11)	0.16 (0.13)	0.18 (0.1)
	Vg	0.36 (0.13)	0.41 (0.12)	0.21 (0.16)	0.23 (0.12)
	Va/Vg	0.64	0.71	0.74	0.77
SA	Va	0.03 (0.02)	0.03 (0.01)	0.02 (0.02)	0.02 (0.01)
	Vg	0.06 (0.02)	0.03 (0.01)	0.03 (0.03)	0.01 (0.01)
	Va/Vg	0.61	1.05	0.78	1.04
Pist	Va	0.14 (0.07)	0.08 (0.04)	0.09 (0.07)	0.05 (0.03)
	Vg	0.17 (0.07)	0.11 (0.04)	0.11 (0.08)	0.06 (0.04)
	Va/Vg	0.80	0.78	0.82	0.82
DTF	Va	1.19 (0.57)	0.25 (0.06)	0.79 (0.55)	0.14 (0.08)
	Vg	2.51 (0.95)	0.28 (0.06)	1.47 (0.95)	0.15 (0.08)
	Va/Vg	0.47	0.9	0.54	0.92
CW	Va	0.37 (0.14)	0.32 (0.11)	0.25 (0.13)	0.2 (0.1)
	Vg	0.74 (0.17)	0.47 (0.13)	0.41 (0.19)	0.27 (0.13)
	Va/Vg	0.50	0.68	0.63	0.75
SA	Va	0.05 (0.02)	0.03 (0.01)	0.03 (0.02)	0.02 (0.01)
	Vg	0.1 (0.03)	0.03 (0.01)	0.05 (0.03)	0.02 (0.01)
	Va/Vg	0.50	0.93	0.66	0.94
Pist	Va	0.19 (0.08)	0.09 (0.04)	0.13 (0.08)	0.06 (0.03)
	Vg	0.32 (0.1)	0.13 (0.04)	0.19 (0.1)	0.08 (0.04)
	Va/Vg	0.59	0.73	0.69	0.78

Figure 1.2. Density plots of bias-corrected V_A calculated with and without epistasis for each trait. Allele frequencies were drawn from a uniform distribution.

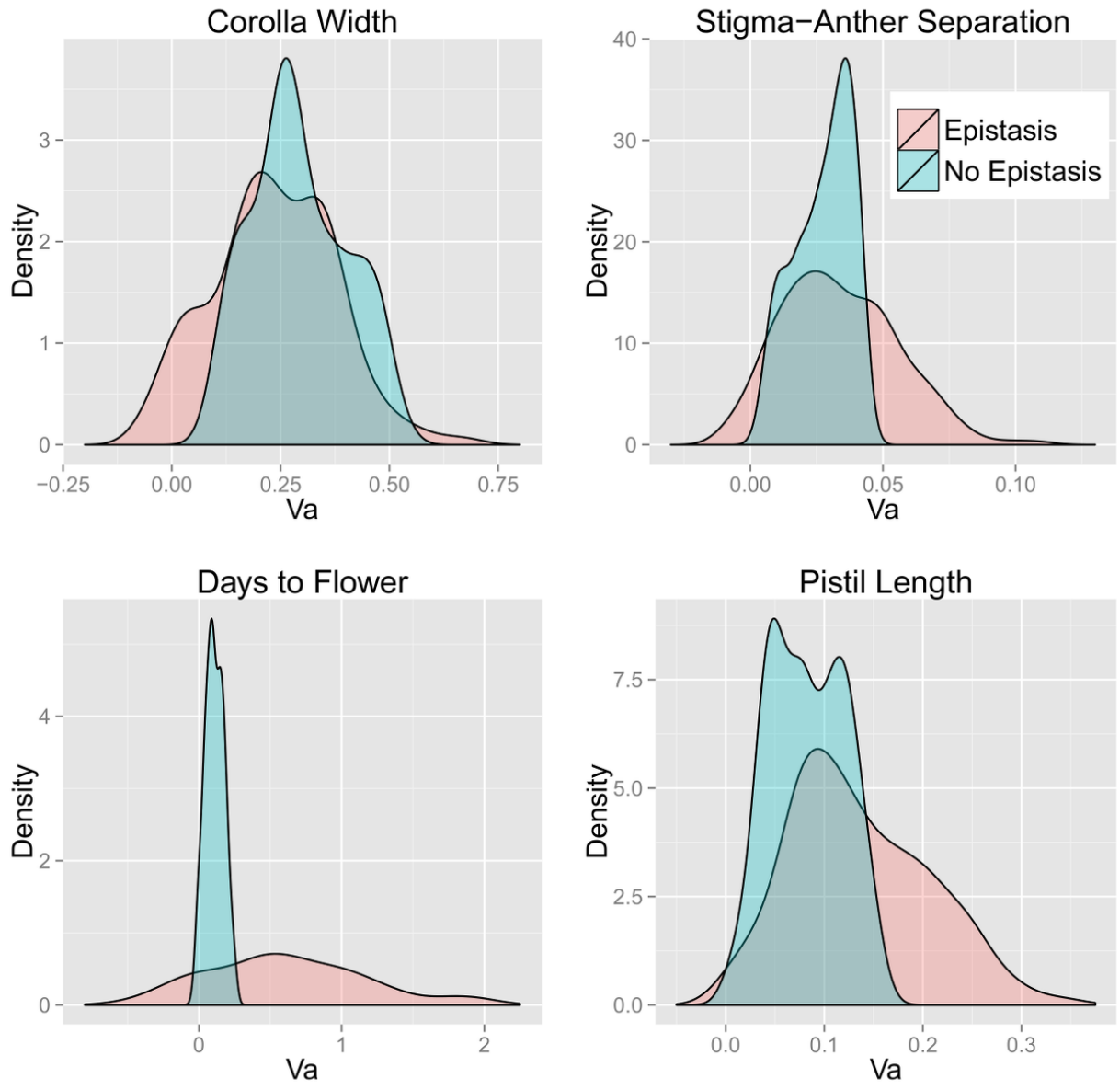

The bias-correction procedure significantly reduced estimated V_G values (particularly for days to flower; DTF) although there was considerable variation among sets (Table 1.2). The larger reduction due to bias-correction of DTF is expected given that estimation error is greatest for this trait and that this estimation error is directly related to the degree of bias in variance calculations. Bias-correction also reduced predicted V_A, but to a lesser extent. As a consequence, the ratio of V_A to V_G is substantially greater for bias-corrected values (60-80% across the four traits) than for uncorrected variance components (45-60%). This is true regardless of whether one calculates V_A/V_G for each simulation replicate and then averages, or takes the ratio of mean V_A to mean V_G (as in (HILL *et al.* 2008)). Occasionally, unrealistic, negative values for V_A result from the bias-correction procedure, and this tendency seems to be exacerbated by greater estimation error of the coefficient estimates. For example, effect estimates for Days to Flower routinely had the largest standard errors, and this is accompanied by many negative values (Fig. 1.2, lower left panel). It should be noted that uncorrected variance estimates also produce negative values albeit to a lesser extent (Appendix 13 and 15) which is true for any estimate whose standard error is large relative to its magnitude.

Table 1.3. Standardized Mean Square Error (MSE) and standardized bias for corrected (Corr.) and uncorrected (Unc.) variance estimates from the bias-correction simulations.

		q=0.5				q=0.05			
		MSE		Std. Bias		MSE		Std. Bias	
		Corr.	Unc.	Corr.	Unc.	Corr.	Unc.	Corr.	Unc.
DTF	Vg	0.07	0.12	-0.04	0.35	0.17	0.24	0.00	0.26
	Va	0.12	0.12	-0.04	0.33	0.23	0.31	0.01	0.28
CW	Vg	0.07	0.15	-0.01	0.27	0.27	0.39	-0.04	0.35
	Va	0.07	0.09	-0.01	0.13	0.30	0.41	-0.04	0.33
SA	Vg	0.10	0.18	-0.02	0.27	0.51	1.16	-0.03	0.76
	Va	0.18	0.24	0.00	0.20	0.79	1.38	-0.04	0.80
Pist	Vg	0.06	0.11	-0.03	0.23	0.17	0.33	-0.02	0.40
	Va	0.09	0.09	-0.03	0.07	0.06	0.10	-0.03	0.41

The distributions resulting from the bias-correction simulations demonstrate that the correction procedure is effective (Table 1.3; Appendix 16 and 17) The mean of corrected estimates matches the truth more closely than uncorrected estimates (Std. Bias in Table 1.3). There is a slight negative bias to the bias corrected estimate (typically 1-4%), perhaps because the sampling (co)variances of estimates are only approximate. The mean square error of corrected statistics is lower than for the uncorrected (Table 1.3). This is due entirely to the bias reductions given that the distributions of the corrected and uncorrected statistics have nearly identical variances.

The V_A for traits is a weighted sum of squared average effects (eqn.'s 14-16). When considering the effects of epistasis on individual loci, we see dependence of the average effect, α, on genetic background (Fig. 1.3 for selected examples; Appendix 7 and 8 for full collection). The points in the figure are α values for a locus calculated from our set of 200 allele frequencies (uniform distribution), and the dashed line represents the best-fit line through the points. The solid black line shows the values for α without epistasis, which depend only on the genetic effects and allele frequency at that locus. If the locus showed entirely additive gene action, this line would be perfectly horizontal, whereas dominance gives rise to a non-zero slope. Over- or under-dominance is implied when lines cross 0 on the y-axis. Deviations between the dashed and solid lines in Fig. 1.3 demonstrate the effect of epistasis averaged over genetic backgrounds. A change in slope between solid and dashed lines indicates the statistical dominance effect depends on epistasis. In Fig. 1.3-A, we see that locus QTL *x10a* is predicted to contribute little to no V_A without epistasis, but exhibits a substantial average effect when epistasis is considered. Fig. 1.3-C indicates a

case in which epistasis does not effect dominance, but changes the sign of α. However, epistasis often affects the dominance properties of a locus as evidenced by differences in the slope of the dashed and solid lines. Epistasis is seen to make an additive locus exhibit dominance (Fig. 1.3-A and 1.3-D), reduce dominance to near additivity (Fig. 1.3-B and 1.3-E), and give rise to over or underdominance (Fig. 1.3-A and 1.3-F). Some loci are relatively less sensitive (more robust) to background than others: Note the small scatter and relatively shallow trajectory of *x5a* relative to *x10a* for Days to Flower (Fig. 1.3-A and 1.3-D).

Figure 1.3. Average effect (Alpha) values for a QTL plotted against frequency of the QTL. The solid black line indicates the alpha value calculated without epistasis whereas the dashed line shows the best-fit line through the scatter of points, which are the alpha values calculated with epistasis included. A.) Days to Flower for QTL x10a; B.) Corolla Width for QTL x10a; C.) Pistil Length for QTL x10a; D.) Days to Flower for QTL x5a; E.) Corolla Width for QTL x8; F.) Stigma-Anther Separation for QTL x5b.

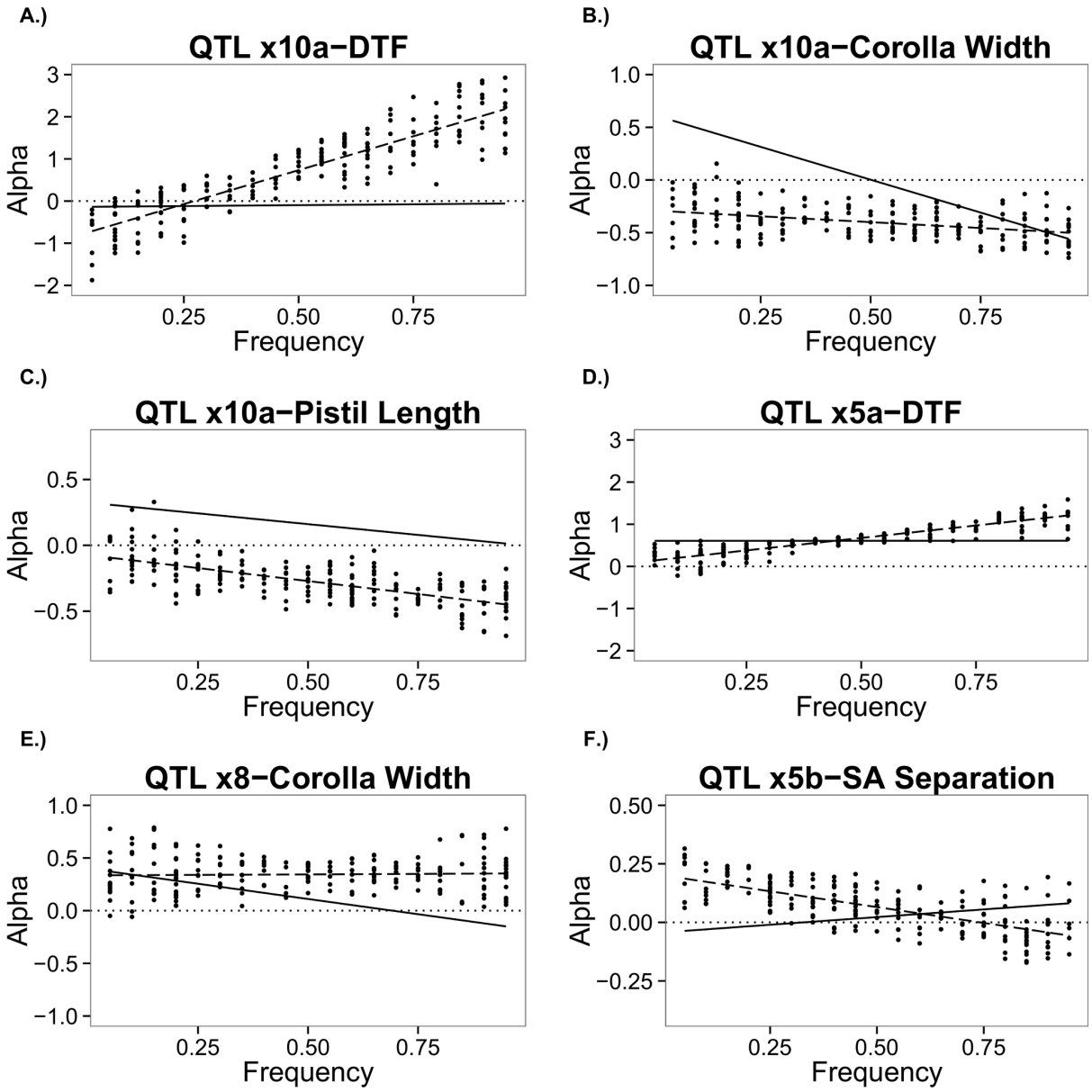

Discussion:

Epistasis is often a major factor in the mapping from genotype to phenotype (MOORE 2003; CARLBORG and HALEY 2004; PHILLIPS 2008; HUANG *et al.* 2012), but its relevance to heritability and evolution remains contentious (CROW 2010; HANSEN 2013). In part, this is due to persistent confusion about how genetic effects are defined and, thus, relate to genetic variation. Kempthorne (KEMPTHORNE 1954) and Cockerham (COCKERHAM 1954) defined genetic effects to be orthogonal, such that additive, dominance, and epistatic variance were each attributed solely to the corresponding genetic effects. The orthogonal property of these models is convenient, and the resulting estimates relate directly to evolutionary change. However, the estimated effects are specific to the population under consideration and depend entirely on allele frequencies. Epistatic effects defined in this way do not contribute to the additive variance (V_A), despite that interactions between genes certainly do affect V_A. This has led many to the incorrect assumption that epistasis is unimportant for evolution. Functional models provide an alternative view that better reflect the physiological or molecular interactions that determine the mapping from genotype to phenotype (CHEVERUD and ROUTMAN 1995). A substantial body of theory and simulation has shown that gene interactions can be an important determinant of heritable variation and, thus, the response to selection (WADE and GOODNIGHT 1998; CARTER *et al.* 2005; PHILLIPS 2008).

Unfortunately, key empirical evidence about how epistasis influences heritability is lacking. Most basically, do interactions among genes tend to increase or decrease V_A on average? How does epistasis affect the evolution of V_A under sustained selection? How do

interactions among QTLs affect the allele frequency dynamics that underpin changes in quantitative traits? While there are many empirical studies demonstrating gene interactions, nearly all lack a clear population context and heritability is a population-specific statistic. While crosses between divergent populations/species routinely reveal epistasis, the loci segregating in these crosses may never have been segregating (simultaneously) within a specific natural population (e.g. Dobzansky-Muller incompatibilities). More importantly, the magnitude and pattern of effects may not be representative of the segregating polymorphisms that determine genetic variation within populations, perhaps due to multiple, subsequent mutation in a locus (McGregor *et al.* 2007) (see (Hansen 2006) for a discussion on the evolution of epistatic interactions). By focusing on epistasis between loci polymorphic in a single, natural population of *M. guttatus*, we provide an empirically calibrated evaluation of how gene interactions alter genetic variance components in nature. We find that epistasis has a net positive effect on both V_A and V_G for most measured traits, providing an empirical demonstration of epistasis in determining heritable variation and the response to selection.

The contribution of epistasis to genetic variance depends, in part, on the existence of particular patterns of epistasis among loci (Carter *et al.* 2005; Le Rouzic 2014). Synergistic epistasis among mutations, termed positive epistasis by (Carter *et al.* 2005) (but see (Phillips *et al.* 2000)), will increase variability among genotypes, whereas diminishing returns epistasis should have the opposite effect. However, when interactions are variable and idiosyncratic as we observe in this study, the effect on genetic variance will likely depend more on allele frequencies in the population than any average pattern across loci.

As allele frequencies change, the balance between positive and negative effects of gene interactions on genetic variance also changes in proportion to the relative frequency of different genotypic combinations. Indeed, we routinely observe both positive and negative effects in the genetic variance predictions for all traits across simulated allele frequency sets (Fig. 1.2). Epistasis will thus facilitate evolution in some cases, but hinder it in others. It may do both at different points in time within the same evolving population.

The average tendency for epistasis to increase genetic variance for days to flower, pistil length, and SA separation suggest a positive average effect of interactions on the additive genetic variance. The exception is corolla width where the mean V_A is slightly lower with epistasis; a result that could be anticipated from the observation in Kelly and Mojica [3] that corolla width QTLs had smaller effects in combination than predicted from individual effects in the isogenic background. For all traits, epistasis increased the variance of the V_A across allele frequency sets (Fig. 1.2; Table 1.2). This speaks directly to how V_A will change under directional selection. With only additive effects, V_A is predicted to change slowly with selection, unless there are major loci and/or if allele frequencies are initially extreme. The greater dispersion of V_A with interactions (Fig. 1.2) suggests that epistasis is likely to generally accelerate changes in V_A.

The strong dependency of the average effect of substitution at a locus on interactions with other genotypes (Fig. 1.3) indicates that epistasis also has important implications for the dynamics of individual loci. With directional selection, the change in allele frequency at a QTL is determined by the locus-specific V_A, which, in turn, is

proportional to the average effect (GRIFFING 1960; KIMURA and CROW 1978). Our results suggest that average effects and, consequently, locus-specific V_A will be highly malleable throughout the selection response as allele frequencies change simultaneously across all loci. This is an important consideration now that we are able to directly monitor allele frequency change within populations under sustained directional selection (HAYES *et al.* 2009; BURKE *et al.* 2010; JOHANSSON *et al.* 2010; TURNER *et al.* 2011; REMOLINA *et al.* 2012; KELLY *et al.* 2013). Allele frequency trajectories will be variable in finite populations, and epistasis is likely to amplify this variability, generating idiosyncratic responses to replicate selection events (SIMÕES *et al.* 2008; SCARCELLI and KOVER 2009; BURKE *et al.* 2010; OROZCO-TERWENGEL *et al.* 2012). Even when genetic drift is inconsequential, sign epistasis and emergent over/under dominance imply that the ultimate loss, fixation, or balance of an allele will depend on the order of fixation of alleles at other loci. A thorough characterization of epistasis is, therefore, necessary if one wishes to understand allelic dynamics in response to selection and how this translates to the observed change in trait means.

Characterizing higher order epistastic interactions involving three or more loci may be necessary for a complete understanding of the selection response in terms of the underlying loci. Nevertheless, studies of pairwise epistasis like this one provide important information on the relative role of at least a subset of possible interactions. First, they provide a baseline estimate of the genetic variance attributable to epistasis. Second, they provide insight regarding the interactive properties of a locus (i.e. how frequently and strongly does the locus exhibit epistasis, and to what degree does this influence the average

effect at the locus). Lastly, pairwise estimates allow us to determine the improvement in predictive ability of the selection response due to the inclusion of epistasis. For example, Carlborg *et al.* (CARLBORG *et al.* 2006) demonstrate that pairwise estimates of epistasis are necessary to predict the long-term selection response in an artificial selection experiment on growth in domestic chickens. While only a first step towards understanding the entire network of epistatic interactions, pairwise estimates illustrate the relevance of epistasis to heritable variation and the evolutionary process.

To extend from genetic effects to genetic variances, it is essential to accommodate estimation error. Otherwise, predictions will necessarily be upwardly biased. Though this issue has been addressed previously (LUO *et al.* 2003), it has gone unnoticed in the vast majority of studies extending genetic effects to variances. Even in studies utilizing highly replicated measurements from inbred lines, such as this one, estimation error is appreciable, and the greater the estimation error, the greater the upward bias in variance predictions. This is particularly disconcerting given the disproportionate effects on variance components documented in this study, as this will impact estimates of heritability in the narrow sense. We have shown that our method of correcting variance calculations does indeed remove this bias and remains as precise as uncorrected calculations, although the latter point is likely to depend on the sample size of a study and the inherent variation of a particular trait. In smaller studies, one must make the choice between the tradeoff of a biased estimate vs. an imprecise one. However, we stress that future studies attempting to unite genetic effects with heritability take greater care to accommodate the potential for estimation error to inflate estimates of genetic variance components.

Conclusion

The results of this study, documenting the role of variable epistasis in determining genetic variance components are timely given the renewed interest and debate on the subject (CROW 2010; HANSEN 2013). Given that most genetic variance remains additive in the presence of epistasis and that additive variance is largely sufficient to predict the response to selection, it would seem, at first glance, as if epistasis is irrelevant. Upon further inspection, we find that epistasis contributes substantially to additive genetic variance, increasing it on average for most traits (Table 1.2, Fig 1.2), which should accelerate the response to selection. We note however that epistasis reduces the additive variance for particular combinations of allele frequencies with all traits. Contrary to the perspective that epistasis will have only transient effects on selection dynamics due to allelic combinations held together by linkage disequilibrium (GRIFFING 1960), our results suggest that the principal effect of epistasis may be as a major determinant of V_A (CARTER *et al.* 2005; HANSEN 2013), although empirical evidence supporting the generality of this conclusion is currently limited (CHEVERUD and ROUTMAN 1995).

Semantics has been a major impediment to connecting epistasis and the additive variance; the terms additive, dominance, and epistatic effects are used in a broad range of genetic effect models, yet differ substantially both in their interpretation as well as their relationship to genetic variance. This has led several authors to make general statements regarding epistasis that may be valid in the context of their own study, but are incorrect generally. For instance, it is not uncommon for authors to simply claim that non-additive

effects, such as dominance and epistasis, do not contribute to additive genetic variance (MAKOWSKY *et al.* 2011) and, therefore, are unimportant for the evolution of polygenic traits (CROW 2010). While this is true of statistical models of genetic effects, it is not true of functional models, as this and several other articles have argued (CHEVERUD and ROUTMAN 1995; CARTER *et al.* 2005; HANSEN 2013). In addition to partially determining additive variance, epistasis implies that allelic dynamics will depend on initial frequencies, such that replicate selection events are expected to be largely idiosyncratic and perhaps unrepeatable in terms of changes at underlying loci. Therefore, understanding functional epistastic interactions are important for understanding the fate of individual genes as well as populations exposed to selection.

CHAPTER 2*

Naturally Segregating Loci Exhibit Epistasis for Fitness

*Monnahan, P. J. and J. K. Kelly (2015). "Naturally segregating loci exhibit epistasis for f fitness." Biology Letters **11**(8): 20150498.

Abstract

The extent to which gene interactions or epistasis contributes to fitness variation *within* populations remains poorly understood, despite its importance to a myriad of evolutionary questions. Here, we report a multi-year field study estimating fitness of *Mimulus guttatus* genetic lines in which pairs of naturally segregating loci exist in an otherwise uniform background. An allele at QTL x5b—a locus originally mapped for its effect on flower size—positively affects survival if combined with one genotype at QTL x10a (aa), but has negative effects when combined with the other genotypes (Aa and AA). The viability differences between genotypes parallel phenotypic differences for the time and node at which a plant flowers. Viability is negatively correlated with fecundity across genotypes indicating antagonistic pleiotropy for fitness components. This tradeoff reduces the genetic variance for total fitness relative to the individual fitness components and thus may serve to maintain variation. Additionally, we find that the effects of each locus and their interaction often vary with the environment.

Introduction:

Heritable variation in fitness is the basis for evolution by natural selection, and understanding the genetic basis of this variation remains a major frontier in biology (CHARLESWORTH 2015). Genetic mapping studies have begun to identify the loci underlying quantitative traits, but the effects of these loci on fitness in nature largely remains unknown. Fitness is a complex function of many traits, few of which are measured in any mapping study. Additionally, the effect of a locus (gene) often depends on the environment experienced by the organism (SCHEINER 1993). Field studies, using genetic lines containing known alleles, have shed light on the evolutionary significance of loci identified in controlled settings (MALMBERG *et al.* 2005; MOJICA *et al.* 2012). However, the common observation in mapping studies that genes interact with one another (i.e. exhibit epistasis) (MOORE 2003; KELLY and MOJICA 2011; HUANG *et al.* 2012) has received limited attention in natural assays.

Natural assays of gene interactions directly address questions about speciation, adaptation, and the evolution of sex (OTTO and FELDMAN 1997). Epistasis is routinely invoked to explain reproductive isolation between species via Dobzhansky-Muller incompatibilities – interactions between heterospecific alleles that cause reduced fitness in hybrids (MOYLE and NAKAZATO 2009; WILLETT 2011). Multiple studies suggest that epistasis contributes to fitness differences between population within a species (KROYMANN and MITCHELL-OLDS 2005), including direct evidence from field assays (FENSTER and GALLOWAY 2000; MALMBERG *et al.* 2005). However, evidence for epistasis in fitness for loci that are naturally segregating *within* populations is limited. Indirect studies, which focus on traits presumably linked to fitness (e.g. flowering time (CAICEDO *et al.* 2004)) suggest a role for

epistasis, but direct evidence from field assays on the magnitude and pattern of epistasis is currently lacking. These details cannot be inferred from the between-population studies because the alleles that differentiate populations or species may never have been simultaneously segregating in any population. Even if they had been, their effects will likely have changed substantially after many generations of isolation due to the accrual of multiple mutations (McGregor *et al.* 2007). Natural assays estimating the magnitude and pattern of epistasis between segregating alleles are necessary to inform important issues such as the maintenance of genetic variation, and thus, the evolutionary potential of populations.

In this paper, we describe a field assay for epistasis between a pair of naturally segregating loci mapped within a single population of *Mimulus guttatus* (yellow monkeyflower). In the greenhouse, these loci exhibit epistasis for multiple floral morphology traits (Appendix 18). In the field, these loci interact to determine the developmental timing of the transition to flowering, as well as several non-floral phenotypes. Importantly, we observe sign epistasis for viability (i.e. probability of living to set seed) wherein an allele has a positive effect in one genetic background and a negative effect in alternate backgrounds. We also document a negative correlation among genotypic values for viability and fecundity (antagonistic pleiotropy), which may contribute to the maintenance of these polymorphisms in nature.

Methods:

Two loci (QTL x10a and QTL x5b), mapped for their effects on flower size, were introgressed into a common isogenic background by intercrossing two Nearly Isogenic

Lines (NILs). The isogenic background is IM767, an inbred line derived from ~15 generations of self-fertilization of field-collected seed. This line has medium floral trait values and genome sequencing reveals it to be highly homozygous (FLAGEL *et al.* 2014). Controlled crossing of the four possible double-homozygous genotypes produces the nine two-locus genotypes that were assayed. Prior to each field season, we confirmed genotypes performing PCR at diagnostic markers for a subset of individuals (KELLY and MOJICA 2011). We germinated seed at the University of Oregon greenhouse at a date matching snowmelt in each year (5/1/12 and 5/15/14). Two weeks after germination, we transplanted seedlings into 98-well trays filled with a mixture of potting soil and soil from the transplant site (44.373238 N, -122.130675 W). Trays were placed in three transects of approximately equal length such that each tray was flush with the surrounding soil. In 2012 and 2014, the study consisted of 430 and 1177 individuals, respectively, split evenly across the 9 two-locus genotypes.

Seedlings that washed out of the wells or died due to transplant shock within the first week were removed from subsequent analyses. The remaining individuals were measured at day of first open flower for corolla width, pistil length, length of internode preceding flowering node, pedicle length, and node of flower. We averaged measurements across flowers, although ~95% of surviving plants produced only one flower. We collected and counted all seed to determine fecundity.

We analyzed the data under the following linear model:

$$Z_{ijkl} = \mu + \alpha_i + \beta_j + Y_k + F_l + \alpha\beta_{ij} + \alpha Y_{ik} + \beta Y_{jk} + \alpha\beta Y_{ijk} \quad \text{(equation 17)}$$

where α_i is the effect of QTL x10a, β_j is the effect of QTL x5b, Y_k is the effect of year, F_{kl} represents the effect of the flat, and all subsequent terms represent interactions between

the relevant factors. F_{kl} was treated as random, while α_i, β_j, and Y_k were fixed factors. A significant effect of $\alpha\beta_{ij}$ indicates epistasis between loci. Non-significant interactions involving Year were removed from the model. Seed count (fecundity) was natural log transformed prior to analysis due to the right-skewed distribution, whereas the raw values were used for all other traits (Appendix 19). Seed count was analyzed only among the individuals that set seed (2012: n = 85 and 2014: n = 714). Traits were analyzed using mixed effects logistic (viability data; 'glmer' function) or linear regression (all other traits; 'lmer' function) as implemented in the 'lme4' package in R. For viability, significance was determined using anova.merMod(),which contrasts nested models with a likelihood ratio test, and Type III Wald Chi-square tests as determined by the 'Anova' function ('car' package) for the remaining traits. We found that Poisson regression for untransformed seed count, which includes individuals that set zero seed, largely mirrors results from viability analysis (Appendix 20); therefore, we opt for analyzing viability and fecundity separately. Genotypic values presented in the figures are the least squares means resulting from the linear model fits ('lsmeans' package) for all traits except viability, in which we calculated the survival probability from the logistic regression coefficients. The percent of explained variance (partial R^2) for each term and significance of post-hoc comparisons were determined with the 'pamer.fnc' and 'mcposthoc.fnc' functions, respectively, ('LMERConvenienceFunctions' package). Greenhouse data comes from a previous study (MONNAHAN and KELLY 2015a) (see Chapter 1).

Results and Discussion:

Epistasis had a highly significant effect on viability, in addition to several morphological and developmental traits (Table 2.1). Point estimates for viability suggest sign epistasis (Figure 2.1): The 'B' allele at QTL x5b has a negative effect on viability in the 'aa' background at QTL x10a, but a positive effect in other backgrounds ('Aa' and 'AA'). The implications of epistatic selection are numerous (WOLF *et al.* 2000; CARTER *et al.* 2005), but

Table 2.1. Summary of linear model fit.

Term	Chisq	Df	P-value	Partial R^2	Term	Chisq	Df	P-value	Partial R^2
	Viability					Fecundity			
Year	52.56	1	< 0.0001	24.684	Year	3.06	1	0.0804	0.331
x10a	23.97	2	< 0.0001	4.221	x10a	6.20	2	0.0450	0.444
x5b	13.46	2	0.0012	2.777	x5b	0.62	2	0.7325	0.266
x10a*x5b	24.61	4	< 0.0001	6.059	x10a*x5b	4.69	4	0.3210	0.529
	Days to Flower					Pedicle Length			
Year	2.85	1	0.0912	0.599	Year	4.83	1	0.0279	0.055
x10a	6.64	2	0.0362	0.740	x10a	31.53	2	< 0.0001	0.017
x5b	0.48	2	0.7856	4.794	x5b	6.59	2	0.0371	4.321
x10a*x5b	12.15	4	0.0163	1.237	x10a*x5b	39.28	4	< 0.0001	1.647
x10a*Year	6.27	2	0.0436	0.093	x10a*Year	24.88	2	< 0.0001	0.404
x5b*Year	2.03	2	0.3626	0.650	x5b*Year	13.69	2	0.0011	1.736
x10a*x5b*Year	11.65	4	0.0201	0.959	x10a*x5b*Year	26.60	4	< 0.0001	2.164
	Corolla Width					Internode Length			
Year	57.43	1	< 0.0001	5.325	Year	52.24	1	< 0.0001	6.851
x10a	5.17	2	0.0752	0.501	x10a	2.64	2	0.2675	0.312
x5b	1.20	2	0.5482	0.278	x5b	3.49	2	0.1743	0.778
x10a*x5b	2.96	4	0.5652	0.196	x10a*x5b	27.60	4	< 0.0001	1.591
x10a*Year	6.57	2	0.0374	0.436	x10a*Year	6.57	2	0.0375	0.390
	Pistil Length					Node			
Year	37.46	1	< 0.0001	3.898	Year	38.71	1	< 0.0001	9.039
x10a	4.81	2	0.0901	0.140	x10a	1.81	2	0.4043	0.465
x5b	2.65	2	0.2656	0.352	x5b	12.03	2	0.0024	4.335
x10a*x5b	2.49	4	0.6464	0.170	x10a*x5b	55.17	4	< 0.0001	3.651
x10a*Year	7.15	2	0.0281	0.482	x10a*Year	12.14	2	0.0023	0.695
					x5b*Year	10.38	2	0.0056	0.716

Figure 2.1. Genetic values for viability of the nine two-locus genotypes for QTL pair x10a-x5b for each year (Left). Different letters indicate significant differences within each 'A' background at $p<0.05$ for 2014 data. Asterisk indicates $p<0.0001$ for the difference between 'B' homozygotes within an 'A' background. Relationship between viability and fecundity for the nine two locus genotypic values (Right; 2012: $r = -0.69$; $p = 0.039$. 2014: $r = -0.80$; $p = 0.008$).

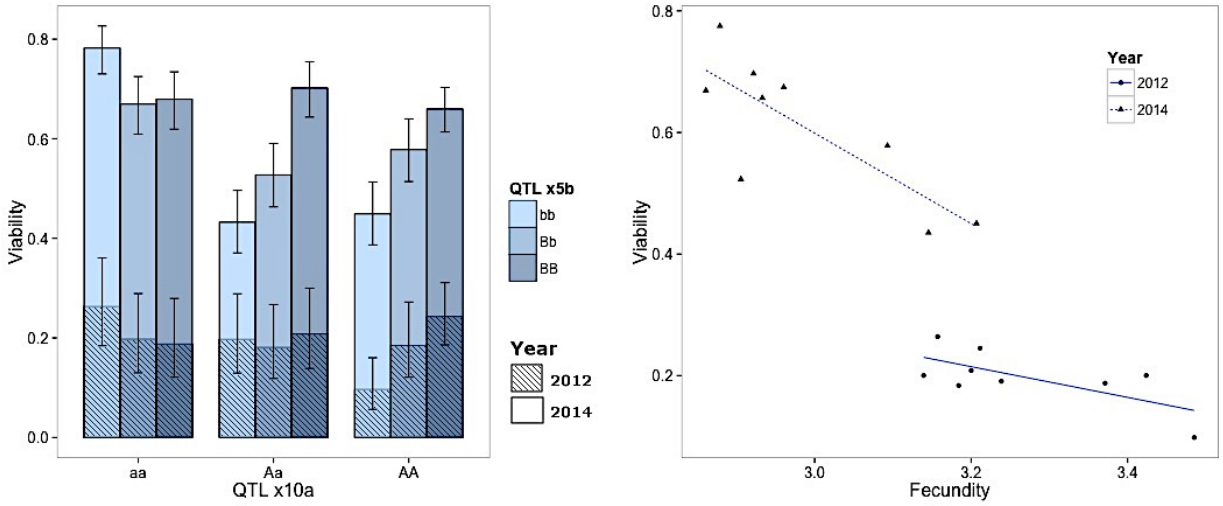

a simple prediction is that allele frequency change at one locus will change depending on allele frequencies at other interacting loci (WADE 2002). In this case, viability selection will favor allele 'b' at x5b, if the 'a' allele at x10a is at high frequency. Conversely, if 'a' is at low frequency, the 'B' allele at x5b will be favored. If selection acts purely through viability, the ultimate loss or fixation of either allele at x5b will be determined by the loss or fixation of alleles at x10a.

The negative correlation between viability and fecundity, the hallmark of antagonistic pleiotropy, should reduce the efficacy of viability selection (Figure 2.1 Right). Considering total fitness as the product of viability and (female) fecundity, the negative correlation between these components implies that variance in total fitness is reduced relative to the individual components. Since the change in allele frequency is proportional to the fitness variance attributable to a locus, the negative tradeoff will slow evolution at these loci, thus promoting the maintenance of polymorphism. In the simplest models, antagonistic pleiotropy between viability and fecundity does not guarantee stable polymorphism unless the total fitness of the heterozygous genotype exceeds both homozygotes (i.e. the locus exhibits overdominance) (HEDRICK 1999). Our point estimates for total fitness are not sufficiently precise to determine whether this condition is satisfied for these loci.

The observed viability-fecundity tradeoff seems to be driven by the epistatic effects of the loci on development time. The negative correlation between node and viability is accompanied by a positive correlation between node and fecundity, particularly in 2014 (Figure 2.2). Genotypes that flowered at a later node were less likely to survive, but

produced more seed if they did survive. This correlation is not significant in 2012, likely because genotypic values are based on very few measurements (~10 individuals per genotype survived to flower). The node at first flower is also positively correlated with the day of flower ($r = 0.864$, $p = 0.0027$; based on least-squares means across years). In annual, alpine *M. guttatus* populations, viability selection primarily acts through the cessation of water availability at the end of the summer (~80% of observed mortality occurred within 10 days in 2014). While individuals that delay flowering to later nodes have the capacity to produce more seed, they run a greater risk of not flowering before senescing.

Other than epistasis and antagonistic pleiotropy, environmental heterogeneity affects polymorphism at these two loci. We observed a strong dependency on environment for both marginal effects (gene-by-environment or GxE interactions) as well as the epistatic/interaction terms (GxGxE) for certain traits (Appendix 21 and Appendix 22). Of the traits for which significant epistasis was observed in the field, only days to flower exhibited epistasis in the greenhouse. We do not see epistasis for corolla width or pistil length in the field, despite observing strong epistasis in the greenhouse, and the opposite is true for internode and pedicle length (Table 2.1 and Appendix 18). Importantly, only surviving plants manifest the phenotype in the field and prior studies have shown these to be non-random with respect to flower size genotype (MOJICA and KELLY 2010).

Marginal and epistatic effects also varied significantly across years for some traits. The two years of this study differed markedly in terms the magnitude and pattern of temperature and precipitation. Excluding fitness traits, a significant interaction with year

Figure 2.2. Relationship between fitness components and developmental stage at which plants flower. (2012: Viability r = -0.47; p = 0.21. Fecundity r = 0.28; p = 0.46). (2014: Viability r = -0.76 p = 0.02. Fecundity r = 0.81 p = 0.008).

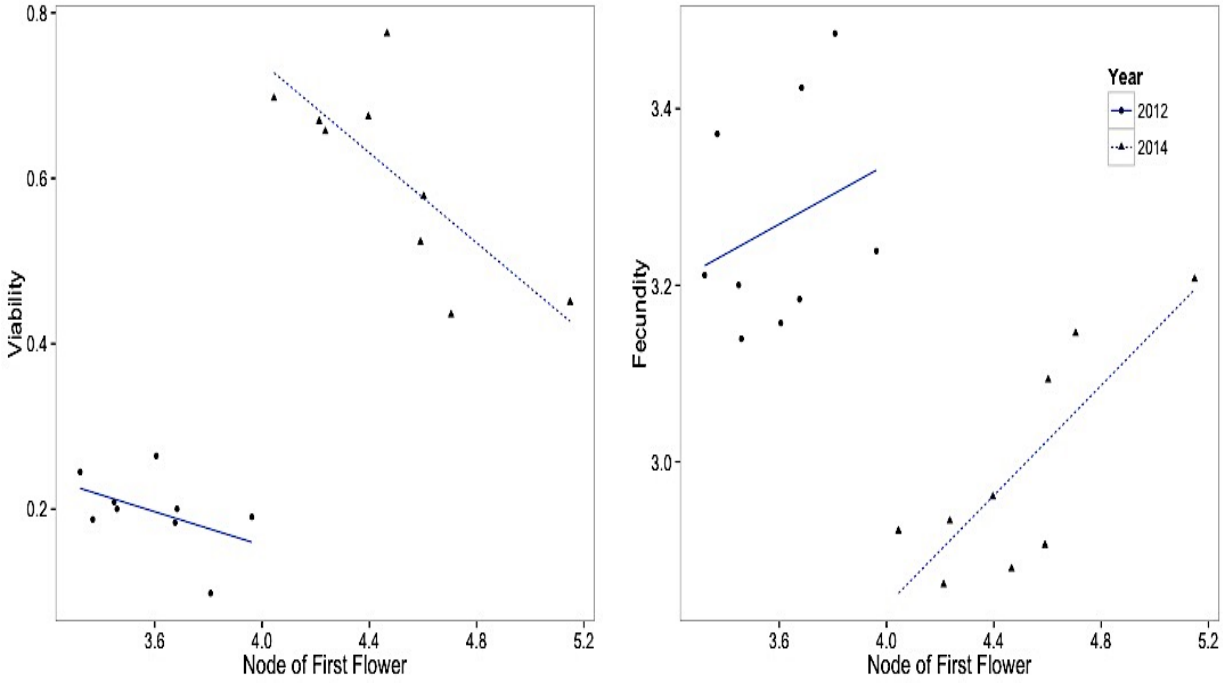

was observed for at least one genetic effect (marginal or epistatic) for each trait (Table 2.1 and Appendix 22). Genetic interactions with the environment are important because even if selection acts consistently on a trait across time and space, change in allele frequency may not be consistent if marginal and/or epistatic genetic effects depend on environment. Although the genetic effects on viability did not differ significantly across years in this study, spatial and temporal variation in selection have been documented for other polymorphisms in this species and locale (MOJICA *et al.* 2012).

In summary, this experiment provides some of the first evidence that alleles segregating within a natural population generate epistasis in fitness. Alleles interact not only with each other, but also with the environment that the organism experiences. Genetic effects are small relative to environmental effects, but on par with the effects of loci differentiating populations (e.g. comparing the portion of explain variance due to genetic effects relative to (MALMBERG *et al.* 2005)). As this study focuses on only two loci, we cannot estimate the quantitative contribution of epistasis to fitness variation. However, this study does demonstrate the importance of natural assays to understand the relevance of genetic mapping studies to evolution in nature.

CHAPTER 3

Comparing the genomic architecture in flowering time across multiple natural populations of *Mimulus guttatus*

Abstract:

The degree to which natural populations share genomic variation in ecologically-relevant traits has important implications for the generality of mapping studies as well as the scale at which we expect to observe parallel evolution. Standard genetic mapping studies are not well suited to this objective. In this study, we develop and implement a novel methodology to compare segregating variation associated with flowering time differences across three neighboring natural populations of *Mimulus guttatus*. We find that although flowering time loci are widely dispersed across the genome, few loci are shared across populations. However, these idiosyncratic sites are often proximal to one another, suggesting that similar gene regions harbor meaningful variation across these populations. A hybrid annual/perennial swarm is seen to harbor the majority of these divergent sites and has more sites/regions in common with both of the typical annual populations than these latter two have with each other, despite the swarm being most geographically isolated. We repeat this study over two years and find that divergence in allele frequency between early and late flowering plants is often year-specific. Overall, our work suggests that genomic variation associated with flowering time across these neighboring populations is highly variable across both time and space.

Introduction:

The standing genomic variation that is present in a population represents a complex history of the four forces of evolution (selection, migration, drift, and mutation), but also serves as the raw material from which future evolution proceeds. Genetic mapping methods can identify the loci underlying genetic variation in fitness and associated traits. However, replicating these studies in multiple populations is cost-prohibitive and prevents a full understanding of their generality. Here, we combine bulk segregant mapping with PoolSeq data to assay genomic variation associated with flowering time within multiple populations of *Mimulus guttatus* in order to determine the degree to which this variation is common versus private to a particular population.

The degree to which genomic variation is shared versus private not only informs the generality of mapping studies, but also our expectations of the repeatability of evolution. The parallel evolution of the same phenotype across multiple conspecific populations can correspond to various scales of parallelism at the genetic level, ranging from mutations in independent genetic pathways (COOLEY *et al.* 2011) to the repeated fixation of the exact same alleles (COLOSIMO *et al.* 2005). Under ideal circumstances in which uniform selection is applied to populations starting with the same initial allele frequencies, the repeated fixation of the same alleles is not certain, even though populations may reach the same phenotypic endpoint (COHAN 1984a; COHAN 1984b). The spatial and genetic structure typically found in natural populations of many species would further promote an idiosyncratic selection response. Although allelic parallelism would seem an unlikely null model, it is worth understanding the scale at which genomic variation is shared to determine if the potential for allelic as well as broader genetic parallelism exists.

The advent of bulk-segregant analysis (BSA) provides a powerful and cost-effective means for such assays and can accommodate multiple data types, including PoolSeq data as well as low-coverage individual sequencing. For the case of PoolSeq data (utilized herein), each pool of DNA is sequenced, and the resulting read counts provide estimates of allele frequency in that pool at variable sites throughout the genome. Divergence in allele frequency between pools that differ in some trait of interest is proportional to an average effect of the locus on the trait, and BSA provides the statistical framework for determining sites that exhibit significant divergence in frequency between pools. PoolSeq data has already been used with great success to investigate a number of issues including population differentiation (FABIAN *et al.* 2012), within-population dynamics of transposable elements (KOFLER *et al.* 2012), and the genomic response to selection (KELLY *et al.* 2013; TOBLER *et al.* 2014). Combing PoolSeq with BSA provides a general means to elucidate genetic architecture in natural and artificial conditions, but unlike other methods, its simplicity facilitates replication, which is central to the goal of the work presented here.

A major difficulty in many Next-Generation sequencing methods is accommodating the variance (in allele frequency estimates in the case of PoolSeq data) introduced by the sampling events subsequent to sequencing. For PoolSeq, these include, but are not limited to, sampling of individuals from populations, sampling DNA's into pools, sampling events during library preparation (particularly, PCR), and sampling of fragments for sequencing. Multiple methods have been proposed to estimate the variance in allele frequency estimates obtained from pooled samples (LAI *et al.* 2007; MAGWENE *et al.* 2011; GAUTIER *et al.* 2013; KELLY *et al.* 2013). Here, we build on a previously developed method (KELLY *et al.* 2013) based on Fisher's angular transformation (FISHER and FORD 1947), in which the

variance of each pool is derived from a series of contrasts between the pools. We construct a general likelihood-based hypothesis testing framework that accommodates information from multiple populations, in addition to allowing for tests within each population.

Although the generality of this method allows for the typical PoolSeq aims of comparing allele frequency divergence across populations, the primary advancement of this method is its power to assay segregating variation associated with particular traits (in this case, divergence between early and late flowering plants within a population). The method also allows tests of whether this associated divergence varies across years, akin to testing for an interaction term in traditional ANOVA style analyses. While we focus on only three proximal populations located in the Central Cascades of Oregon, the method can accommodate an arbitrary number of populations. Given the affordability of sequencing for PoolSeq, one could utilize this method to provide a comprehensive survey of within-population genomic variation across the species' entire range.

Flowering time is an excellent candidate for studies of genomic architecture because of the central role that it plays in many ecological and evolutionary processes. For many plants (particularly annuals), progression to flowering is a major determinant of fitness because access to pollination and resources necessary to complete reproduction (set seed) vary over the course of a growing season. This is particularly true for annual *M. guttatus,* in which plants must flower and set seed before the cessation of water availability. Although plants that delay flowering tend to produce more seed than their faster developing counterparts, they run the risk of not leaving enough time to set seed prior to desiccation.

This tradeoff may explain why genetic variation in flowering time is maintained, but will also surely play a role in how these populations evolve in response to a changing climate. Indeed, shifts in flowering time due to climate change have already been observed for a number of species (FITTER and FITTER 2002). Ideally, our study would be repeated multiple times in the coming decades to determine not only if these populations experience a shift in flowering time, but also if allele frequencies change in the expected direction given the results of this study.

That said, this two-year study provides many striking observations regarding the structure of genomic variation associated with flowering time differences within multiple populations. Several thousand SNPs, broadly distributed throughout the genome, differ in frequency between early and late flowering plants, and the vast majority of these are idiosyncratic to a specific population. One population in particular, a recently established annual/perennial hybrid swarm, harbors far more early-late divergent sites compared to the other two, and the allele frequency divergence at these sites tends to be more consistent across years. We also corroborate the hybrid nature of the population via identification of multiple segregating inversions characteristic of life-history divergence in *M. guttatus* and identify potential copy number variation associated with flowering time in this and one other population.

The apparent idiosyncrasy of genomic sites associated with flowering time is surprising given the physical proximity of these populations and modest levels of genetic differentiation (MONNAHAN *et al.* 2015a). This has important implications regarding the

potential for genetic parallelism in the response of these populations to uniform selection. As we consider larger genomic scales, we find that, although sites appear idiosyncratic, there is appreciable overlap in the genomic regions harboring this variation, suggesting that parallel evolution may occur at the genetic (but not the nucleotide) level. However, ascertainment bias hampers our ability to make firm conclusions regarding the scale of idiosyncrasy (i.e. a site may exhibit similar changes in some populations, but fail to simultaneously reach significance), and we find some evidence for this in at least one of pair of populations in 2014. More generally, identifying these shared genomic regions informs the probability of genetic parallelism as well as supports the utility of mapping studies in identifying gene regions that likely harbor meaningful allelic variation in natural populations. Overall, this paper demonstrates the power and efficiency of the analytical framework introduced herein to identify segregating variation within multiple populations in order to inform the scale at which genomic variation is shared.

Methods:

Plant Collection and phenotyping:

We focus on three natural, neighboring populations in the Central Cascades of Oregon: Quarry (44.3454243 N, –122.1362023 W; Elevation ~1200 meters), IM (44.402217 N, –122.153317 W; Elevation ~1400 meters), and BR (44.373238 N, –122.130675 W; Elevation ~1200 meters). IM (Iron Mountain) is ~6.5 miles north/northwest of Quarry, and BR (Browder Ridge) is approximately halfway between IM and Quarry. IM and BR are typical alpine, annual populations whereas Quarry is a phenotypically-diverse potential annual/perennial hybrid population (MONNAHAN *et al.* 2015b).

From each population in each year (2013 and 2014), we collected and measured 100 early flowering and 100 late flowering plants. We established several parallel transects of approximately equal length spanning each population. We sampled whole plants at a rate of ~2 plants per ~30 cm, choosing sampling times based on density of plants along a transect. A transect would be sampled as soon as plant density was such that 2 plants could be found within 15 cm on either side of the transect for each foot of transect. Collection times were similar across years albeit slightly earlier for all 'early' bulks in 2014 and slightly later for the 'late' bulk in Quarry (Appendix 24). We collected tissue into 2 mL tubes and stored in dry ice until it could be stored at -20° C. There was a very hot and dry spell that wiped out the BR population shortly after collecting the 'early' bulk; therefore there was no 'late' bulk to collect. Aside from the variance calculations (described in 'Likelihood framework' section below), that data from Browder Ridge in 2014 is excluded from the study.

***Sequencing*:**

We extracted DNA from each individual collected over 2013 and 2014 using a standard CTAB protocol. We pooled individuals' DNA in equal amounts (20 ng/sample; quantified via Qubit) corresponding to the year, population, and bulk in which they were collected. We whole-genome sequenced each sample on an Illumina HiSeq 2500 (Paired-end 100bp reads). We sequenced the 2013 samples across 3 High-Output lanes, while the 2014 samples were sequenced with just two High-Output lanes. We sequenced the samples in two additional rapid-runs in order to equilibrate coverage across samples.

We combined data from the different lanes to create 11 fastq files corresponding to each of the sampling bulks. We ran Scythe (https://github.com/vsbuffalo/scythe) and Sickle (https://github.com/najoshi/sickle) for each fastq file to remove adaptors and trim low quality sites, respectively. We mapped reads to the *Mimulus guttatus* v2 genome build using BWA. We used Samtools to create bam files, which were converted to a vcf file using the GATK UnifiedGenotyper. Prior to creating the vcf, we removed PCR duplicates using Picard Tools. The read counts in the vcf corresponding to each of the sampling bulks serve as the input for all of our subsequent likelihood analysis.

Likelihood framework:

Our likelihood framework for testing for divergence in allele frequency generalizes the method of (KELLY *et al.* 2013) to accommodate additional populations across multiple years. This method was originally developed as a window-based approach to detect soft-sweeps resulting from divergent selection on a common starting population. We opt for a site-based approach given the highly outbred nature of these populations, but utilize a similar variance estimation procedure. Briefly, we transform estimates of allele frequency using Fisher's angular transformation to create new variables that are independent and approximately normally distributed under the assumption that divergence in allele frequency is due solely to neutral processes. The variance of such a variable is a function of the sampling events leading to the observed read counts. In this case, the relevant sampling events would correspond to the following: sampling of individuals (or rather, alleles) from the population, sampling of DNA into the pooled library, PCR sampling during library preparation, and sampling of fragments on the flowcell of the sequencer (i.e.

variance due to finite read depth). Each of these sampling events contributes additively to the variance and in a reciprocal manner (1 on the number of units sampled). The variance due to the first and last of these sampling events for each bulk can be readily estimated: 100 individuals (200 alleles) were sampled for each bulk, and a known number of reads was sampled at each site upon sequencing. The variance due to the remaining sampling events must be inferred from the data. PCR duplicates were removed bioinformatically, which should reduce the variance contributed by differential PCR amplification. To calculate the remaining variance, we first perform a series of contrasts between the four bulks within a population. This is beneficial because the contrasts will be centered on zero with a variance equal to the sum of the variances of the relevant bulks. In other words,

$$E[x_E - x_L] = 0 \quad \text{(equation 18)}$$

$$Var[x_E - x_L] = Var[x_E] + Var[x_L] = \frac{1}{m_E} + \frac{1}{m_L} + v_E + v_L \quad \text{(equation 19)}$$

,

where the *x*'s are the transformed allele frequencies, the *m* values are the read depth in each sample, and the *v* terms are the remaining sampling variance (hereafter, denoted RS variance). This RS variance effectively bins all sources of error upstream of read sampling. We assume these to be common to all SNPs in a sample. The *E* and *L* subscripts denote the 'Early' and 'Late' samples.

The actual distribution of the contrasts will contain a mixture of neutral and selected SNPs. We utilize the interquartile range to approximate the true variance of the neutral distribution, as this is robust to the presence of extreme values caused by selected SNPs. We can use the IQR to calculate the variance of the neutral contrasts and subtract off the mean of the variance due to sampling of fragments (the sum of 1 on read count in each

bulk) to arrive at the RS variance for each sample. For the IM and Q populations, this equates to solving 6 equations (one for each contrast) for 4 unknowns (variances), keeping in mind that each variance component appears in two of the resulting equations from the contrasts. This system is technically overdetermined (i.e. there are more equations than unknowns) and lacks an exact solution; however, we utilize the method of General Least Squares to obtain a 'best-compromise' solution for the RS variances (LYNCH and WALSH 1998). The only additional information necessary are estimates of the (co)variance of the 6 contrast variances. We obtain these (co)variances via jackknifing the original data set of read counts, recalculating the contrast variances after deleting a portion of the original data. The RS variance calculation is much simpler for the BR population as there are only 3 samples resulting in three equations with 3 unknowns. These produce an exact solution for the RS variance of BR Early 2013 and BR Late 2013.

With estimates of these variance components, we can easily implement a set of likelihood calculations for each site based on the normal density function in which we allow one or more parameters of interest to vary. In the simplest case, we focus on a single population in a single year and ask whether there is a significant difference in allele frequency between the early bulk and the late flowering bulk. The log-likelihood of the constrained model in which we enforce a single mean frequency in the population is simply:

$$LL = \frac{-(x_E - \hat{\mu})^2}{2\hat{\sigma}_E^{\,2}} + \frac{-(x_L - \hat{\mu})^2}{2\hat{\sigma}_L^{\,2}} \qquad \text{(equation 20)}$$

Here, the *x* values are the transformed allele frequencies in each sample and the σ_k^2 terms are the RS variance plus the reciprocal of the read depth in each sample. The maximum likelihood estimate of the transformed population allele frequency is simply:

$$\hat{\mu} = \frac{x_E w_E + x_L w_L}{w_E + w_L} \quad , \qquad \text{(equation 21)}$$

where *w* is the reciprocal of the sample-specific variance. The greater the variance in a particular sample, the lower the weight that it exhibits on the estimate of the mean. This can be compared to an unconstrained model in which a separate mean is estimated for each sample. Since there is only one observation (allele frequency) in each sample, the estimate of the mean is simply the observation, and the likelihood of the unconstrained model becomes zero. A likelihood ratio test statistic simply becomes -2 times the log likelihood of the constrained model, and a significant test indicates that the unconstrained model fits the data significantly better. This likelihood ratio test can be compared to a chi-square distribution, where the degrees of freedom equals the difference in the number of free parameters between the two models.

Under the assumption that neutral, drift processes govern divergence among bulks, the above likelihoods are independent across populations and years, and therefore, can be summed to perform an omnibus test of divergence between early and late flowering samples. This likelihood takes the general form:

$$LL = \sum_{i=0}^{Y} \sum_{j=0}^{P} \sum_{k=0}^{B} \frac{-(x_{ijk} - \hat{\mu}_{ij})^2}{2\hat{\sigma}_{ijk}^{\ 2}} \quad , \qquad \text{(equation 22)}$$

where the summations are across Years, Populations, and Bulk (Early/Late). For the unconstrained model, there are 20 free parameters (one mean and one variance for each sample), whereas there are 15 free parameters in the constrained model (one variance for each sample (10) and one mean for each population (5)). This results in 5 degrees of freedom for the test.

The testing procedure is very general. We can test for divergence between early and late flowering plants within a single population/year, within a population across years, across populations within a year, and across populations for both years. Additionally, we can use this same framework to test if allele frequency differs significantly across years or across populations. Lastly, we can determine if there is a significant interaction between the effect of bulk (early or late flowering) and the year (i.e. does the change in allele frequency between early and late plants depend on the year in question). For the interaction test, the constrained model has a single mean for each year/population and a single effect of bulk, α, which applies to both years. The maximum likelihood estimates are substantially more complex for this model and become intractable upon scaling to multiple populations; therefore, we restrict the interaction test for individual populations. The MLEs for the means and α term takes the form:

$$\hat{\mu}_{13E} = \frac{(v_{13E} + v_{14E} + v_{14L})x_{13L} + (x_{13E} - x_{14E} + x_{14L})v_{13L}}{(v_{13E} + v_{13L} + v_{14E} + v_{14L})} \quad \text{(equation 23)}$$

$$\hat{\mu}_{14E} = \frac{(v_{13E} + v_{13L} + v_{14E})x_{14L} + (x_{14E} - x_{13E} + x_{13L})v_{14L}}{(v_{13E} + v_{13L} + v_{14E} + v_{14L})} \quad \text{(equation 24)}$$

$$\alpha = \frac{(v_{14E} + v_{14L})(x_{13E} - x_{13L}) + (v_{13E} + v_{13L})(x_{14E} - x_{14L})}{(v_{13E} + v_{13L} + v_{14E} + v_{14L})} \quad \text{(equation 25)}$$

Note that the means are defined for the early bulk. The mean for the late bulk in a particular year is simply the mean for the early bulk plus α.

We applied a series of filters for each of the implemented tests. For all of the tests, we required that both samples from a population and year have at least 25 reads and less than 100 reads. For the omnibus test, in which likelihoods are aggregated across years and populations, failure of a population/year to pass filter simply resulted in dropping this population/year from the likelihood calculation and adjusting the degrees of freedom appropriately. Additionally, we required the reference allele frequency, averaged across the relevant samples, to be between 0.05 and 0.95. For example, with the bulk test, this was enforced for each population/year combination, but for the population test, the average was taken across all samples. For all tests, we apply a false discovery rate of 0.1 to establish significance.

Enrichment Analysis:

For the significant tests from the combined analysis of all the populations, we performed a GO enrichment test using Blast2Go (again, with FDR = 0.1). We use a previously annotated transcriptome (COLICCHIO *et al.* 2015) as the reference set.

Additionally, we perform an enrichment test specifically for a list of homologous loci corresponding to flowering time genes in *Arabidopsis thaliana*(gene list compiled by J. Friedman and B. Blackman). Using the v2 *M. guttatus* annotation, each gene was classified as either a flowering time gene or not as well as whether there existed a significant Δp_{EL} (allele frequency divergence between early and late flowering plants) SNP within the gene boundary. With these four counts, we conducted a Fisher's exact test. We repeated this procedure for regions 2 kb upstream of the gene start site.

Results:

Genome Scan:

In total, we identified approximately 7.5 million SNPs passing filter, most of which are segregating in more than one population (Appendix 26). Our testing procedure was able to identify numerous significant sites for each of the null hypotheses that were tested. The focal test of this study, whether allele frequency differs between early and late flowering plants (hereafter, Δp_{EL}) provides a general characterization of the genomic distribution of variant sites exhibiting an association with flowering time and suggests that, across these three populations, approximately 0.2% of the variant sites exhibit a significant association with flowering time divergence (Appendix 23; Fig 3.1A).

Figure 3.1. A.) –log10(p) for divergence between early and late flowering plants for each population. Red = Browder Ridge; Green = Iron Mountain; Blue = Quarry. Only significant tests are shown. Triangles denote tests in which a significant interaction between year and bulk was observed. B.) Mean and variance for the difference in allele frequency in 1 Mb windows. C.) Overlap in significance for tests of bulk, population, or year. D.) Overlap in significance of the bulk test in the three different populations for 2013 data (Left to right: individual sites, 30 kb windows, and 1 Mb windows)

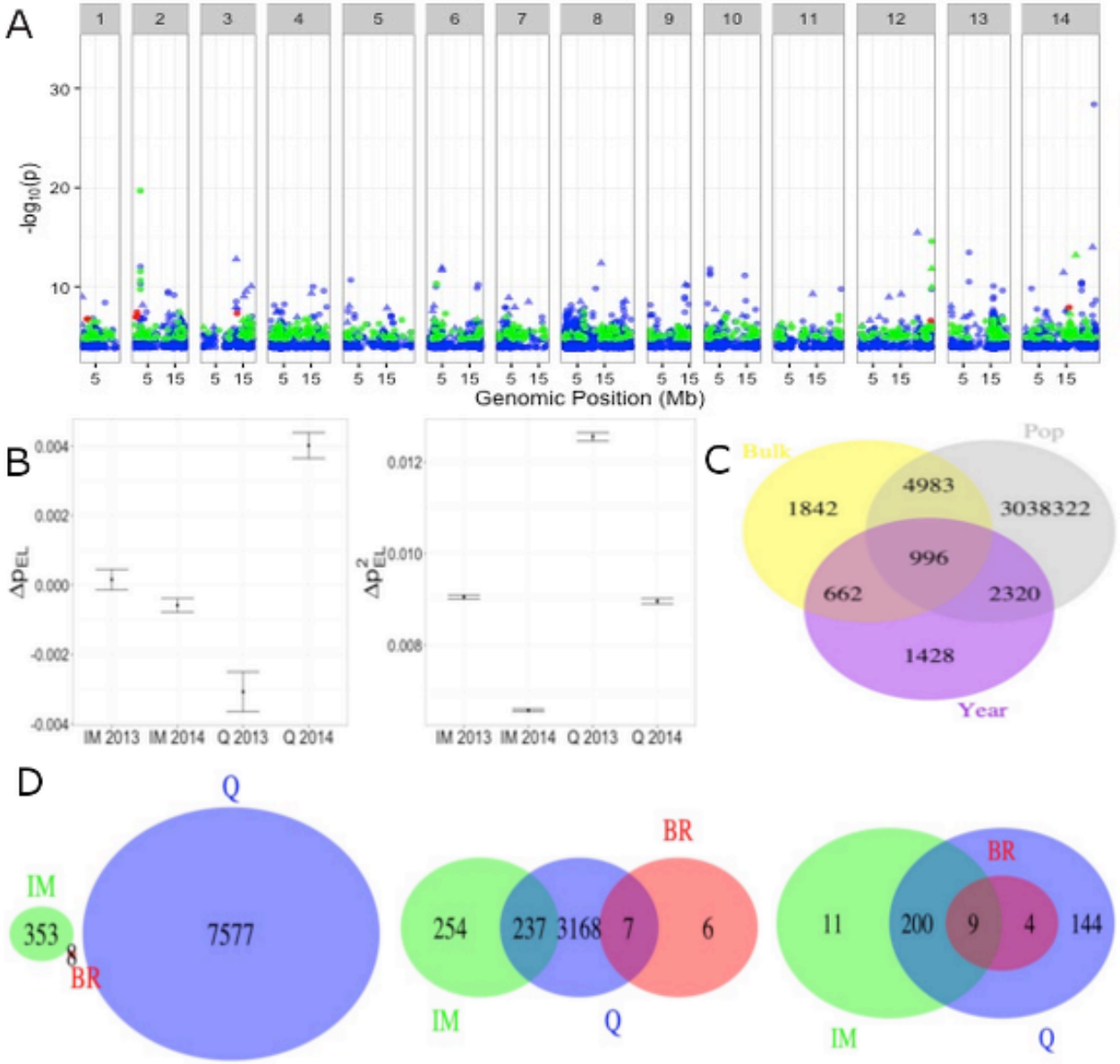

The test for spatial divergence (allele frequency difference between populations; Δp_{Pop}) suggests that nearly two thirds of the variant sites in our sample exhibit significant divergence among populations. The test for temporal divergence indicates that a much smaller albeit still substantial number of sites change significantly across years (~0.1% of variant sites; Δp_Y; Appendix 23). Furthermore, the allele frequency difference between early and late flowering plants often depends on the year in question. Genome-wide, the Quarry population exhibits the greatest difference in mean Δp_{EL} across years (Figure 3.1B); however, among sites exhibiting significant Δp_{EL} a greater proportion of sites exhibit a significant interaction between year and bulk in IM (154/909 = 16.9% in IM; 262/8808 = 2.9% in Quarry; Appendix 23). We are unable to make the analogous test in Browder Ridge due to the lack of the 2014 Late sample.

Comparing across the three major hypotheses tested (Bulk, Year, and Population) we see that many of the same SNPs are often deemed significant for multiple tests, indicating that the same site not only associates with flowering time divergence, but is also divergent across time and space (Fig 3.1C).

There is a great disparity between the number of significant sites identified in the three different populations, when considering the year (2013) in which we have complete data for all populations (Appendix 23; Fig 3.1A). Quarry exhibits vastly more sites with significant divergence between early and late flowering plants than do Iron Mountain or Browder Ridge, the latter of which shows very few significant sites. This is generally in line with genome-wide patterns of allele frequency differences between early and late flowering plants. In both years, the average difference in allele frequency in Quarry was much greater (and more variable), than Iron Mountain (Fig 3.1B-1 and 3.1B-2) or Browder

Ridge (not shown). These statistics were calculated for 1 Mb sliding windows (sliding by 100 kb at a time), and the variance values that are displayed are the mean of the variance in allele frequency differences within windows. Interestingly, we find very few significant sites when considering only the 2014 data for IM and Quarry (~250 per population).

Regarding the central focus of this study, we find no sites to be simultaneously significant in two or more populations, at least in the 2013 data (Fig 3.1D-1). In the 2014 data, only 8 sites are found to be significant in both Q and IM. If we zoom out to consider 30 kb or 1 Mb windows, there is more overlap between populations (Fig 3.1D-2 and 3.1D-3. A window is considered shared if two or more populations each have a significant SNP within the window. Of the 1 Mb windows assayed, all of the windows in which Browder Ridge exhibited at least one significant SNP also contained significant SNPs within Quarry. This is largely true of Iron Mountain and Quarry as well. Regardless of the scale of observation, Browder Ridge and Iron Mountain have a greater number of divergent regions in common with Quarry than they do with each other.

Figure 3.2. Correlation in Δp_{EL} across populations in 2013. The red points are sites deemed significant for the population on the x-axis, and the grey points are non-significant. The black lines are the best fit through the red points, and the blue line is the best fit line through the grey points.

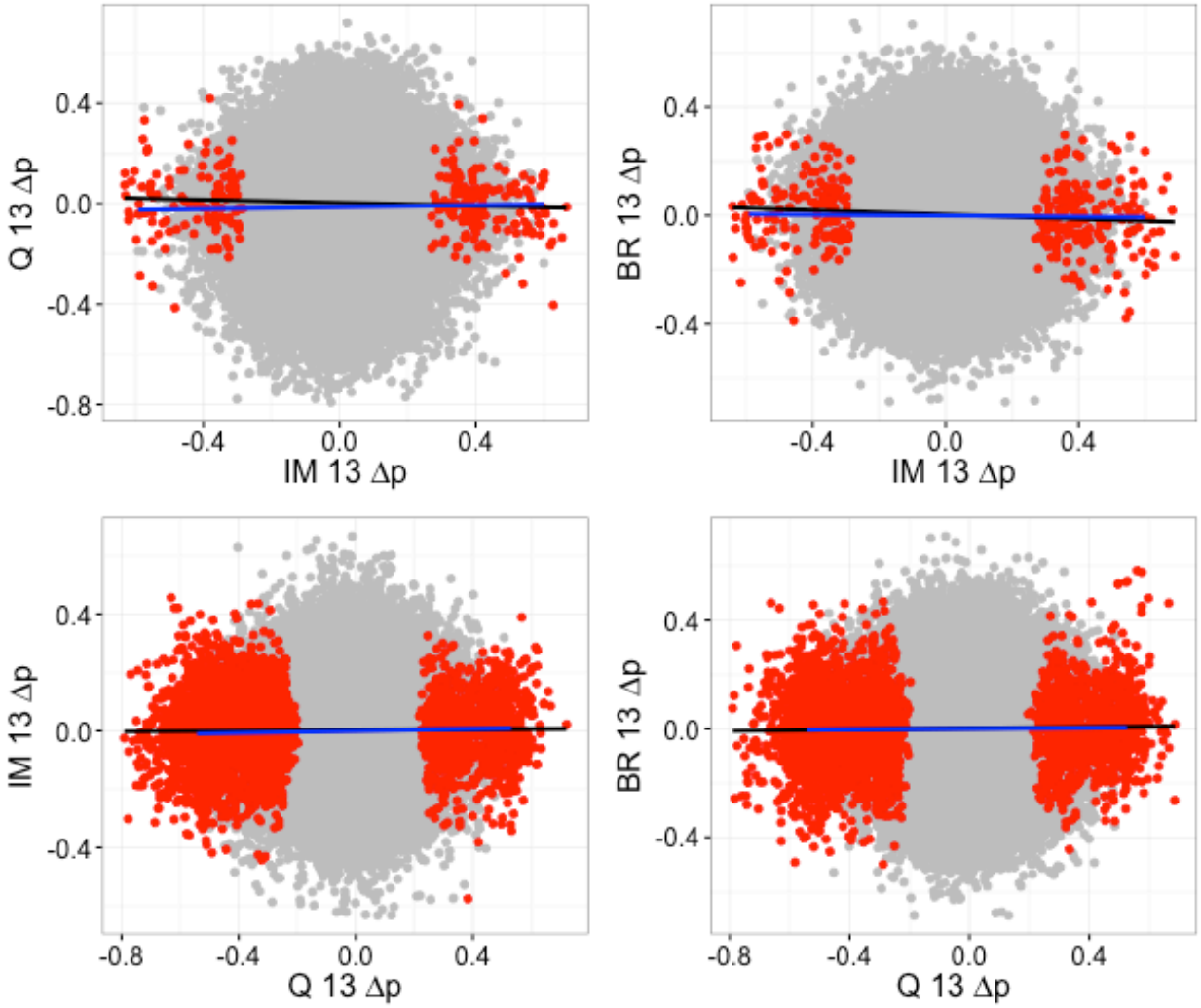

Figure 3.3. Top Panel: Correlation in Δp_{EL} across populations in 2014. The red points are sites deemed significant for the population on the x-axis, and the grey points are non-significant. The black lines are the best fit through the red points, and the blue line is the best fit line through the grey points. Bottom Panel: Correlation in Δp_{EL} across populations in 2014 for the sites found to be simultaneously significant in both populations in 2014.

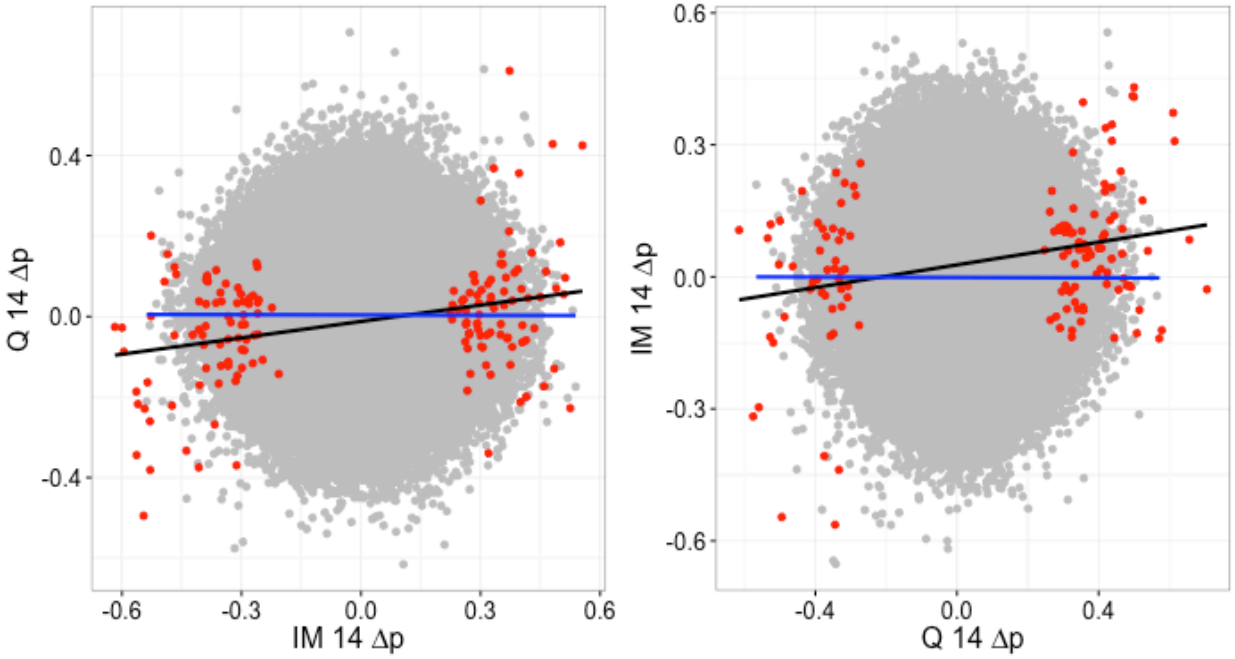

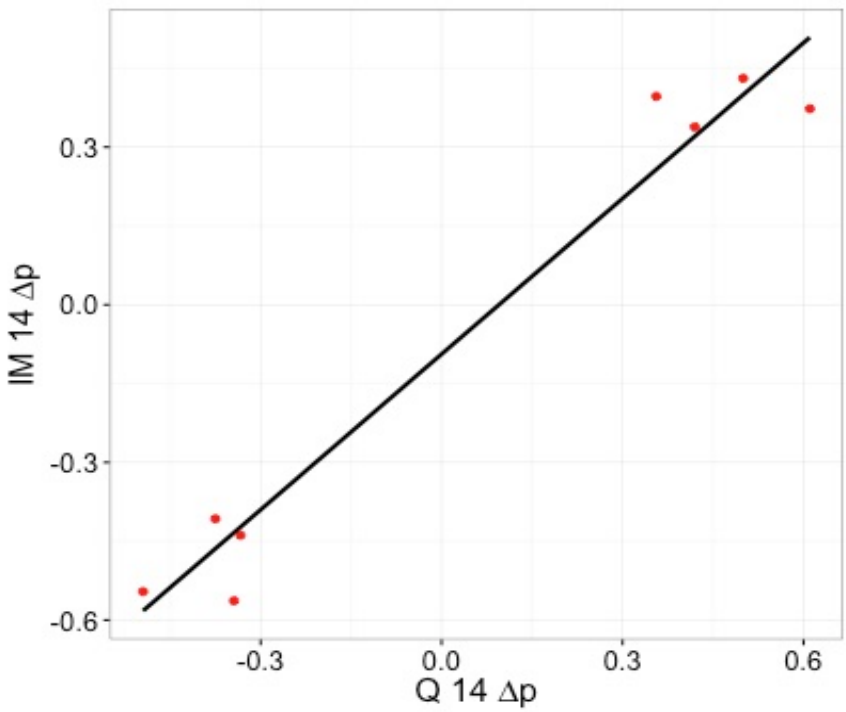

Spatial and Temporal consistency in Δp_{EL}

Spatial consistency varies greatly across the two years of this study. In 2013, not only is there no overlap in significance with regard to individual sites, but also there is little to no correlation in Δp_{EL} across populations for significant sites (Figure 3.2). For these figures, it is important to note that we only include sites that are polymorphic in both populations as including non-polymorphic sites would downwardly bias correlation estimates. Additionally, we remove the sites corresponding to the suspected copy number variants (discussed in section below). In contrast to the 2013 data, both IM and Q reciprocally show a strong positive correlation for sites deemed significant in each population in 2014 (Figure 3.3; Top Panel). Focusing in on the 8 shared significant sites in 2014, we see a striking positive correlation (Figure 3.3; Bottom Panel). This suggests that the spatial consistency in Δp_{EL} varies across years.

Similarly, we find that temporal consistency Δp_{EL} varies across space. Though it remains true that Δp_{EL} is generally more variable in the Quarry population (Figure 3.1B-2), there are also a greater number of sites that exhibit a consistent Δp_{EL} across the two years of the study (Figure 3.4; Top Panel). For both populations depicted, the same filtration steps were applied to the SNP set. To be included in the graph, a SNP must fall in the top 75th percentile of Δp_{EL} in 2013, as well as in the lower 25th percentile for the squared difference in Δp_{EL} for the two years of study. This filtration will select for SNPs that have a large, positive yet consistent Δp_{EL} over time. The same filtration criteria applied to both IM and Q yields a much greater number of SNPs in Quarry that exhibit large, consistent

Δp_{EL}. Note that the choice to filter for positive versus negative Δp_{EL} is arbitrary as the point of the graph is merely to demonstrate the greater preponderance of sites passing filters in Quarry versus IM. This greater consistency of Δp_{EL} is reiterated in the scatter plots of Figure 3.4 (Bottom Panel). This is in line with the results for the test of interaction between Δp_{EL} and year presented in Appendix 23. Though Quarry had a greater number of SNPs exhibiting a significant interaction compared to IM, this represented a lower proportion of the total sites exhibiting a significant Δp_{EL}. With regard to significance, only 13 sites were found to be significant in Quarry in both years and only 6 were found for both years in IM.

Figure 3.4. Top Panel: Reference frequency across the four sampling events for a subset of sites exhibiting the greatest degree of consistency in Δp_{EL} across the two years of study. Bottom Panel: Scatter plots depicting correlation in Δp_{EL} across the two years of study within IM and Q.

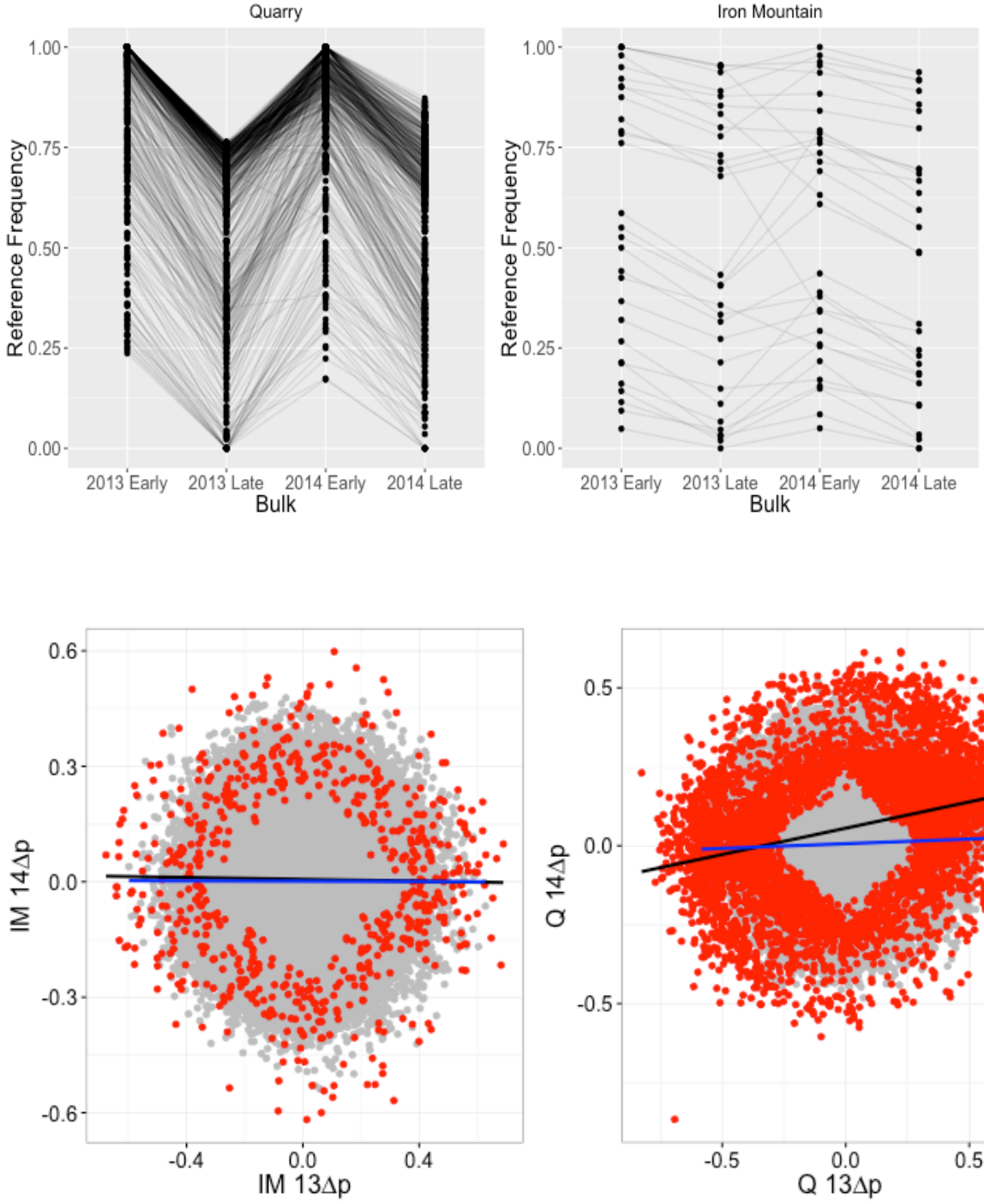

Candidate Genes and Enrichment Analysis:

Using the list of 10,985 sites exhibiting significant Δp_{EL}, we searched the *M. guttatus* annotation for potential candidate genes. We identified approximately 1,800 candidate genes based on whether or not the gene boundary contained at least one significant site for the Δp_{EL} test; however, many of these matches were driven primarily by the Quarry population. Out of all candidate genes, 13 possessed significant Δp_{EL} sites for both IM and Q. Interestingly, 7 of these are annotated as histone superfamily proteins.

With the list of compiled *A. thaliana* flowering time gene homologs in *M. guttatus,* we found 41 (16%) had at least one significant site within the gene boundary. For the remainder of the 27,326 non-flowering time genes, 3653 (13%) were found to contain at least one significant site. A Fisher's exact test on these counts suggests that flowering time genes were not significantly more likely to harbor significant Δp_{EL} sites than expected by chance (p = 0.2091). We repeated this test for significant sites located 2 kb upstream of gene regions, again finding no association between significance and flowering time gene identity. However, this procedure identified several candidate genes harboring significant sites with clear, previously identified roles in determining natural variation in flowering time like FLC, FT, Frigida-like genes, and LFY.

Gene Ontology enrichment analysis on the list of sites exhibiting a significant Δp_{EL} or Δp_Y identified no significant GO terms for Δp_{EL} and 5 terms for Δp_Y. After reducing these 5 GO terms to the most specific terms, there remained only one, which was 'nucleotide

binding'. For the test of Δp_{Pop} we find 20 enriched GO terms (after reducing to the most specific set; Appendix 25) some of which make sense in light of population differences (e.g. pollination, anatomical structure morphogenesis, response to abiotic stimulus, etc.).

Structural and copy number variation:

A targeted investigation of allele frequency divergence in the Quarry population provides evidence for the segregation of multiple previously identified inversions (Figure 3.5). These inversions typically occur as fixed differences between annual and perennial populations. Since the reference genome is of an annual individual, the reference base should tag the annual version of the inversion and vice versa. A broad pattern of positive Δp_{EL} (indicating a higher reference base frequency in the early flowering plants) suggests that the inversion is segregating within Quarry. The average Δp_{EL} in windows in the inversion are substantially larger and positive relative to the genome-wide average in either year (2013 Δp_{EL} Inversion = 0.02929344; 2013 Δp_{EL} genome-wide = -0.003076053; 2014 Δp_{EL} Inversion = 0.01596762; 2013 Δp_{EL} genome-wide = 0.004017341). Though Δp_{EL} is positive in this region for Iron Mountain as well (2013 Δp_{EL} Inversion = 0.0009626377; 2013 Δp_{EL} genome-wide = 0.0001560661; 2014 Δp_{EL} Inversion = 0.0008536093; 2013 Δp_{EL} genome-wide = -0.0005833527), the magnitude of the difference from the genome-wide average does not implicate a segregating inversion in IM. We also find evidence for the presence of a previously identified meiotic drive locus in the Quarry population that was initially discovered in the Iron Mountain population. The

negative Δp_{EL} throughout this region implies that the alternate allele frequency is higher in the early bulk (Figure 3.5).

Along several different chromosomes (2, 8, 10, and 14), we noticed serial discrepancies of read depth across our samples indicative of copy number variation. Figure 3.6 provides an example of this on chromosome 14, wherein normalized read depth is two-fold greater in the 2014 early sampling event at Iron Mountain as compared to the remaining bulks. This region corresponds to a known RNA-ligase gene (Migut.N02091), whose primary function is in the maturation of tRNAs. The remaining regions also display read depth discrepancies albeit to a lesser extent. Interestingly, all of these regions correspond to genes encoding histone subunits (both h3 and h4).

Figure 3.5. Δp_{EL} for Quarry 2013 (top), Quarry 2014 (middle), and IM 2013 (bottom) plotted along select chromosomes calculated for 1 Mb sliding windows (step size = 100 kb). From left to right: Chromosomes 7, 8, 10, and 11. The approximate locations of two putative inversions (chromosome 8 and 10) and a meiotic drive locus (chromosome 11) are given by the blue bars.

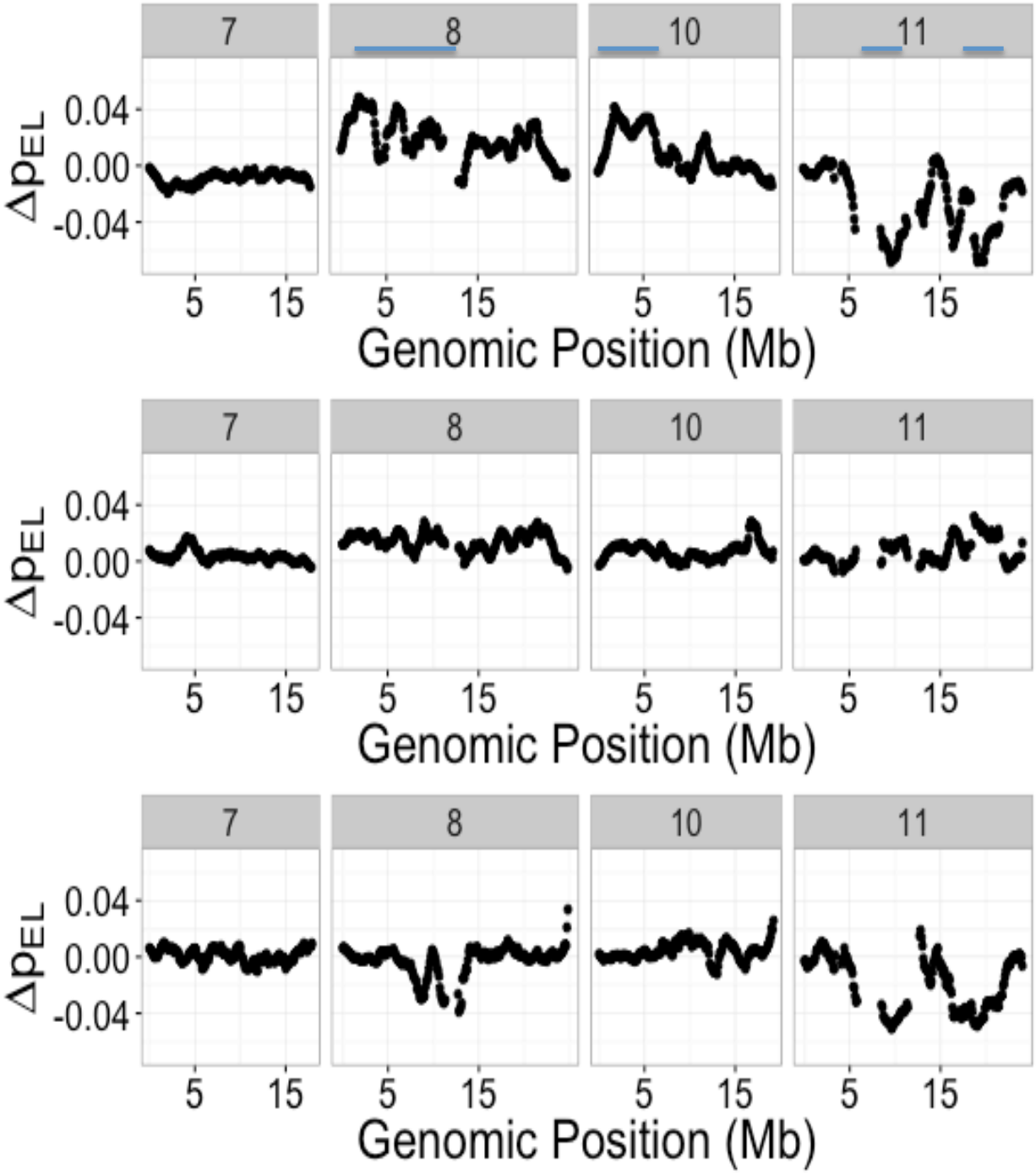

Figure 3.6. Normalized read depth (smoothed using 'loess' function in R) for Iron Mountain samples across the region on chromosome 14.

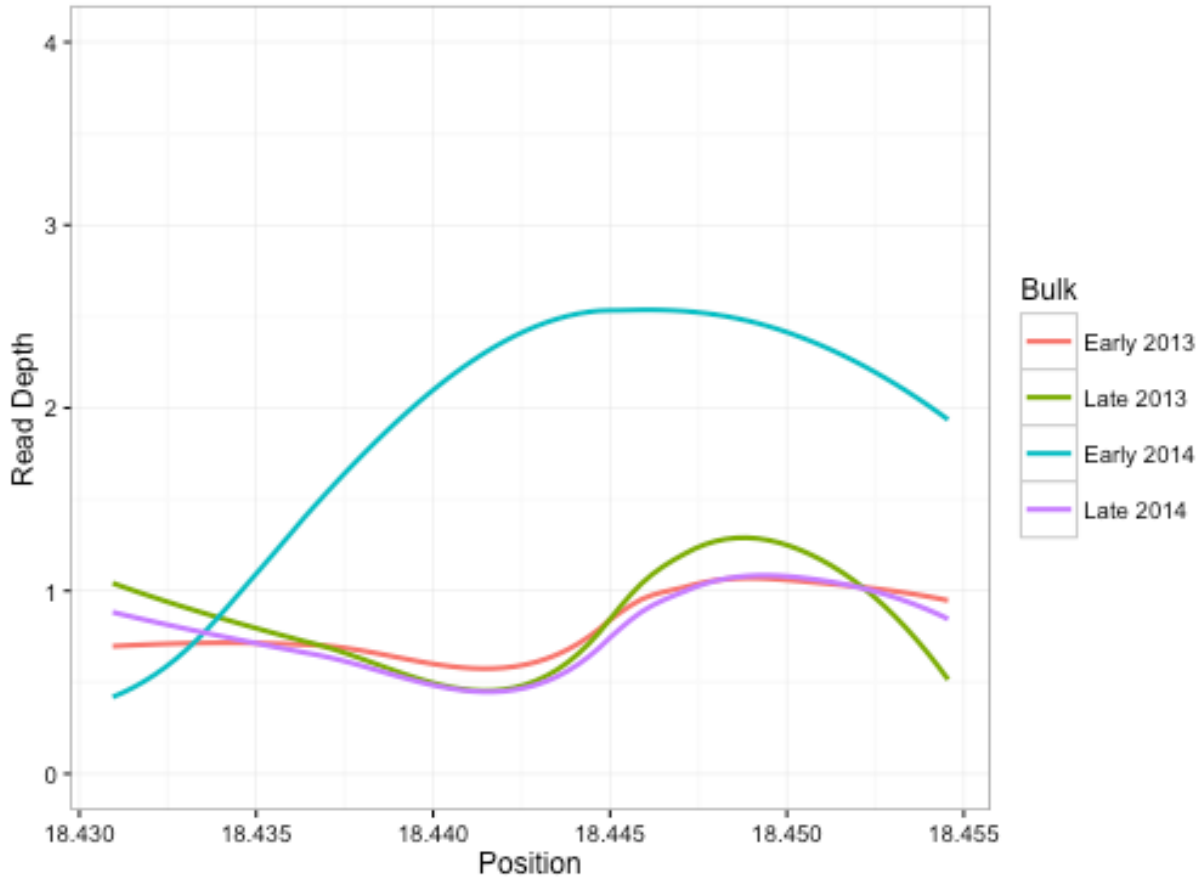

DISCUSSION:

Overview:

To what extent is the genomic variation in quantitative traits private to a particular population versus shared among neighboring populations? Within a population, how consistent are the components of variation from one generation to the next? These questions are fundamental, determining both the generality of genetic mapping studies as well as the repeatability of the evolutionary process. To address these questions, we develop a novel analytical method suitable to bulked-population samples (PoolSeq data). The application of this analysis elucidates genomic variation associated with flowering time in three natural populations of *M. guttatus*, identifying thousands of divergent sites broadly distributed throughout the genome.

The general picture that emerges is that the sites associated with flowering time are largely idiosyncratic to a particular population; however, these sites often reside in common regions. Given that loci identified by common QTL mapping methods are often megabases in size, mapping the segregating variation in any one of these populations would, therefore, likely identify a substantial portion of the loci or QTL contributing to variation in neighboring populations. It also follows the intuition that the response(s) of neighboring, natural populations to uniform selection will be highly polygenic, although the fixation of particular alleles or haplotypes may be idiosyncratic, and that the selection response may involve similar genetic pathways, even in the absence of recurrent migration and/or strong selection,

We find that idiosyncrasy with regard to divergence in allele frequency between early and late flowering plants applies across time as well, likely reflective of the temporal

environmental variation characteristic of this species' habitat. In fact, most of the significantly divergent sites that we identify are found in just one population and in one year (Quarry 2013). In the following paragraphs, we discuss the possible reasons and consequences for such spatial and temporal disparity in allelic divergence associated with flowering time and highlight several novel observations on the nature of this segregating variation.

Why does Δp_{EL} vary across time and space?

The observed variation of Δp_{EL} across time and space is likely a product of actual biological differences as well as statistical artifact. Regarding the latter, if many sites within a region show a weak association with flowering time, the sites where Δp_{EL} is overestimated will more likely be deemed significant and vice versa. This will generate the appearance that more sites are idiosyncratic to a particular population versus shared. This effect is exacerbated by the highly restrictive significance thresholds imposed by FDR adjustment on genomic datasets with millions of tests. Therefore, basing conclusions regarding idiosyncrasy solely on overlap of significance as in Figure 3.1D is not sufficient. Alternatively, one can consider whether sites deemed significant in one population tend to exhibit a similar sign and magnitude Δp_{EL} in other populations (Figure 3.2 and 3.3). Interestingly, the two years of this study exhibit opposite patterns with little to no correlation in Δp_{EL} across populations in 2013, but consistent positive correlations in 2014. Additionally, we find 8 overlapping significant sites in 2014 between IM and Q, whereas no overlapping sites were found in 2013 despite the vastly greater number of significant sites in 2013. This discrepancy between 2013 and 2014 directly relates to variation in Δp_{EL}

across time within each population as well. Most notably, vastly fewer sites were identified as significantly divergent between early and late flowering plants in 2014, and these were largely nonoverlapping with the significant sites from 2013 (only 18 in common between the two years). Together, this suggests an appreciable degree of idiosyncrasy with regard to sites associated with flowering time across both time and space and that the degree of idiosyncrasy of Δp_{EL} across space varies over time.

There are a number biological explanations for why Δp_{EL} might vary across time and space. Innumerable studies over the past few decades have demonstrated the context-dependent nature of allelic effects, both in terms of the genomic background and environmental conditions in which the allele is expressed. Gene-by-environment (GxE) interactions are a routine observation in QTL-based experiments and can be of appreciable magnitude relative to the marginal effect across environments (SCHEINER 1993; MARAIS *et al.* 2013). Despite the physical proximity of these populations, they differ consistently in a number of environmental variables that may generate a differential response on flowering time (e.g. edaphic substrate, water availability, aspect, etc.). The habitat of *M. guttatus* is also characterized by appreciable variation across years, which likely results in corresponding temporal variation in Δp_{EL}. This spatial and temporal variation in environment will directly generate variation in Δp_{EL} across time and space via GxE interactions, but also indirectly via genomic divergence resulting from local adaptation.

It is generally accepted that the genomic background in which an allele is expressed is often a critical determinant of that allele's effect. Divergence in allele frequency across

populations due to local adaptation or even simply drift processes results in a change in the relative representations of genomic backgrounds. In *M. guttatus,* several recent papers have demonstrated a major role of epistasis (i.e. genomic background) for the segregating variants affecting developmental and fitness components in IM (KELLY and MOJICA 2011; MONNAHAN and KELLY 2015a; MONNAHAN and KELLY 2015b). Even with the modest genomic differentiation among these populations, allele frequency differences would be expected to generate substantial variation in allelic effects (MONNAHAN and KELLY 2015a), and this will likely be exacerbated by elevated divergence among genes underlying local adaptation. The relevance of this last statement is evidenced by a previous study, in which we document the ability of local adaptation to maintain genomic divergence between Quarry and the other two populations despite recurrent migration (MONNAHAN *et al.* 2015a). Along with the aforementioned reasons, these differences in genomic background due to local adaptation are a likely explanation for some of the spatial variation in Δp_{EL} variation, although at this stage we are unable to quantify the relative contributions of these different sources.

What is the functional significance of Δp_{EL} sites?

Up until now, we have focused the discussion on the general patterns of significant tests and allele frequency differences. However, the most direct result from our data is a list of candidate genes in which we find one or more significantly divergent sites. For the test of Δp_{EL}, it is first worth considering what kind of genes we might expect to associate with natural differences in flowering time. Genes with direct effects on the flowering time pathway are expected to appear, but so too are genes with any indirect effects on flowering

time (e.g. germination time, growth-rate, etc.) or traits associated with flowering time. In our search of the *M. guttatus* annotation, ~3k of the significant Δp_{EL} sites were within annotated gene regions, and 56 of these genes correspond to flowering time gene homologs. Most interestingly, all populations surveyed exhibit segregating variation within both FLC and Frigida, which are two major flowering time genes known to interact to determine flowering time in natural populations of *A. thaliana* (CAICEDO et al. 2004). Δp_{EL} is significant in both of these genes in the Quarry population. Of the ~3k annotated gene regions, 13 had significant Δp_{EL} in both IM and Q. Interestingly, 7 of these 13 are annotated as "Histone Superfamily Protein", which generally refer to the core subunits of the actual histone proteins. Although there exist a set of 'universal' histone core subunits that exhibit extreme conservation among taxa, a number of histone core subunit variants have been described in various species with diverse regulatory, organizational, and epigenetic effects (TALBERT and HENIKOFF 2010). Our results suggest that histone variation may be a common source of developmental variation across populations. Additionally, both IM and Q show significant Δp_{EL} for GDSL-motif lipase 5, which belongs to a class of lipases with broad, ecologically-relevant functions including microbial defense (OH *et al.* 2005; KWON *et al.* 2009), morphogenesis and development (RIEMANN *et al.* 2007; LEE *et al.* 2009), and abiotic stress responses (HONG *et al.* 2007). While this gene may play a direct role in promoting/hindering development, it may just as well function in defense of a pest associated with early or late season conditions. Regardless, this list of genes provides a number of avenues for further investigation.

Our results also provide evidence that macro-mutations such as structural and copy number polymorphisms may be important determinants of natural variation in ecologically-relevant traits. A number of inversion polymorphisms have been identified in *M. guttatus* that differentiate annual and perennial ecotypes (LOWRY and WILLIS 2010; HOLESKI *et al.* 2014). The most well-studied of these, *DIV1*, is often a major distinguishing character between annual populations and both coastal and inland perennial ecotypes (LOWRY and WILLIS 2010). This is a large ~6 Mb paracentric inversion on the eighth chromosome containing hundreds of genes and exhibiting large effects on traits that differentiate annual/perennial ecotypes such as flowering time, anthocyanin production, and growth-related traits. To our knowledge, this is the first time in which this inversion has been found to be actively segregating in a natural population, and its presence confirms that the admixture of this population is of both annual and perennial origin. While segregating inversions have previously been shown to contribute to genetic (co)variation in natural *M. guttatus* populations (SCOVILLE *et al.* 2009; LEE *et al.* 2016), this is the first evidence that the inversion has originated via hybridization. Although the Quarry population is somewhat unique in its environment and phenotypic composition, there are certainly many other annual populations with overlapping environmental and phenotypic distributions in which a similar scenario could lead to maintenance of an inversion polymorphism, at least temporarily.

We also find evidence for copy number variation at several loci within both IM and Q populations as suggested by tracks of elevated read depth in certain samples. Interestingly, four of these regions are composed of histone core proteins (either h3 or h4),

suggesting that copy number variation in addition to allele frequency divergence in histones may underlie developmental variation in natural populations. The remaining region suggestive of a CNV also points to modifications of basic cellular processes. This region contains an RNA-ligase gene, which is involved in the maturation of tRNAs. Recently, it was discovered that mutants of a RNA-ligase gene in *Arabidopsis thaliana* exhibited defects, specifically, in auxin-related growth processes (LEITNER *et al.* 2015). Though one would expect a mutant in such a fundamental process as tRNA maturation would have innumerable abnormalities, reduced tRNA availability was shown to have specific effects on auxin distribution and signaling. While a CNV for RNA-ligase has a clearer link to flowering time variation via the link to the major plant morphogenesis hormone, all of the putative CNVs we identify suggest that modifications to basic cellular processes at least partly underlie natural variation in flowering time.

Role of population history

The Quarry population was established no more than 40 generations ago when a rock quarry fell into disuse and was subsequently colonized by nearby *Mimulus* (perhaps even by IM or BR). Patterns of linkage disequilibrium confirm that the population remains highly admixed (MONNAHAN *et al.* 2015a), which likely reflects both the young age of the population and continued immigration. The plants at Quarry are phenotypically striking and highly variable. Although there are many plants of the typical annual form, producing one main shoot and relatively few flowers, there are also many large, almost perennial-looking plants. These plants are highly branched, produce numerous flowers, and sometimes possess rhizomatous structures characteristic of perennials. There is a

relatively even gradation within Quarry between these two extreme forms. That this is a potential annual-perennial hybrid swarm is also suggested by the fact that an inversion on LG 8, characteristic of the perennial ecotype, seems to be segregating in the population. A founder event followed by mixing of diverse ecotypes could have provided a great deal of additive genetic variation in traits such as flowering time. Combined with the highly heterogeneous landscape that Quarry occupies, migrant alleles from BR and IM may be more likely to be maintained in this environment than in older, well-established populations such as BR and IM. This may explain why Quarry seems to share more variation with IM and BR than IM and BR share with each other.

The highly admixed nature of Quarry, and consequently high level of linkage disequilibrium, also presents considerable difficulties for interpreting some of our major results. Regardless of the population, many of the sites exhibiting significant Δp_{EL} are likely not causal but are due to linkage to a causal site. Although the young, admixed nature of Quarry might imply that much of the segregating variation in flowering time has yet to be fixed (resulting in more significant Δp_{EL} sites), the elevated LD will tend to inflate the number of significant tests in Quarry relative to the other populations. LD will also likely increase or exaggerate our observation in the temporal consistency of Δp_{EL} across the two years (Figure 3.5). Indeed, about half of the sites in Figure 3.4A are within the inversion on chromosome 8. That said, the remainder are relatively evenly dispersed throughout the genome and still vastly outnumber sites showing temporal consistency in IM. This would suggest that although some of the pattern of temporal consistency in Δp_{EL} is due to linkage, it is likely the case that there are simply more sites exhibiting a consistent difference

between early and late flowering plants. One may expect for this to be the case in a population that is a hybrid of annuals and perennials. The segregating alleles affecting flowering time are likely to have relatively large effects compared to the alleles segregating in IM, and therefore, may be more likely to end up in one or the other sampling pools. Additionally, these large effect alleles may be more resilient to environmental differences across years.

Conclusion:

The scale at which genomic variation in ecologically-relevant traits is shared across populations versus idiosyncratic has important implications for fundamental questions in evolutionary genetics such as the likelihood of parallel evolution at different scales as well as the generality of genetic mapping studies. Here, we find that despite populations sharing a great deal of standing variation, the variation associated with divergence in flowering time appears largely idiosyncratic at the scale of individual sites. However, much of this variation exists in common regions supporting the ability of mapping studies to identify important genomic regions. Throughout the course of our analysis, we identified many other interesting features of these populations that warrant future investigation. These include several candidate genes, some of which are suggestive of copy number variation as well as segregating inversions that likely arose via the hybridization of annual and perennial ecotypes.

Conclusion

In this dissertation, I provide a detailed characterization of the standing variation within and across multiple natural populations and describe the implications for evolution with regard to the response to natural selection. I find that epistasis plays an important role not only in determining an individual's phenotype, but also for the rate and genetic trajectory of evolution. Two populations experiencing uniform selection and possessing the exact same allelic variation will likely fix unique sets of alleles depending on the starting allele frequencies at interacting loci.

Indeed, looking across populations, it seems that, despite a great deal of shared polymorphism, the sites influencing within-population variation in flowering time are not shared across populations. Given widespread divergence in allele frequency across the genome for the surveyed populations, the idiosyncrasy of variants associated with flowering time may be the signature of epistasis as implied in the first two chapters of this dissertation. However, allelic effects that are determined by the environmental differences across populations could also drive this observation. Regardless, the cumulative message of this dissertation is one of idiosyncrasy with regard to the evolutionary trajectory as implied by observations of standing genetic variation in natural populations.

Although this is fascinating from an evolutionary point of view, it is somewhat unfortunate from a practical standpoint. Despite advances in genetic methodologies, statistical requirements to detect and characterize pairwise, and especially, higher order epistasis and to do so in multiple populations suggest that much of evolution will always retain an element of unpredictability.

Literature Cited

ÁLVAREZ-CASTRO, J. M., and Ö. CARLBORG, 2007 A unified model for functional and statistical epistasis and its application in quantitative trait loci analysis. Genetics **176:** 1151-1167.

BATES, D., M. MARTIN, B. BEN and S. WALKER, 2014 lme4: Linear mixed effects models using Eigen and S4.(R package v. 1.0–6), pp. See http://CRAN. R-project. org/package= lme4.

BLOOM, J. S., I. M. EHRENREICH, W. T. LOO, T.-L. V. LITE and L. KRUGLYAK, 2013 Finding the sources of missing heritability in a yeast cross. Nature **494:** 234-237.

BURKE, M. K., J. P. DUNHAM, P. SHAHRESTANI, K. R. THORNTON, M. R. ROSE *et al.*, 2010 Genome-wide analysis of a long-term evolution experiment with Drosophila. Nature **467:** 587-590.

CAICEDO, A. L., J. R. STINCHCOMBE, K. M. OLSEN, J. SCHMITT and M. D. PURUGGANAN, 2004 Epistatic interaction between Arabidopsis FRI and FLC flowering time genes generates a latitudinal cline in a life history trait. Proceedings of the National Academy of Sciences of the United States of America **101:** 15670-15675.

CARLBORG, O., and C. S. HALEY, 2004 Epistasis: too often neglected in complex trait studies? Nat Rev Genet **5:** 618-625.

CARLBORG, Ö., L. JACOBSSON, P. ÅHGREN, P. SIEGEL and L. ANDERSSON, 2006 Epistasis and the release of genetic variation during long-term selection. Nature genetics **38:** 418-420.

CARLBORG, Ö., S. KERJE, K. SCHÜTZ, L. JACOBSSON, P. JENSEN *et al.*, 2003 A global search reveals epistatic interaction between QTL for early growth in the chicken. Genome research **13:** 413-421.

CARTER, A. J. R., J. HERMISSON and T. F. HANSEN, 2005 The role of epistatic gene interactions in the response to selection and the evolution of evolvability. Theoretical Population Biology **68:** 179-196.

CHARLESWORTH, B., 2015 Causes of natural variation in fitness: Evidence from studies of Drosophila populations. Proceedings of the National Academy of Sciences**:** 201423275.

CHEVERUD, J. M., and E. J. ROUTMAN, 1995 Epistasis and its contribution to genetic variance components. Genetics **139:** 1455-1461.

COCKERHAM, C. C., 1954 An extension of the concept of partitioning hereditary variance for analysis of covariances among relatives when epistasis is present. Genetics **39:** 859.

COHAN, F. M., 1984a Can uniform selection retard random genetic divergence between isolated conspecific populations? Evolution**:** 495-504.

COHAN, F. M., 1984b Genetic divergence under uniform selection. I. Similarity among populations of Drosophila melanogaster in their responses to artificial selection for modifiers of ciD. Evolution**:** 55-71.

COLICCHIO, J. M., P. J. MONNAHAN, J. K. KELLY and L. C. HILEMAN, 2015 Gene expression plasticity resulting from parental leaf damage in Mimulus guttatus. New Phytologist **205:** 894-906.

COOLEY, ARIELLE M., JENNIFER L. MODLISZEWSKI, MEGAN L. ROMMEL and JOHN H. WILLIS, 2011 Gene Duplication in Mimulus Underlies Parallel Floral Evolution via Independent trans-Regulatory Changes. Current Biology **21:** 700-704.

CROW, J. F., 2010 On epistasis: why it is unimportant in polygenic directional selection. Philosophical Transactions of the Royal Society B: Biological Sciences **365:** 1241-1244.

FABIAN, D. K., M. KAPUN, V. NOLTE, R. KOFLER, P. S. SCHMIDT *et al.*, 2012 Genome-wide patterns of latitudinal differentiation among populations of Drosophila melanogaster from North America. Molecular Ecology **21:** 4748-4769.

FALCONER, D. S., T. F. MACKAY and R. FRANKHAM, 1996 Introduction to Quantitative Genetics (4th edn). Trends in Genetics **12:** 280.

FENSTER, C. B., and L. F. GALLOWAY, 2000 Inbreeding and Outbreeding Depression in Natural Populations of Chamaecrista fasciculata (Fabaceae)

Depresión por Endogamia y Exogamia en Poblaciones Naturales de Chamaecrista fasciculata (Fabaceae). Conservation Biology **14:** 1406-1412.

FISHER, R. A., 1919 XV.—The correlation between relatives on the supposition of Mendelian inheritance. Transactions of the royal society of Edinburgh **52:** 399-433.

FISHER, S. R. A., and E. B. FORD, 1947 *The spread of a gene in natural conditions in a colony of the moth Panaxia dominula L*. Oliver & Boyd.

FITTER, A., and R. FITTER, 2002 Rapid changes in flowering time in British plants. Science **296:** 1689-1691.

FLAGEL, L. E., J. H. WILLIS and T. J. VISION, 2014 The standing pool of genomic structural variation in a natural population of Mimulus guttatus. Genome biology and evolution **6:** 53-64.

GAUTIER, M., J. FOUCAUD, K. GHARBI, T. CÉZARD, M. GALAN *et al.*, 2013 Estimation of population allele frequencies from next-generation sequencing data: pool-versus individual-based genotyping. Molecular Ecology **22:** 3766-3779.

GIBSON, G., 1996 Epistasis and pleiotropy as natural properties of transcriptional regulation. Theoretical population biology **49:** 58-89.

GOODNIGHT, C. J., 1987 On the effect of founder events on epistatic genetic variance. Evolution**:** 80-91.

GRIFFING, B., 1960 Theoretical consequences of truncation selection based on the individual phenotype. Australian Journal of Biological Sciences **13:** 307-343.

HANSEN, T. F., 2006 The evolution of genetic architecture. Annual Review of Ecology, Evolution, and Systematics**:** 123-157.

HANSEN, T. F., 2013 Why epistasis is important for selection and adaptation. Evolution **67:** 3501-3511.

HAYES, B., A. CHAMBERLAIN, S. MACEACHERN, K. SAVIN, H. MCPARTLAN *et al.*, 2009 A genome map of divergent artificial selection between Bos taurus dairy cattle and Bos taurus beef cattle. Animal genetics **40:** 176-184.

HEDRICK, P. W., 1999 Antagonistic pleiotropy and genetic polymorphism: a perspective. Heredity **82:** 126-133.

HILL, W. G., M. E. GODDARD and P. M. VISSCHER, 2008 Data and theory point to mainly additive genetic variance for complex traits. PLoS Genetics **4:** e1000008.

HOLESKI, L. M., P. MONNAHAN, B. KOSEVA, N. MCCOOL, R. L. LINDROTH *et al.*, 2014 A high-resolution genetic map of yellow monkeyflower identifies chemical defense QTLs and recombination rate variation. G3: Genes| Genomes| Genetics **4:** 813-821.

HONG, J. K., H. W. CHOI, I. S. HWANG, D. S. KIM, N. H. KIM *et al.*, 2007 Function of a novel GDSL-type pepper lipase gene, CaGLIP1, in disease susceptibility and abiotic stress tolerance. Planta **227:** 539-558.

HUANG, W., S. RICHARDS, M. A. CARBONE, D. ZHU, R. R. ANHOLT *et al.*, 2012 Epistasis dominates the genetic architecture of Drosophila quantitative traits. Proceedings of the National Academy of Sciences **109:** 15553-15559.

JOHANSSON, A. M., M. E. PETTERSSON, P. B. SIEGEL and Ö. CARLBORG, 2010 Genome-Wide Effects of Long-Term Divergent Selection. PLoS Genet **6:** e1001188.

KELLY, J., 2008 Testing the rare-alleles model of quantitative variation by artificial selection. Genetica **132:** 187-198.

KELLY, J. K., 1999 Response to selection in partially self-fertilizing populations. I. Selection on a single trait. Evolution**:** 336-349.

KELLY, J. K., 2005 Epistasis in Monkeyflowers. Genetics **171:** 1917-1931.

KELLY, J. K., B. KOSEVA and J. P. MOJICA, 2013 The genomic signal of partial sweeps in Mimulus guttatus. Genome biology and evolution **5:** 1457-1469.

KELLY, J. K., and J. P. MOJICA, 2011 Interactions among flower-size QTL of Mimulus guttatus are abundant but highly variable in nature. Genetics **189:** 1461-1471.

KELLY, J. K., and S. WILLIAMSON, 2000 Predicting response to selection on a quantitative trait: a comparison between models for mixed-mating populations. Journal of theoretical biology **207:** 37-56.

KEMPTHORNE, O., 1954 The correlation between relatives in a random mating population. Proceedings of the Royal Society of London. Series B-Biological Sciences **143:** 103-113.

KIMURA, M., and J. F. CROW, 1978 Effect of overall phenotypic selection on genetic change at individual loci. Proceedings of the National Academy of Sciences **75:** 6168-6171.

KOFLER, R., A. J. BETANCOURT and C. SCHLÖTTERER, 2012 Sequencing of Pooled DNA Samples (Pool-Seq) Uncovers Complex Dynamics of Transposable Element Insertions in <italic>Drosophila melanogaster</italic>. PLoS Genet **8:** e1002487.

KROYMANN, J., and T. MITCHELL-OLDS, 2005 Epistasis and balanced polymorphism influencing complex trait variation. Nature **435:** 95-98.

KWON, S. J., H. C. JIN, S. LEE, M. H. NAM, J. H. CHUNG *et al.*, 2009 GDSL lipase‐like 1 regulates systemic resistance associated with ethylene signaling in Arabidopsis. The Plant Journal **58:** 235-245.

LAI, C.-Q., J. LEIPS, W. ZOU, J. F. ROBERTS, K. R. WOLLENBERG *et al.*, 2007 Speed-mapping quantitative trait loci using microarrays. Nature methods **4:** 839-841.

LE ROUZIC, A., 2014 Estimating directional epistasis. Frontiers in genetics **5**.

LEE, D. S., B. K. KIM, S. J. KWON, H. C. JIN and O. K. PARK, 2009 Arabidopsis GDSL lipase 2 plays a role in pathogen defense via negative regulation of auxin signaling. Biochemical and Biophysical Research Communications **379:** 1038-1042.

LEE, Y. W., L. FISHMAN, J. K. KELLY and J. H. WILLIS, 2016 Fitness Variation Is Generated by a Segregating Inversion in Yellow Monkeyflower (Mimulus guttatus). Genetics.

LEITNER, J., K. RETZER, N. MALENICA, R. BARTKEVICIUTE, D. LUCYSHYN *et al.*, 2015 Meta-regulation of Arabidopsis Auxin Responses Depends on tRNA Maturation. Cell Reports **11:** 516-526.

LI, Z., S. R. PINSON, W. D. PARK, A. H. PATERSON and J. W. STANSEL, 1997 Epistasis for three grain yield components in rice (Oryxa sativa L.). Genetics **145:** 453-465.
LOWRY, D. B., and J. H. WILLIS, 2010 A widespread chromosomal inversion polymorphism contributes to a major life-history transition, local adaptation, and reproductive isolation. PLoS biology **8:** 2227.
LUO, L., Y. MAO and S. XU, 2003 Correcting the bias in estimation of genetic variances contributed by individual QTL. Genetica **119:** 107-114.
LYNCH, M., and B. WALSH, 1998 *Genetics and analysis of quantitative traits*. Sinauer Sunderland, MA.
MAGWENE, P. M., J. H. WILLIS and J. K. KELLY, 2011 The statistics of bulk segregant analysis using next generation sequencing. PLoS Comput Biol **7:** e1002255.
MÄKI-TANILA, A., and W. G. HILL, 2014 Influence of gene interaction on complex trait variation with multilocus models. Genetics **198:** 355-367.
MAKOWSKY, R., N. M. PAJEWSKI, Y. C. KLIMENTIDIS, A. I. VAZQUEZ, C. W. DUARTE *et al.*, 2011 Beyond missing heritability: prediction of complex traits. PLoS genetics **7:** e1002051.
MALMBERG, R. L., S. HELD, A. WAITS and R. MAURICIO, 2005 Epistasis for fitness-related quantitative traits in Arabidopsis thaliana grown in the field and in the greenhouse. Genetics **171:** 2013-2027.
MARAIS, D. L. D., K. M. HERNANDEZ and T. E. JUENGER, 2013 Genotype-by-Environment Interaction and Plasticity: Exploring Genomic Responses of Plants to the Abiotic Environment. Annual Review of Ecology, Evolution, and Systematics **44:** 5-29.
MCGREGOR, A. P., V. ORGOGOZO, I. DELON, J. ZANET, D. G. SRINIVASAN *et al.*, 2007 Morphological evolution through multiple cis-regulatory mutations at a single gene. Nature **448:** 587-590.
MOJICA, J. P., and J. K. KELLY, 2010 Viability selection prior to trait expression is an essential component of natural selection. Proceedings of the Royal Society B: Biological Sciences**:** rspb20100568.
MOJICA, J. P., Y. W. LEE, J. H. WILLIS and J. K. KELLY, 2012 Spatially and temporally varying selection on intrapopulation quantitative trait loci for a life history trade‐off in Mimulus guttatus. Molecular ecology **21:** 3718-3728.
MONNAHAN, P. J., J. COLICCHIO and J. K. KELLY, 2015a A genomic selection component analysis characterizes migration-selection balance. Evolution**:** n/a-n/a.
MONNAHAN, P. J., J. COLICCHIO and J. K. KELLY, 2015b A genomic selection component analysis characterizes migration‐selection balance. Evolution **69:** 1713-1727.
MONNAHAN, P. J., and J. K. KELLY, 2015a Epistasis Is a Major Determinant of the Additive Genetic Variance in <italic>Mimulus guttatus</italic>. PLoS Genet **11:** e1005201.
MONNAHAN, P. J., and J. K. KELLY, 2015b *Naturally segregating loci exhibit epistasis for fitness*.
MOORE, J. H., 2003 The ubiquitous nature of epistasis in determining susceptibility to common human diseases. Human heredity **56:** 73-82.
MOYLE, L. C., and T. NAKAZATO, 2009 Complex Epistasis for Dobzhansky–Muller Hybrid Incompatibility in Solanum. Genetics **181:** 347-351.
OH, I. S., A. R. PARK, M. S. BAE, S. J. KWON, Y. S. KIM *et al.*, 2005 Secretome Analysis Reveals an Arabidopsis Lipase Involved in Defense against Alternaria brassicicola. The Plant Cell **17:** 2832-2847.

OROZCO‐TERWENGEL, P., M. KAPUN, V. NOLTE, R. KOFLER, T. FLATT *et al.*, 2012 Adaptation of Drosophila to a novel laboratory environment reveals temporally heterogeneous trajectories of selected alleles. Molecular ecology **21:** 4931-4941.

OTTO, S. P., and M. W. FELDMAN, 1997 Deleterious mutations, variable epistatic interactions, and the evolution of recombination. Theoretical population biology **51:** 134-147.

PHILLIPS, P. C., 2008 Epistasis [mdash] the essential role of gene interactions in the structure and evolution of genetic systems. Nat Rev Genet **9:** 855-867.

PHILLIPS, P. C., S. P. OTTO and M. C. WHITLOCK, 2000 Beyond the average. Epistasis and the evolutionary process**:** 20-38.

REMOLINA, S. C., P. L. CHANG, J. LEIPS, S. V. NUZHDIN and K. A. HUGHES, 2012 GENOMIC BASIS OF AGING AND LIFE‐HISTORY EVOLUTION IN DROSOPHILA MELANOGASTER. Evolution **66:** 3390-3403.

RIEMANN, M., C. GUTJAHR, A. KORTE, M. RIEMANN, B. DANGER *et al.*, 2007 GER1, a GDSL Motif-Encoding Gene from Rice is a Novel Early Light- and Jasmonate-Induced Gene. Plant Biology **9:** 32-40.

SCARCELLI, N., and P. X. KOVER, 2009 Standing genetic variation in FRIGIDA mediates experimental evolution of flowering time in Arabidopsis. Molecular ecology **18:** 2039-2049.

SCHEINER, S. M., 1993 Genetics and evolution of phenotypic plasticity. Annual review of ecology and systematics**:** 35-68.

SCOVILLE, A., Y. W. LEE, J. H. WILLIS and J. K. KELLY, 2009 Contribution of chromosomal polymorphisms to the G‐matrix of Mimulus guttatus. New Phytologist **183:** 803-815.

SHIMOMURA, K., S. S. LOW-ZEDDIES, D. P. KING, T. D. STEEVES, A. WHITELEY *et al.*, 2001 Genome-wide epistatic interaction analysis reveals complex genetic determinants of circadian behavior in mice. Genome research **11:** 959-980.

SIMÕES, P., J. SANTOS, I. FRAGATA, L. D. MUELLER, M. R. ROSE *et al.*, 2008 How repeatable is adaptive evolution? The role of geographical origin and founder effects in laboratory adaptation. Evolution **62:** 1817-1829.

TALBERT, P. B., and S. HENIKOFF, 2010 Histone variants—ancient wrap artists of the epigenome. Nature reviews Molecular cell biology **11:** 264-275.

TOBLER, R., S. U. FRANSSEN, R. KOFLER, P. OROZCO-TERWENGEL, V. NOLTE *et al.*, 2014 Massive habitat-specific genomic response in D. melanogaster populations during experimental evolution in hot and cold environments. Molecular biology and evolution **31:** 364-375.

TURNER, T. L., A. D. STEWART, A. T. FIELDS, W. R. RICE and A. M. TARONE, 2011 Population-Based Resequencing of Experimentally Evolved Populations Reveals the Genetic Basis of Body Size Variation in <italic>Drosophila melanogaster</italic>. PLoS Genet **7:** e1001336.

VAN DER VEEN, J., 1959 Tests of non-allelic interaction and linkage for quantitative characters in generations derived from two diploid pure lines. Genetica **30:** 201-232.

WADE, M., 2002 A gene's eye view of epistasis, selection and speciation. Journal of Evolutionary Biology **15:** 337-346.

WADE, M. J., and C. J. GOODNIGHT, 1998 Perspective: the theories of Fisher and Wright in the context of metapopulations: when nature does many small experiments. Evolution**:** 1537-1553.

WALSH, B., 2004 Population-and quantitative-genetic models of selection limits. Plant breeding reviews **24:** 177-226.

WEIR, B., and C. C. COCKERHAM, 1977 *Two-locus theory in quantitative genetics*. North Carolina State University. Institute of Statistics.

WILLETT, C., 2011 The nature of interactions that contribute to postzygotic reproductive isolation in hybrid copepods. Genetica **139:** 575-588.

WILLIS, J. H., 1999 The Role of Genes of Large Effect on Inbreeding Depression in Mimulus guttatus. Evolution **53:** 1678-1691.

WOLF, J. B., E. D. BRODIE and M. J. WADE, 2000 *Epistasis and the evolutionary process*. Oxford University Press.

WU, C., D. LOWRY, A. COOLEY, K. WRIGHT, Y. LEE *et al.*, 2007 Mimulus is an emerging model system for the integration of ecological and genomic studies. Heredity **100:** 220-230.

ZUK, O., E. HECHTER, S. R. SUNYAEV and E. S. LANDER, 2012 The mystery of missing heritability: Genetic interactions create phantom heritability. Proceedings of the National Academy of Sciences **109:** 1193-1198.

Appendix 1—List of diagnostic markers used to determine genotype at each locus.

QTL name	Linkage Group	Diagnostic Marker
x10a	10	MgSTS 70, MgSTS 82
X9	9	MgSTS 523
X1	1	MgSTS 757, MgSTS 198
X5a	5	MgSTS 40
X5b	5	MgSTS 641/764, MgSTS 385
X10b	10	MgSTS 308
X8	8	MgSTS 432, MgSTS 736, MgSTS 31

Appendix 2—Estimated additive and dominance genetic effects for each locus and for each trait. * = 0.1 > p > 0.01 ; ** = 0.01 > p >0.001 ; *** = p < 0.001. The p-value correspond to a test of the null hypothesis that the term is equal to 0.

QTL	Parameter	Corolla Width (**CW**)	Pistil Length (**Pist**)	Days to Flower (**DTF**)	Stigma-Anther Separation (**SA**)
x10a	a	0.009	-0.152**	0.101	0.018
	d	0.654***	0.17*	-0.004	-0.051
x9	a	0.404***	0.285***	0.166	0.268***
	d	0.108	0.388***	-0.111	-0.034
x1	a	-0.076	-0.099*	0.144	0.09***
	d	0.109	-0.166*	-0.051	-0.083
x5a	a	0.191*	-0.064	-0.598**	0.017
	d	-0.04	-0.102	-0.022	-0.025
x5b	a	-0.575***	-0.037	0.227	-0.023
	d	0.092	0.034	0.367	-0.076
x10b	a	0.362***	0.187***	0.371*	-0.043
	d	0.794***	-0.106	0.111	0.03
x8	a	-0.119	-0.227***	0.24	0.019
	d	0.313*	0.189*	0.181	0.056

Appendix 3—Estimates of the four epistatic terms for each QTL pair and their significance (H_0: term is equal to 0). * = 0.1 > p > 0.01 ; ** = 0.01 > p >0.001 ; *** = p < 0.001

QTL Pair	Parameter	**CW**	**Pistil**	**DTF**	**SA**
x10a & x1	aa	-0.035	0.099*	0.172	-0.015
	ad	0.171	0.177*	-0.49	-0.013
	da	-0.162	0.009	-0.52	-0.033
	dd	-0.027	-0.048	1.083	0.085
x10a & x5a	aa	-0.02	0.005	-0.039	0.005
	ad	0.436**	0.236*	-0.296	0.094*
	da	-0.058	0.02	-0.256	0.119*
	dd	-0.529	-0.259	-0.585	0.047
x10a & x5b	aa	0.181*	0.136*	-0.285	0.081**
	ad	0.246	0.092	0.03	0.052
	da	-0.027	-0.038	-0.343	0.041
	dd	-0.071	0.186	-0.21	0.266*
x10a & x8	aa	-0.04	-0.017	-0.184	-0.043*
	ad	0.012	0.113	-0.825**	-0.014
	da	0.068	0.19*	-0.887**	0.076
	dd	-0.49	-0.361*	0.563	-0.012
x9 & x1	aa	0.095	0.102*	0.063	0.106***
	ad	-0.217	0.015	-0.316	0.118*
	da	0.269	0.035	-0.7*	-0.048
	dd	0.194	0.026	0.268	0.15
x9 & x5a	aa	-0.089	-0.09*	0.066	-0.085**
	ad	-0.048	0.107	-0.309	-0.032
	da	0.297	0.11	-0.046	0.094
	dd	0.112	-0.194	0.69	0.045
x9 & x5b	aa	-0.14*	-0.034	-0.096	-0.068**
	ad	0.121	0.263**	-0.365	0.064
	da	-0.045	-0.128	0.141	-0.109*
	dd	0.201	-0.237	0.247	-0.06
x9 & x8	aa	-0.015	0.149**	-0.403*	-0.002
	ad	-0.254	-0.156	0.214	-0.1*
	da	0.161	-0.091	0.481	0.044
	dd	0.207	-0.055	-0.903	0.273*
x1 & x5b	aa	0.084	0.026	0.223	-0.027
	ad	-0.05	0.066	-0.631*	-0.038
	da	-0.179	0.024	0.213	-0.008
	dd	-0.337	0.024	-0.558	0.135
x1 & x10b	aa	-0.045	-0.027	-0.283*	-0.045*

	ad	-0.179	-0.192*	0.436	-0.029
	da	-0.118	-0.147	-0.071	0.078
	dd	-0.279	-0.196	-0.415	-0.117
x10b & x8	aa	-0.158*	-0.14**	-0.242	0.048*
	ad	0.23	0.092	0.01	0.004
	da	-0.256	0.031	-0.064	-0.083
	dd	-0.681*	-0.116	0.204	-0.058

Appendix 4—Full collection of graphs equivalent to Figure 1.1 for each pair of loci. Trait values (in mm's) for selected DNILs as deviations from the reference genotype (IM767) estimated by the linear model. Genotypic mean values are given by bars, whereas non-epistatic values are given by the X's.

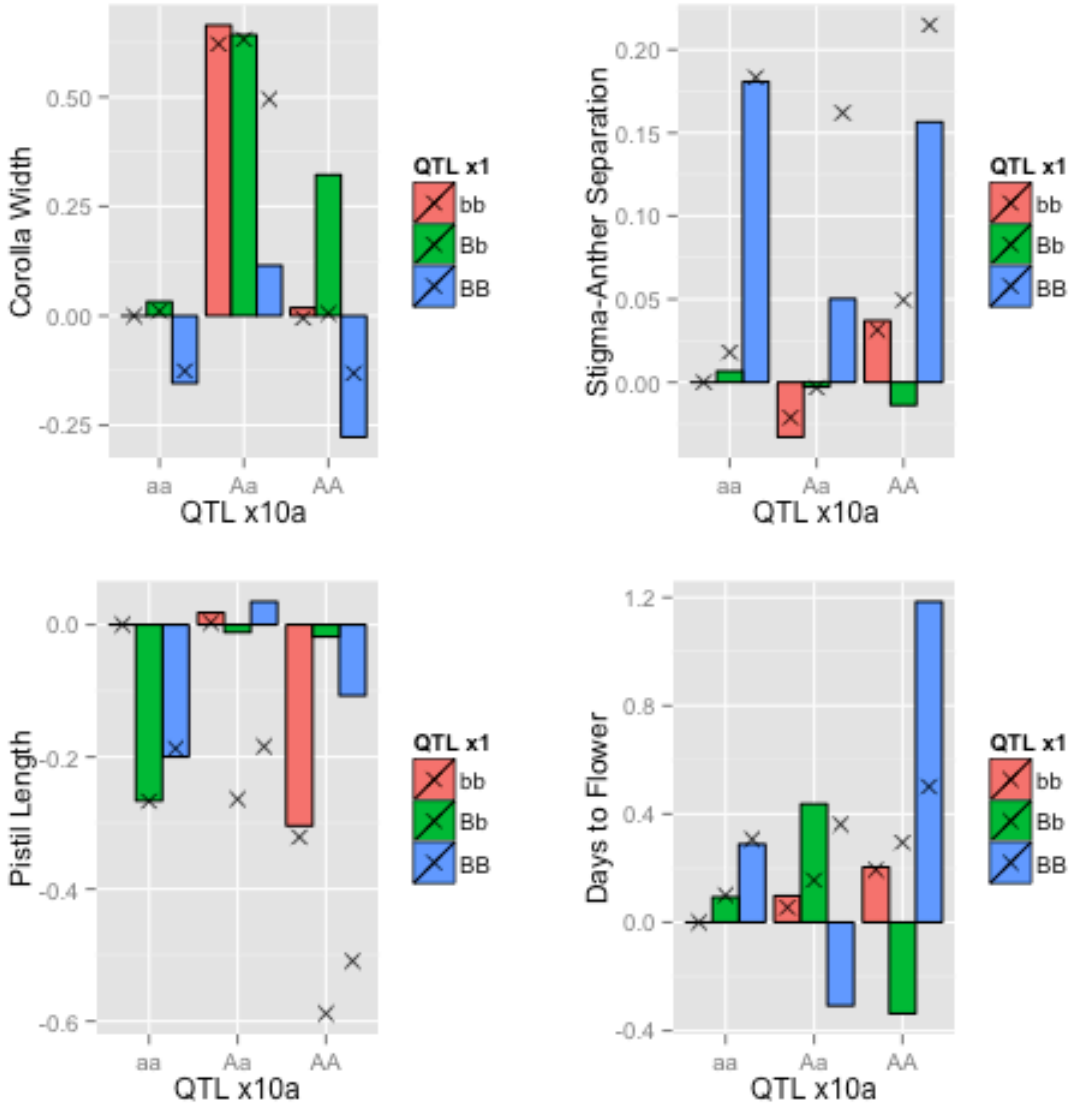

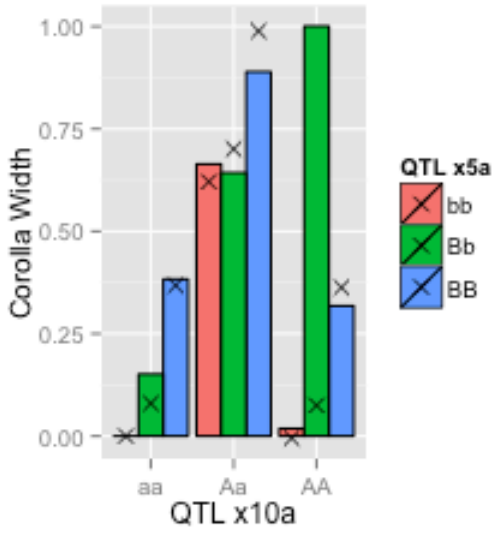
Corolla Width
1.00
0.75
0.50
0.25
0.00
aa
Aa
AA
QTL x10a
QTL x5a
bb
Bb
BB

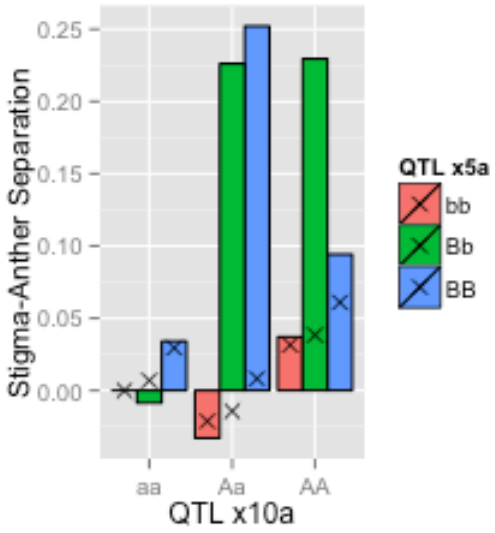
Stigma-Anther Separation
0.25
0.20
0.15
0.10
0.05
0.00
aa
Aa
AA
QTL x10a
QTL x5a
bb
Bb
BB

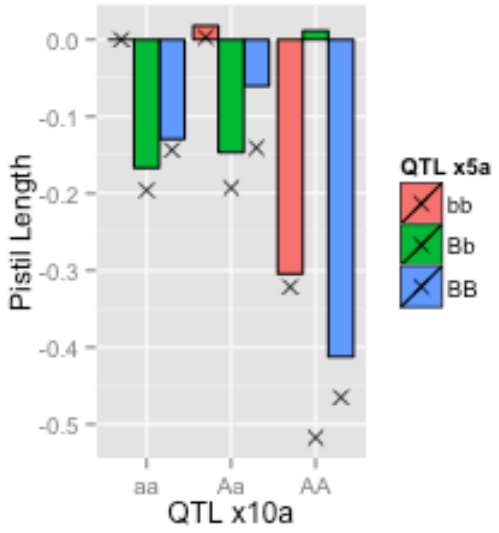
Pistil Length
0.0
-0.1
-0.2
-0.3
-0.4
-0.5
aa
Aa
AA
QTL x10a
QTL x5a
bb
Bb
BB

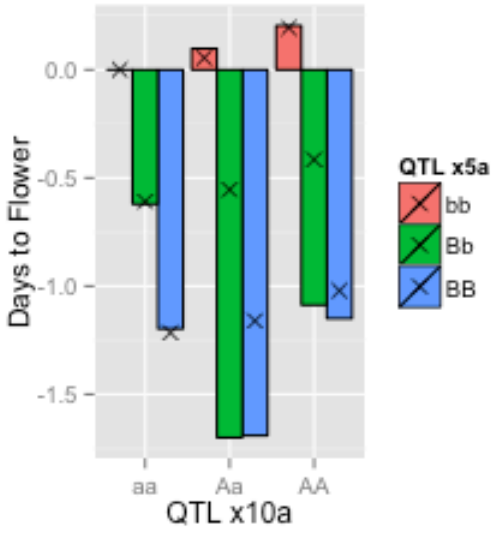
Days to Flower
0.0
-0.5
-1.0
-1.5
aa
Aa
AA
QTL x10a
QTL x5a
bb
Bb
BB

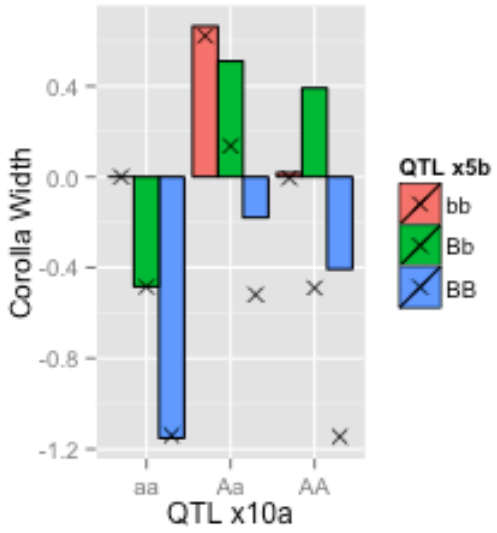
Corolla Width
0.4
0.0
-0.4
-0.8
-1.2
aa
Aa
AA
QTL x10a
QTL x5b
bb
Bb
BB

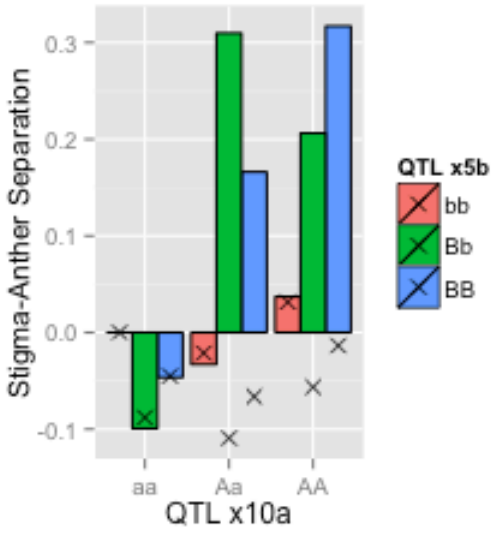
Stigma-Anther Separation
0.3
0.2
0.1
0.0
-0.1
aa
Aa
AA
QTL x10a
QTL x5b
bb
Bb
BB

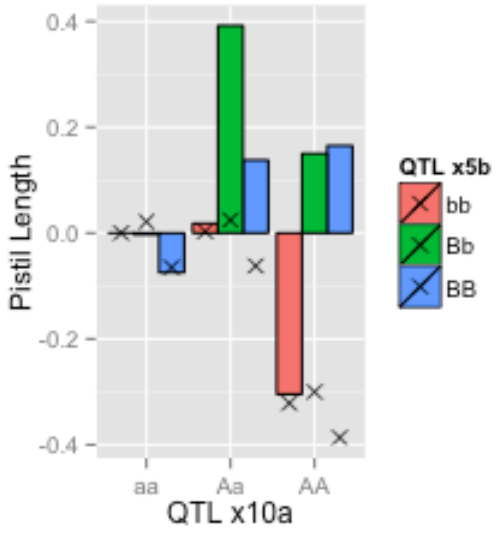
Pistil Length
0.4
0.2
0.0
-0.2
-0.4
aa
Aa
AA
QTL x10a
QTL x5b
bb
Bb
BB

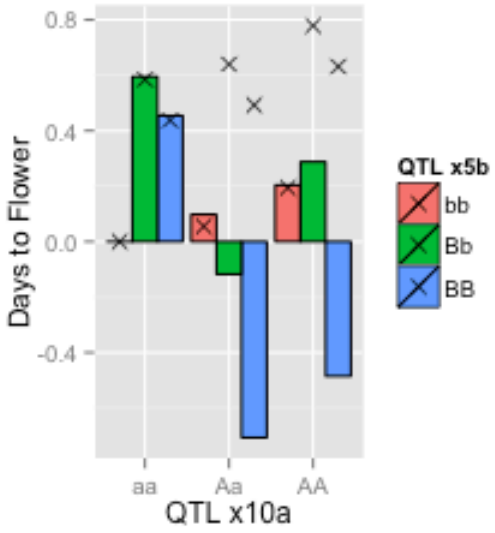
Days to Flower
0.8
0.4
0.0
-0.4
aa
Aa
AA
QTL x10a
QTL x5b
bb
Bb
BB

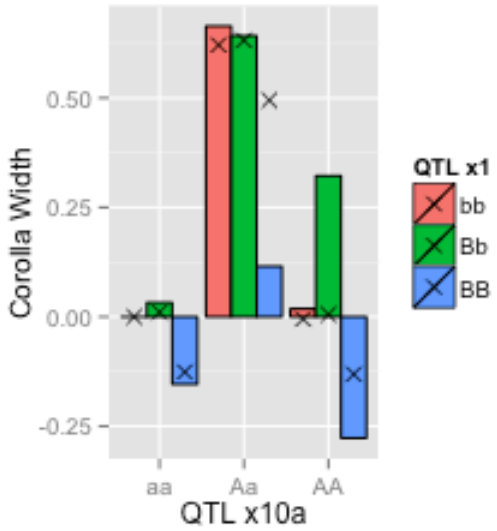
Corolla Width
0.50
0.25
0.00
-0.25
aa
Aa
AA
QTL x10a
QTL x1
bb
Bb
BB

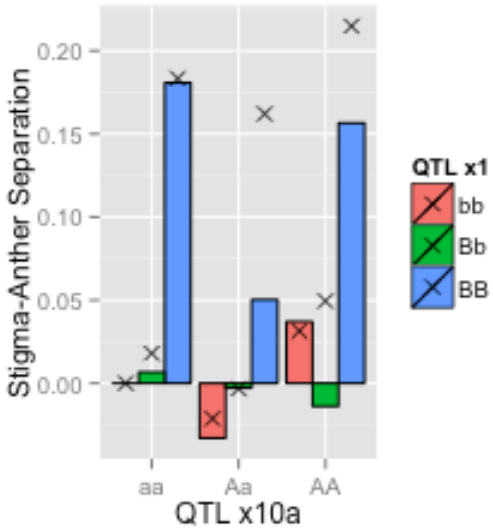
Stigma-Anther Separation
0.20
0.15
0.10
0.05
0.00
aa
Aa
AA
QTL x10a
QTL x1
bb
Bb
BB

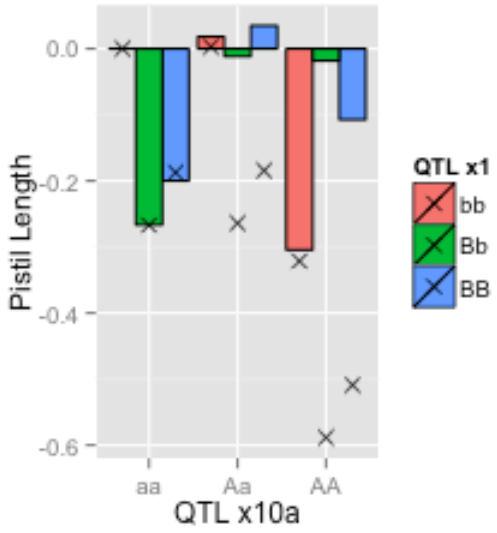
Pistil Length
0.0
-0.2
-0.4
-0.6
aa
Aa
AA
QTL x10a
QTL x1
bb
Bb
BB

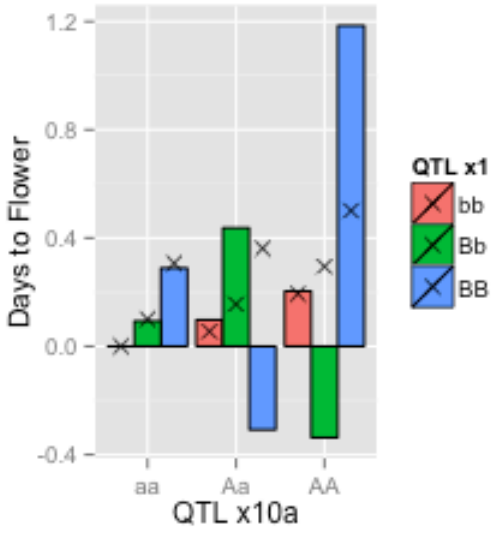
Days to Flower
1.2
0.8
0.4
0.0
-0.4
aa
Aa
AA
QTL x10a
QTL x1
bb
Bb
BB

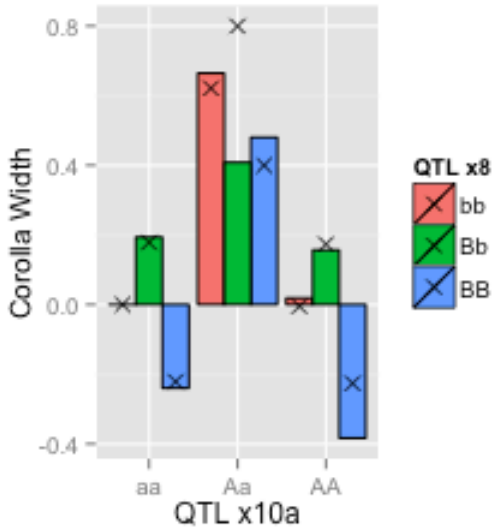
Corolla Width
0.8
0.4
0.0
-0.4
aa
Aa
AA
QTL x10a
QTL x8
bb
Bb
BB

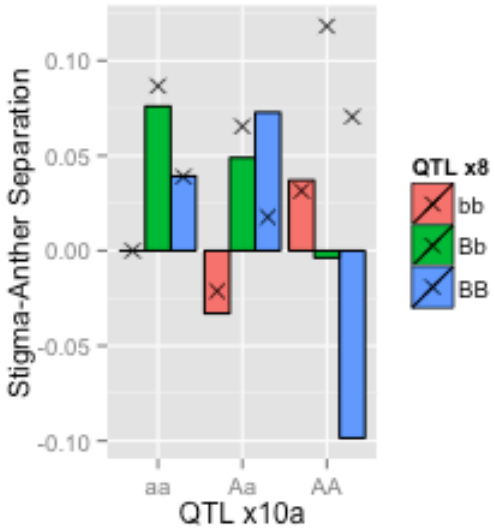
Stigma-Anther Separation
0.10
0.05
0.00
-0.05
-0.10
aa
Aa
AA
QTL x10a
QTL x8
bb
Bb
BB

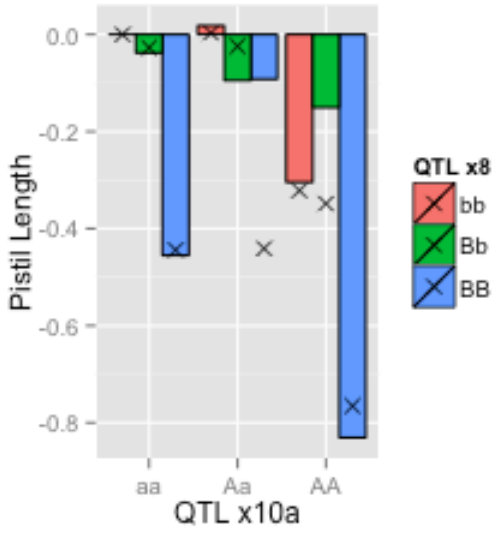
Pistil Length
0.0
-0.2
-0.4
-0.6
-0.8
aa
Aa
AA
QTL x10a
QTL x8
bb
Bb
BB

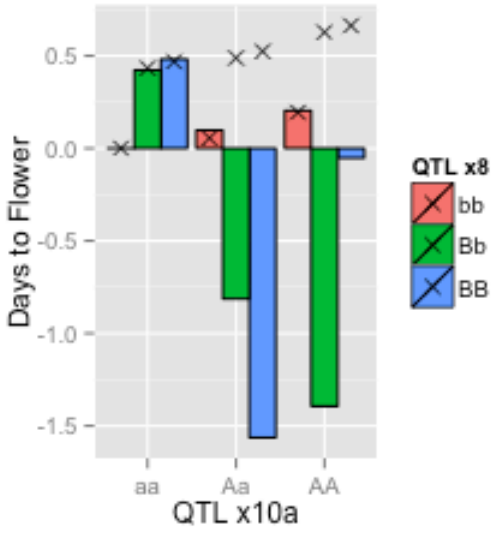
Days to Flower
0.5
0.0
-0.5
-1.0
-1.5
aa
Aa
AA
QTL x10a
QTL x8
bb
Bb
BB

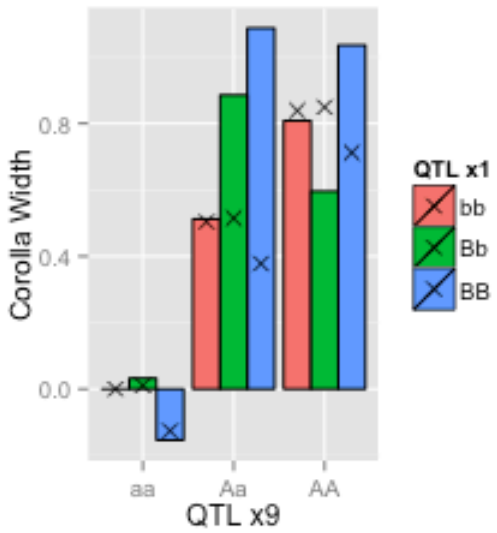
Corolla Width
0.8
0.4
0.0
aa
Aa
AA
QTL x9
QTL x1
bb
Bb
BB

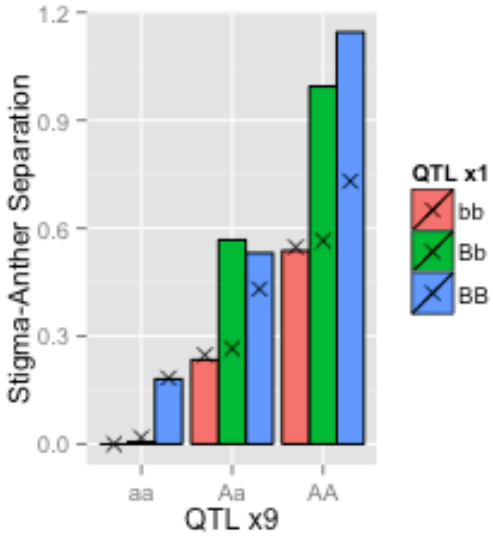
Stigma-Anther Separation
1.2
0.9
0.6
0.3
0.0
aa
Aa
AA
QTL x9
QTL x1
bb
Bb
BB

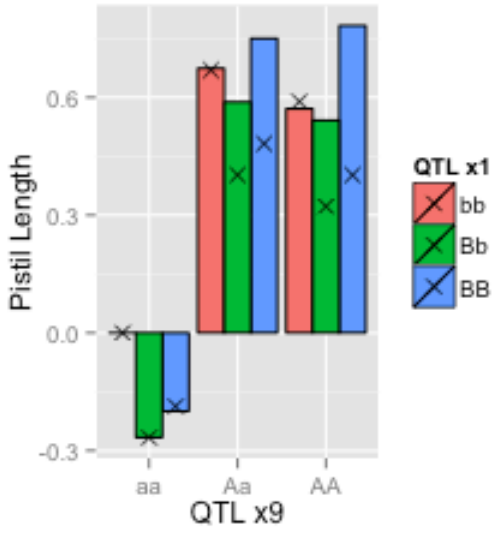
Pistil Length
0.6
0.3
0.0
-0.3
aa
Aa
AA
QTL x9
QTL x1
bb
Bb
BB

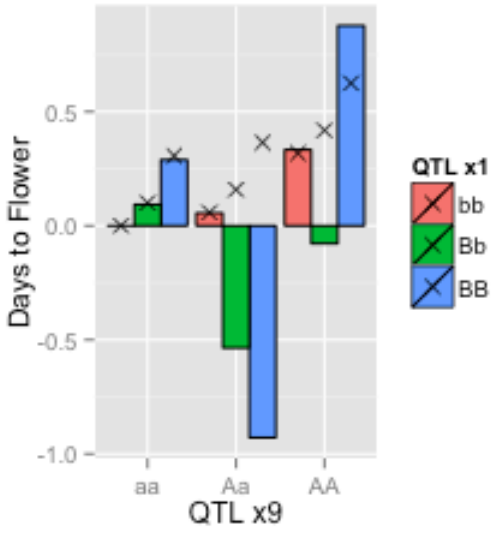
Days to Flower
0.5
0.0
-0.5
-1.0
aa
Aa
AA
QTL x9
QTL x1
bb
Bb
BB

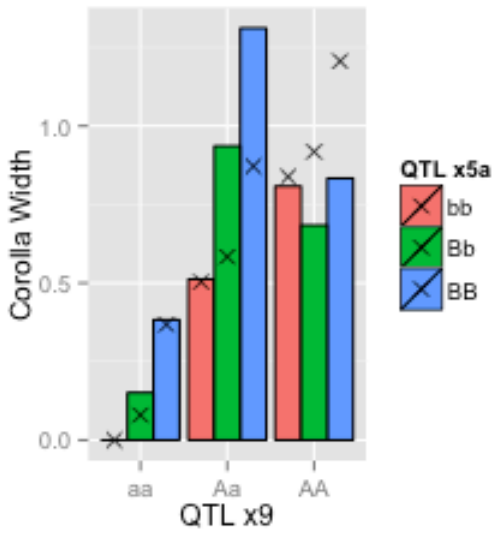
Corolla Width
1.0
0.5
0.0
aa
Aa
AA
QTL x9
QTL x5a
bb
Bb
BB

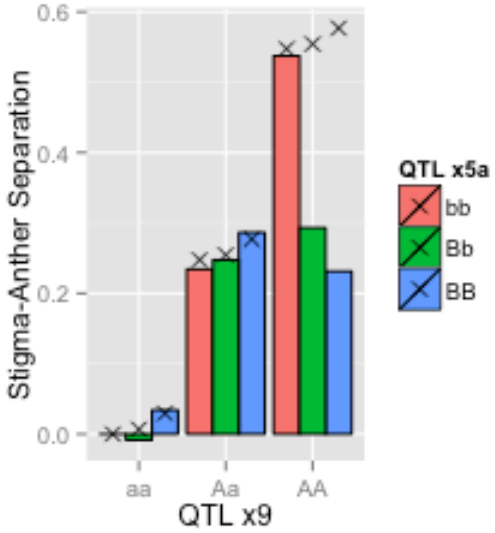
Stigma-Anther Separation
0.6
0.4
0.2
0.0
aa
Aa
AA
QTL x9
QTL x5a
bb
Bb
BB

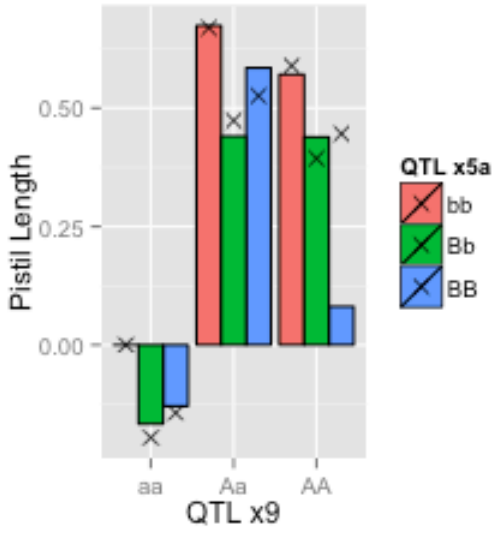
Pistil Length
0.50
0.25
0.00
aa
Aa
AA
QTL x9
QTL x5a
bb
Bb
BB

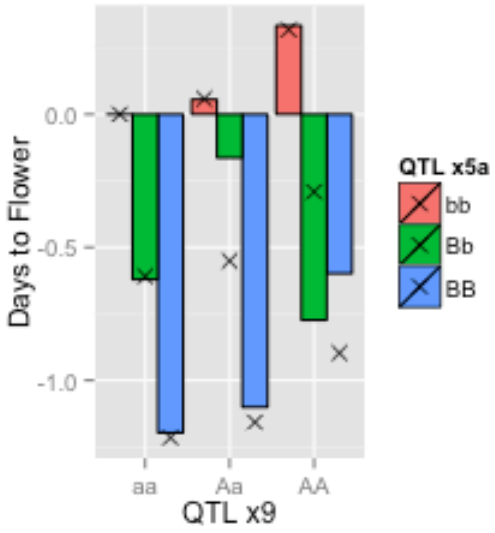
Days to Flower
0.0
-0.5
-1.0
aa
Aa
AA
QTL x9
QTL x5a
bb
Bb
BB

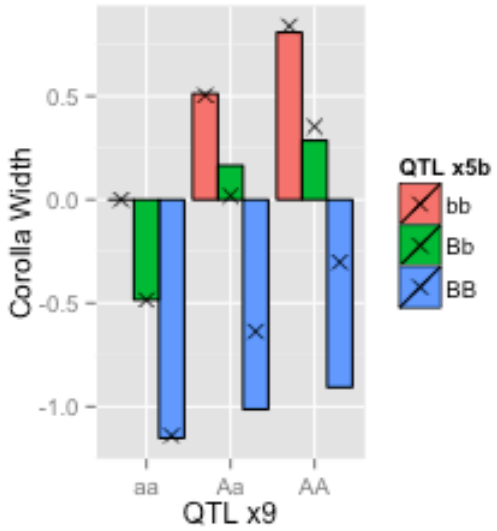
Corolla Width
0.5
0.0
-0.5
-1.0
aa
Aa
AA
QTL x9
QTL x5b
bb
Bb
BB

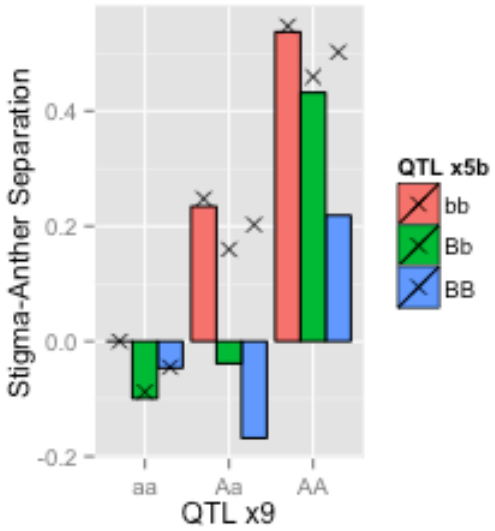
Stigma-Anther Separation
0.4
0.2
0.0
-0.2
aa
Aa
AA
QTL x9
QTL x5b
bb
Bb
BB

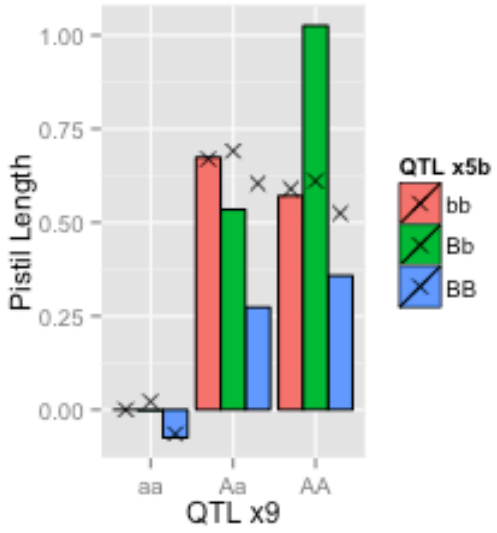
Pistil Length
1.00
0.75
0.50
0.25
0.00
aa
Aa
AA
QTL x9
QTL x5b
bb
Bb
BB

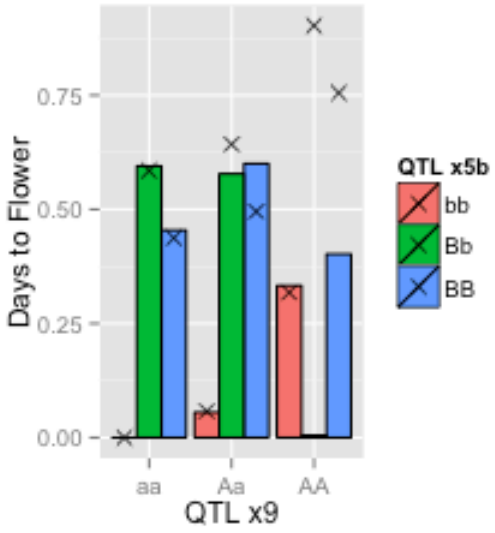
Days to Flower
0.75
0.50
0.25
0.00
aa
Aa
AA
QTL x9
QTL x5b
bb
Bb
BB

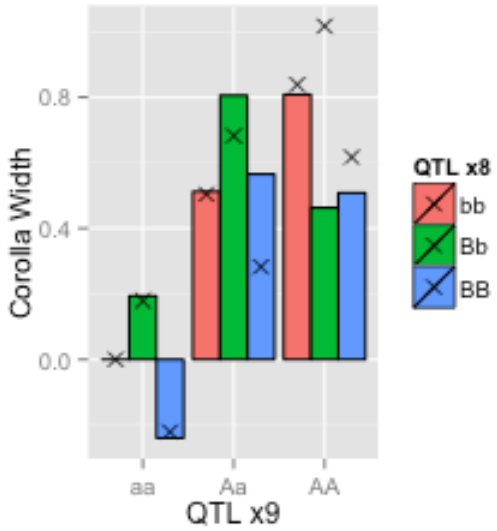
Corolla Width
0.8
0.4
0.0
aa
Aa
AA
QTL x9
QTL x8
bb
Bb
BB

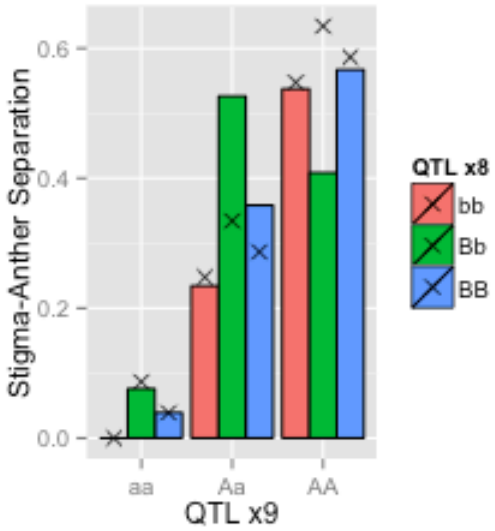
Stigma-Anther Separation
0.6
0.4
0.2
0.0
aa
Aa
AA
QTL x9
QTL x8
bb
Bb
BB

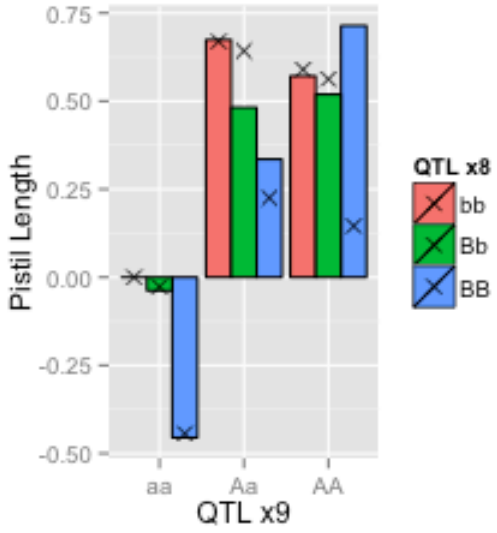
Pistil Length
0.75
0.50
0.25
0.00
-0.25
-0.50
aa
Aa
AA
QTL x9
QTL x8
bb
Bb
BB

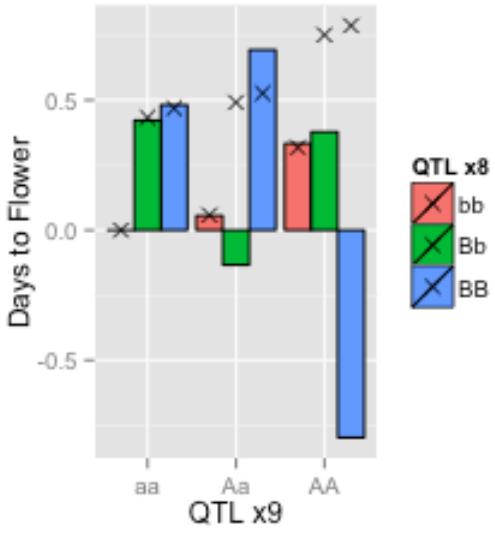
Days to Flower
0.5
0.0
-0.5
aa
Aa
AA
QTL x9
QTL x8
bb
Bb
BB

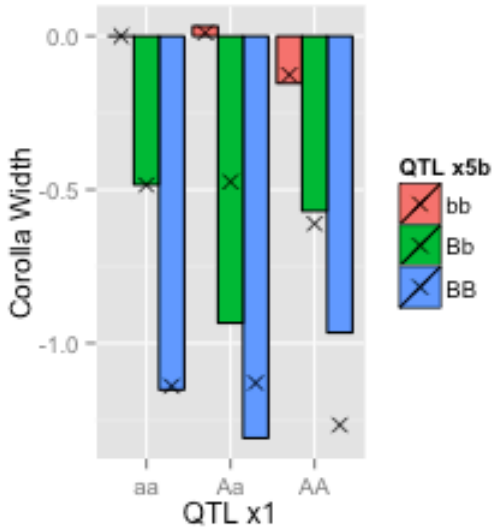
Corolla Width
0.0
-0.5
-1.0
aa
Aa
AA
QTL x1
QTL x5b
bb
Bb
BB

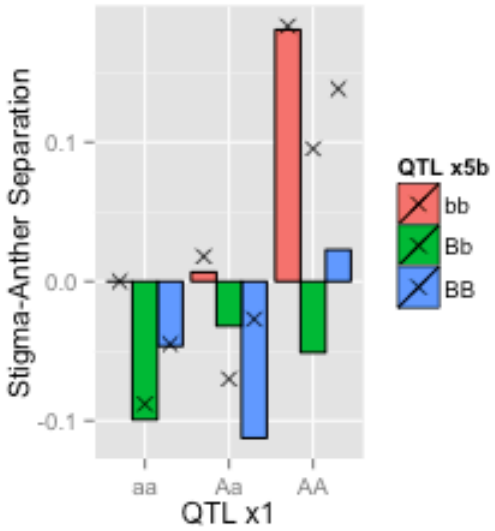
Stigma-Anther Separation
0.1
0.0
-0.1
aa
Aa
AA
QTL x1
QTL x5b
bb
Bb
BB

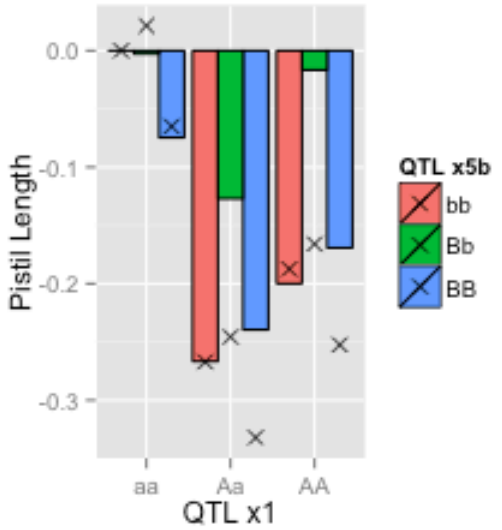
Pistil Length
0.0
-0.1
-0.2
-0.3
aa
Aa
AA
QTL x1
QTL x5b
bb
Bb
BB

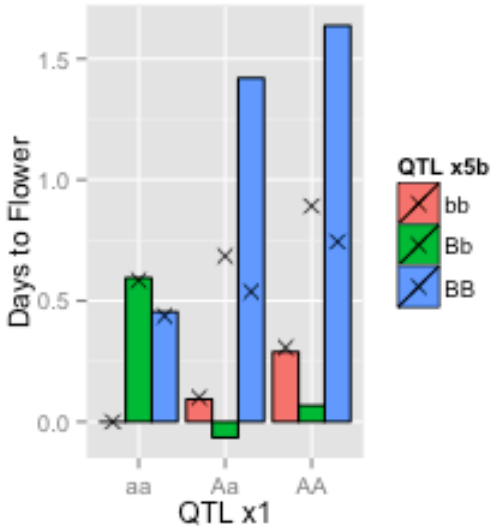
Days to Flower
1.5
1.0
0.5
0.0
aa
Aa
AA
QTL x1
QTL x5b
bb
Bb
BB

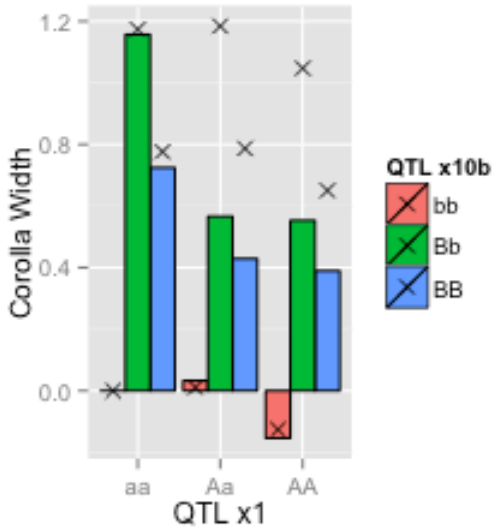
Corolla Width
1.2
0.8
0.4
0.0
aa
Aa
AA
QTL x1
QTL x10b
bb
Bb
BB

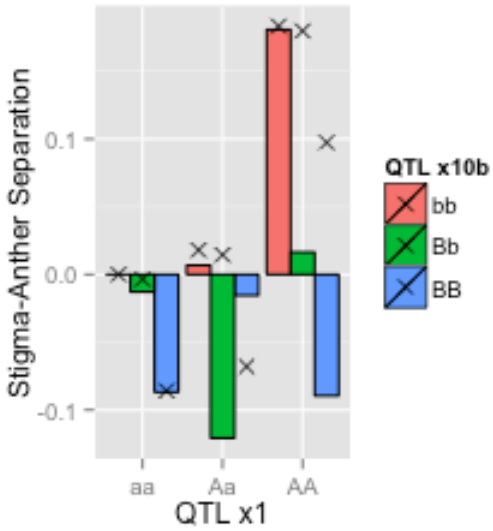
Stigma-Anther Separation
0.1
0.0
-0.1
aa
Aa
AA
QTL x1
QTL x10b
bb
Bb
BB

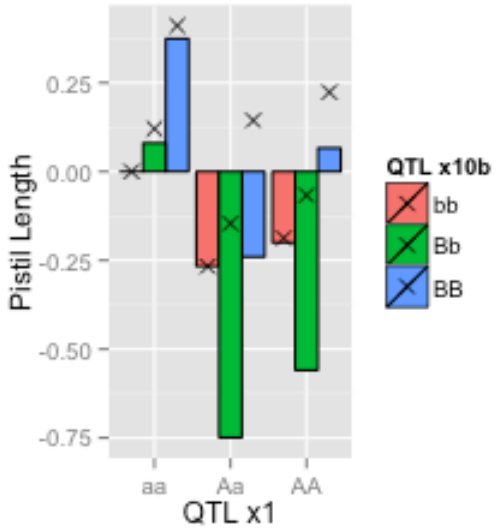
Pistil Length
0.25
0.00
-0.25
-0.50
-0.75
aa
Aa
AA
QTL x1
QTL x10b
bb
Bb
BB

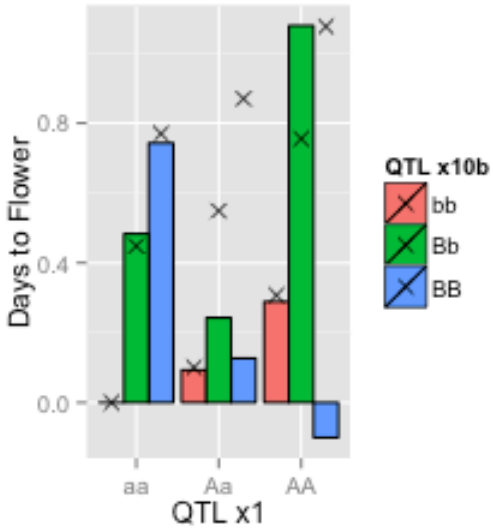
Days to Flower
0.8
0.4
0.0
aa
Aa
AA
QTL x1
QTL x10b
bb
Bb
BB

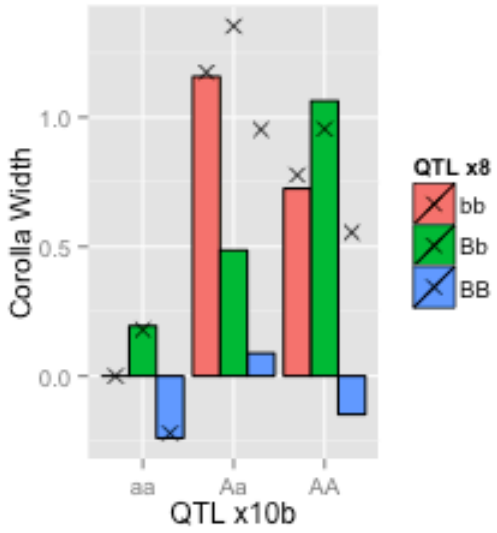
Corolla Width
1.0
0.5
0.0
aa
Aa
AA
QTL x10b
QTL x8
bb
Bb
BB

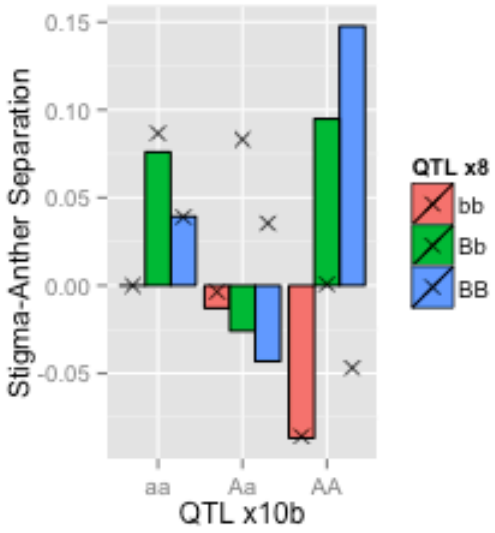
Stigma-Anther Separation
0.15
0.10
0.05
0.00
-0.05
aa
Aa
AA
QTL x10b
QTL x8
bb
Bb
BB

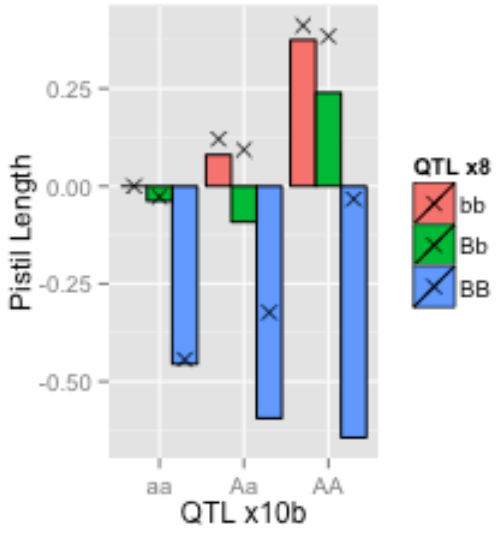
Pistil Length
0.25
0.00
-0.25
-0.50
aa
Aa
AA
QTL x10b
QTL x8
bb
Bb
BB

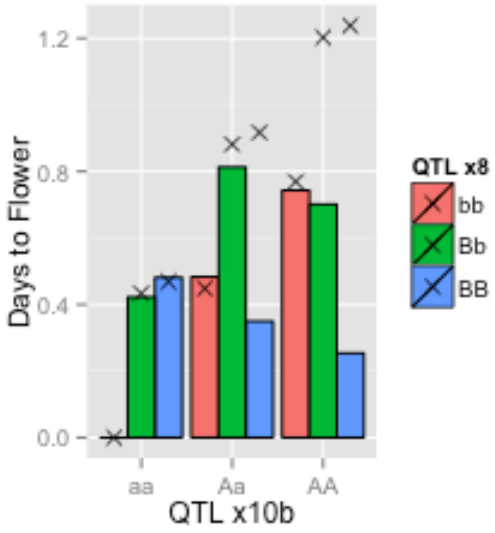
Days to Flower
1.2
0.8
0.4
0.0
aa
Aa
AA
QTL x10b
QTL x8
bb
Bb
BB

Appendix 5— Correlations between effect estimates for each trait.

EFFECTS

Effect 1	Effect 2	Correlation	Count	Lower 95%	Upper 95%	P-value
Pist	CW	0.465	58	0.2349	0.6458	0.0002
DTF	CW	-0.0039	58	-0.2619	0.2546	0.9768
DTF	Pist	-0.2844	58	-0.5055	-0.0281	0.0305
SA	CW	0.2082	58	-0.0529	0.4427	0.1167
SA	Pist	0.2865	58	0.0305	0.5073	0.0292
SA	DTF	-0.1353	58	-0.3803	0.1274	0.3111

Appendix 6— Correlations between phenotypic traits.

TRAITS

Trait 1	Trait 2	Correlation	Count	Lower 95%	Upper 95%	P-value
CWmm	day1	0.2997	10430	0.2821	0.3171	<.0001
SA_mm	day1	-0.0689	10027	-0.0884	-0.0494	<.0001
SA_mm	CWmm	0.1646	10045	0.1455	0.1836	<.0001
pist_mm	day1	0.2433	10125	0.2249	0.2615	<.0001
pist_mm	CWmm	0.4656	10144	0.4502	0.4807	<.0001
pist_mm	SA_mm	0.3202	10037	0.3026	0.3377	<.0001

Appendix 7—Full collection of graphs for each QTL for each trait analogous to Figure 1.3, where allele frequencies are drawn from a Uniform distribution. Average effect (Alpha) values for a QTL plotted against frequency of the QTL. The solid black line indicates the alpha value calculated without epistasis whereas the dashed line shows the best-fit line through the scatter of points, which are the alpha values calculated with epistasis included.

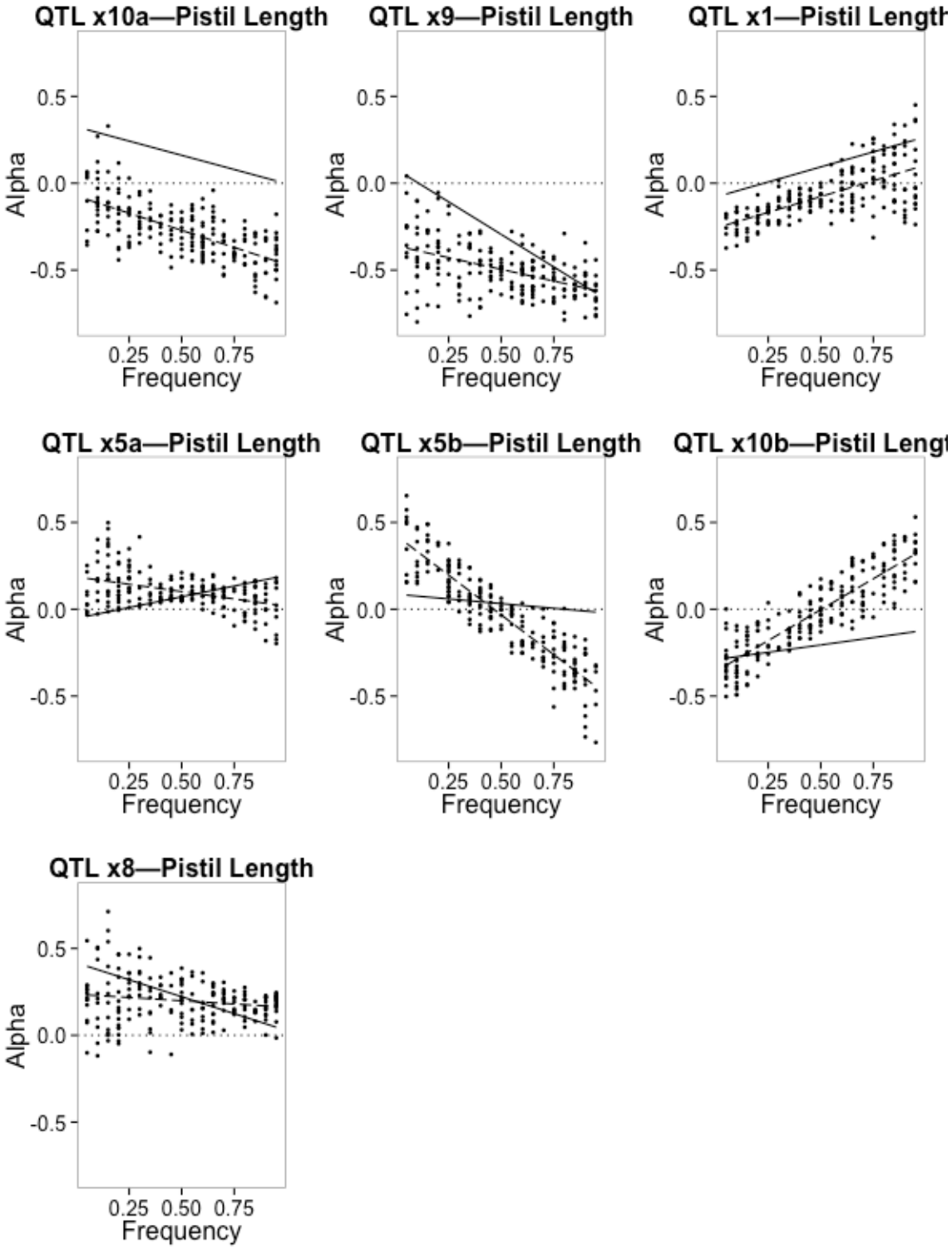

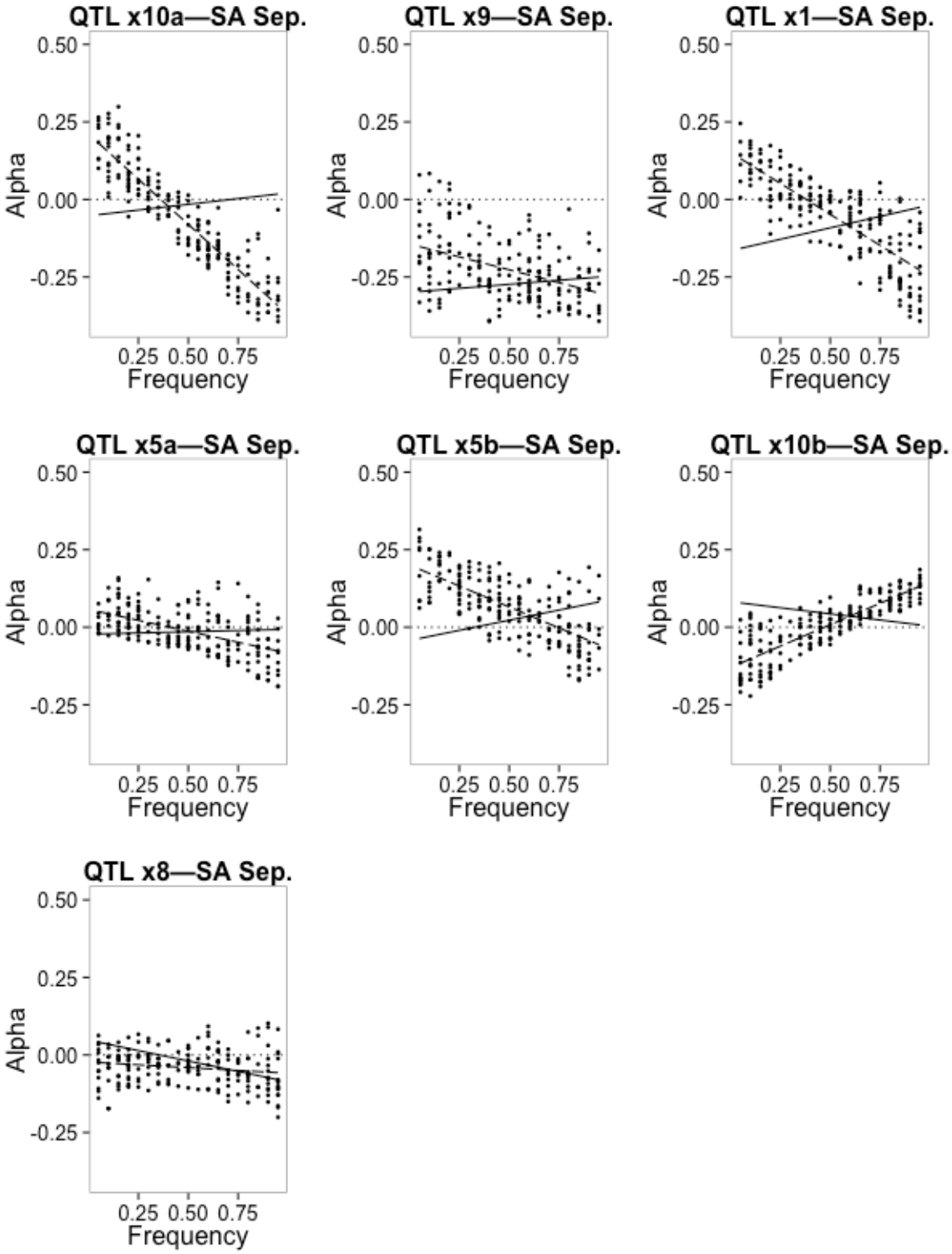
QTL x10a—SA Sep.
QTL x9—SA Sep.
QTL x1—SA Sep.
QTL x5a—SA Sep.
QTL x5b—SA Sep.
QTL x10b—SA Sep.
QTL x8—SA Sep.
Alpha
Frequency
0.50
0.25
0.00
-0.25
0.25 0.50 0.75

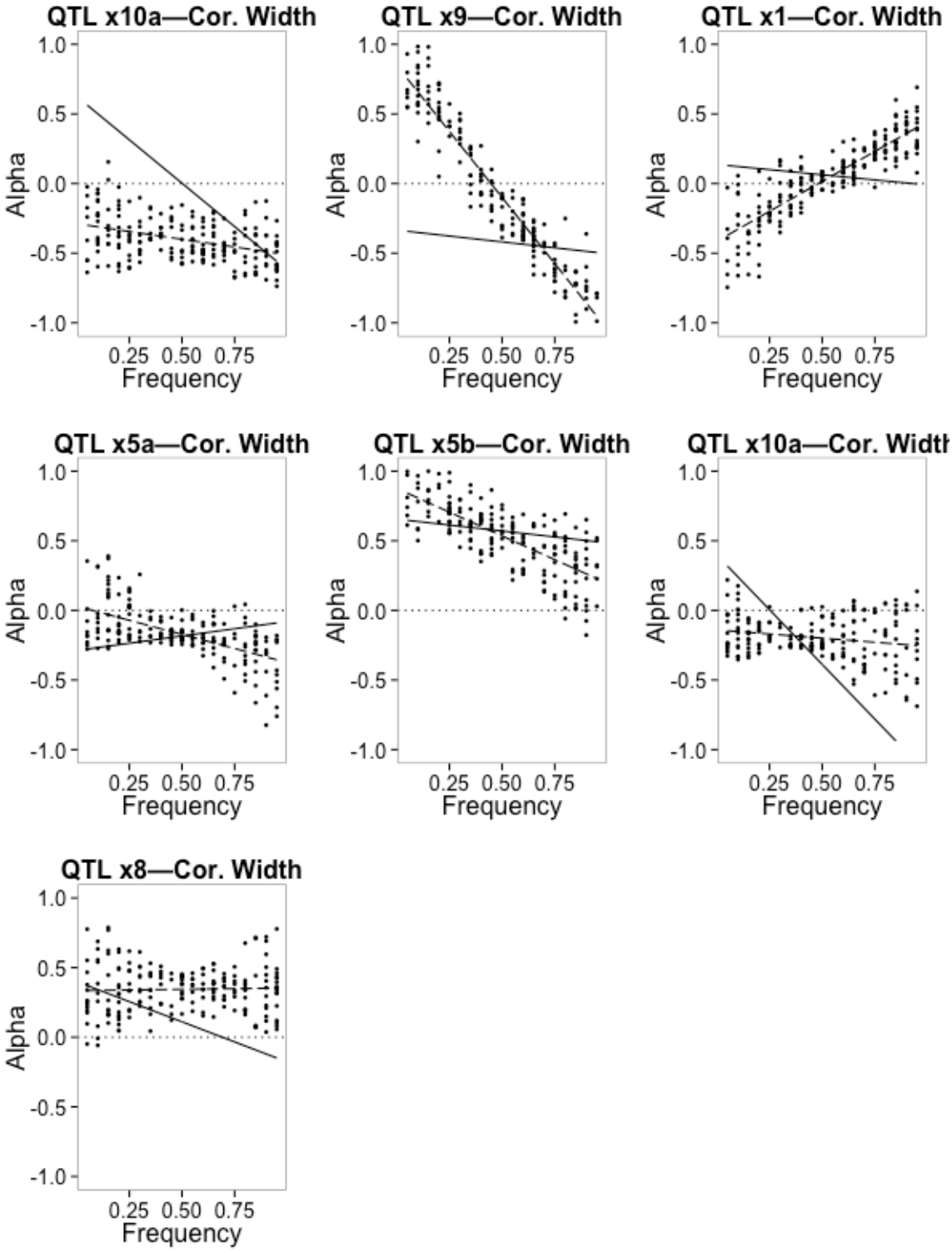
QTL x10a—Cor. Width
QTL x9—Cor. Width
QTL x1—Cor. Width
QTL x5a—Cor. Width
QTL x5b—Cor. Width
QTL x10a—Cor. Width
QTL x8—Cor. Width
Alpha
Frequency
1.0
0.5
0.0
-0.5
-1.0
0.25 0.50 0.75

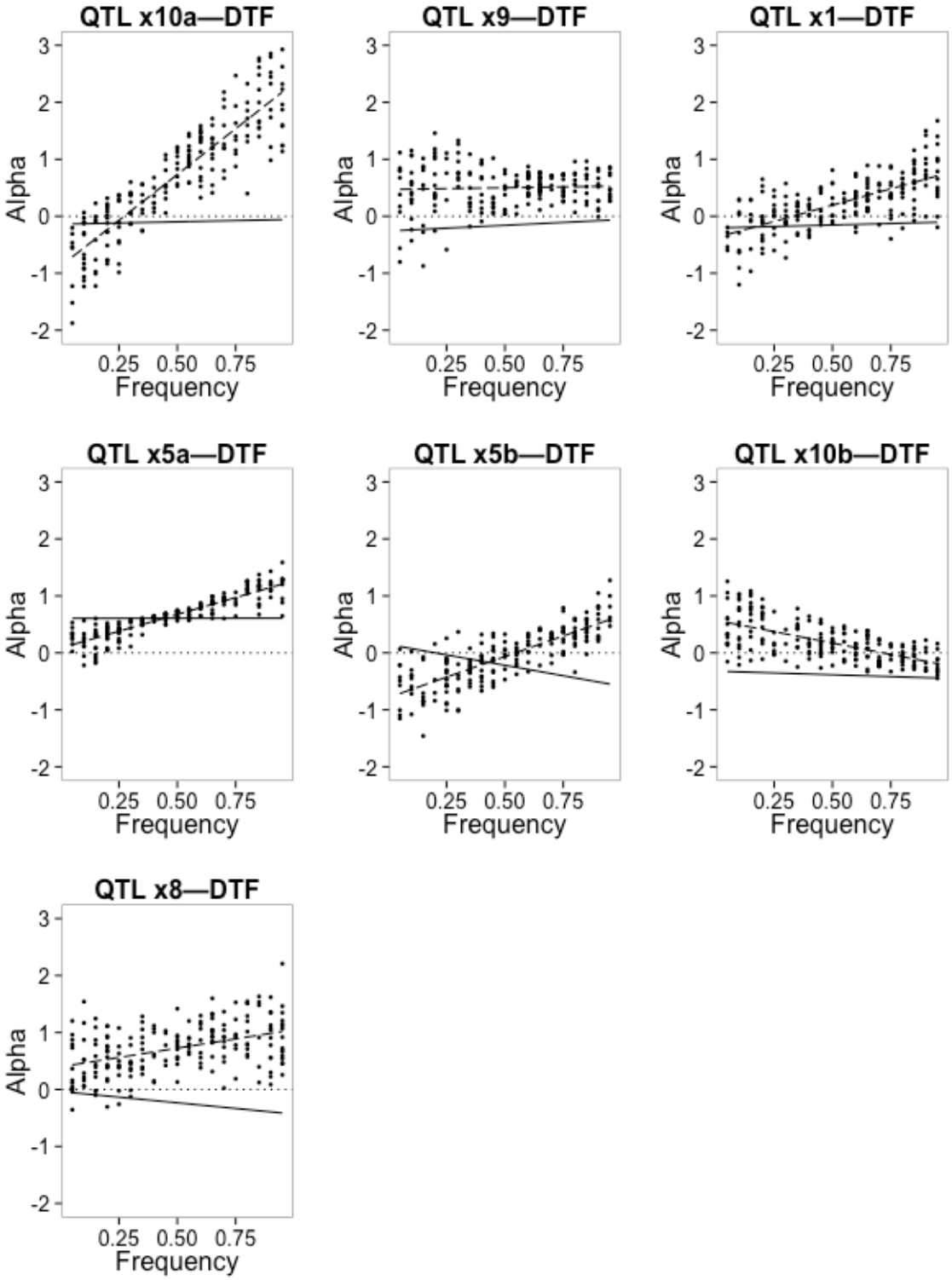
QTL x10a—DTF
QTL x9—DTF
QTL x1—DTF
QTL x5a—DTF
QTL x5b—DTF
QTL x10b—DTF
QTL x8—DTF
Alpha
Frequency
3
2
1
0
-1
-2
0.25
0.50
0.75

Appendix 8—Full collection of graphs for each QTL analgous to Figure 1.3, except that allele frequencies are drawn from a U-shaped distribution. Average effect (Alpha) values for a QTL plotted against frequency of the QTL. The solid black line indicates the alpha value calculated without epistasis whereas the dashed line shows the best-fit line through the scatter of points, which are the alpha values calculated with epistasis included.

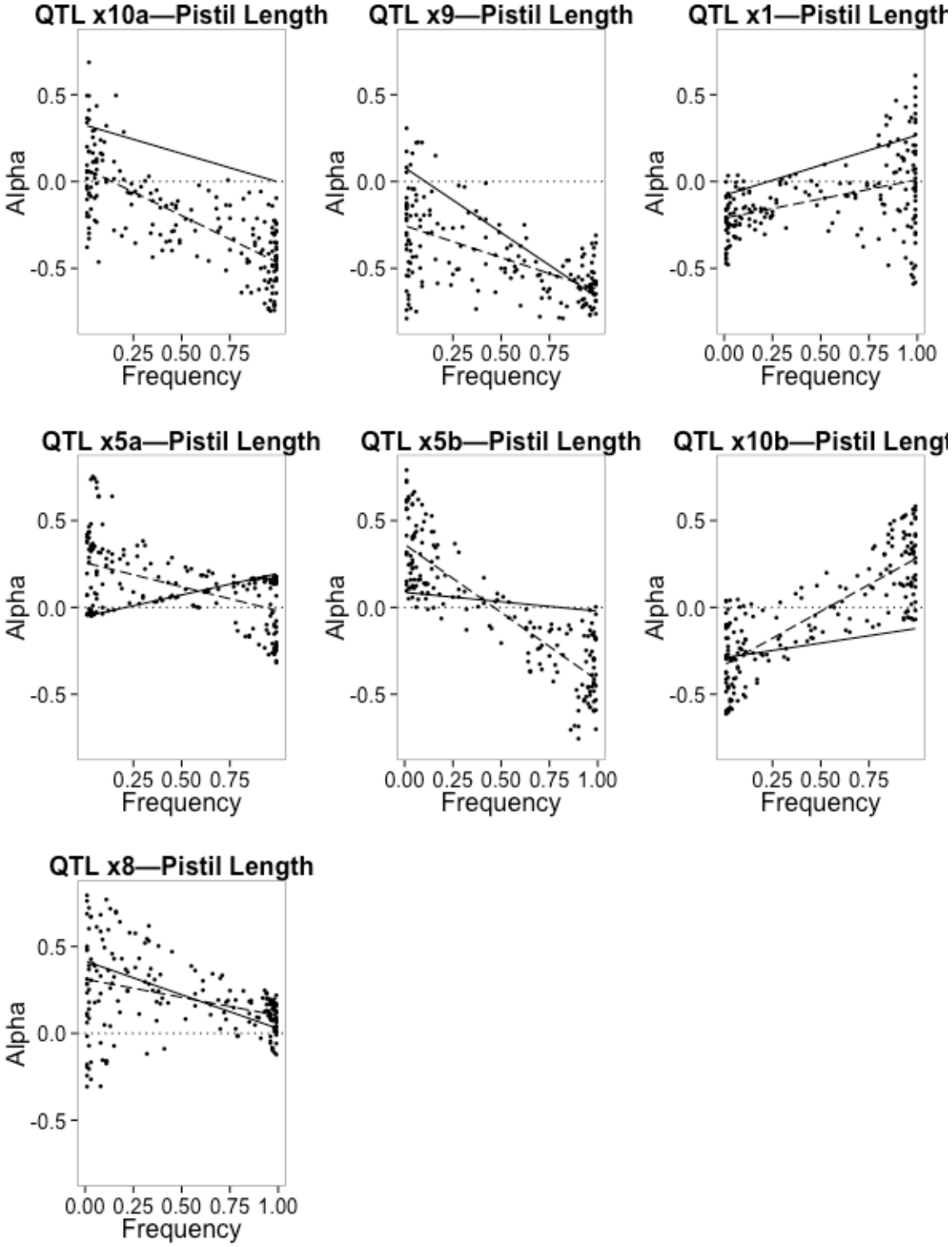

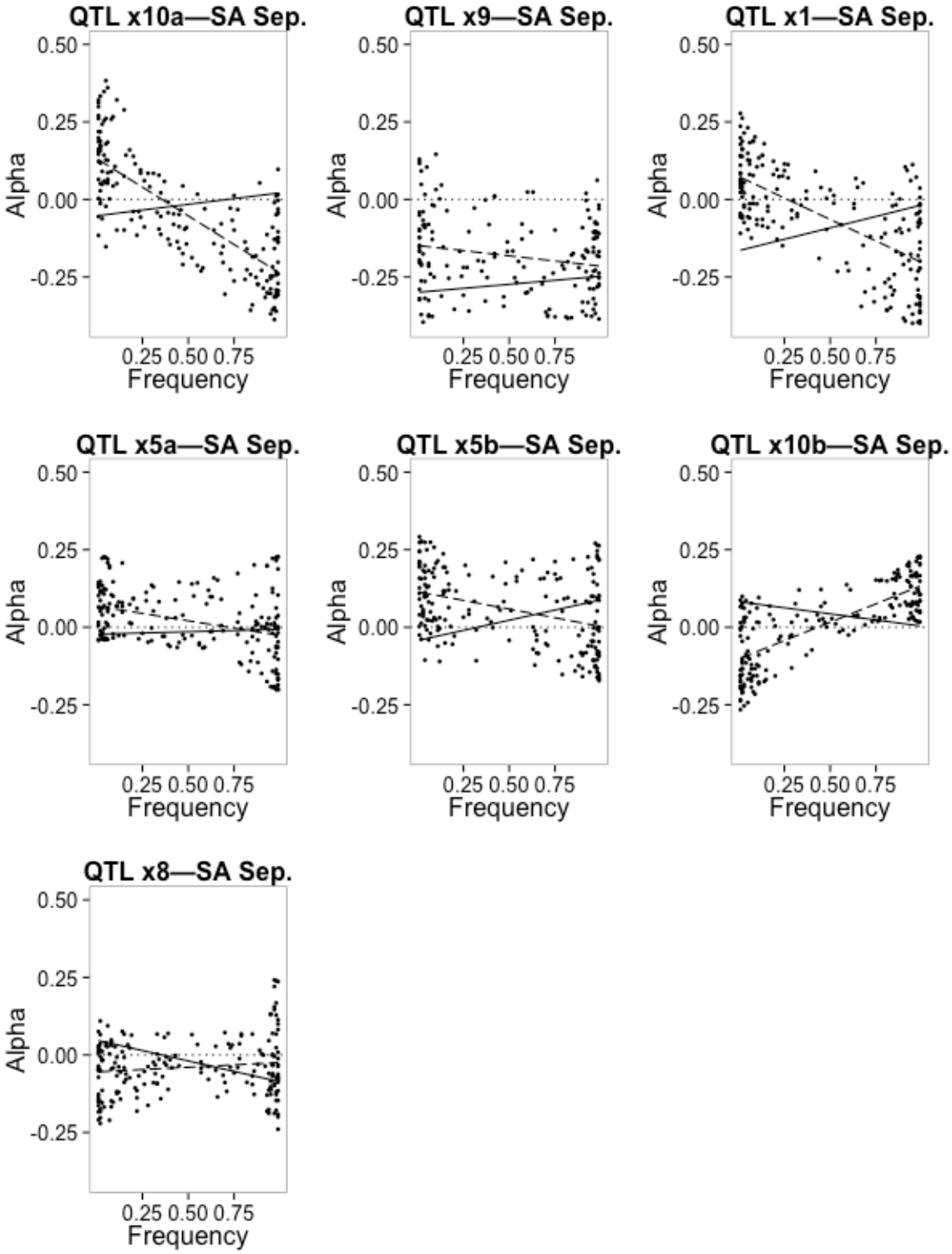
QTL x10a—SA Sep.
QTL x9—SA Sep.
QTL x1—SA Sep.
QTL x5a—SA Sep.
QTL x5b—SA Sep.
QTL x10b—SA Sep.
QTL x8—SA Sep.
Alpha
0.50
0.25
0.00
-0.25
0.25 0.50 0.75
Frequency

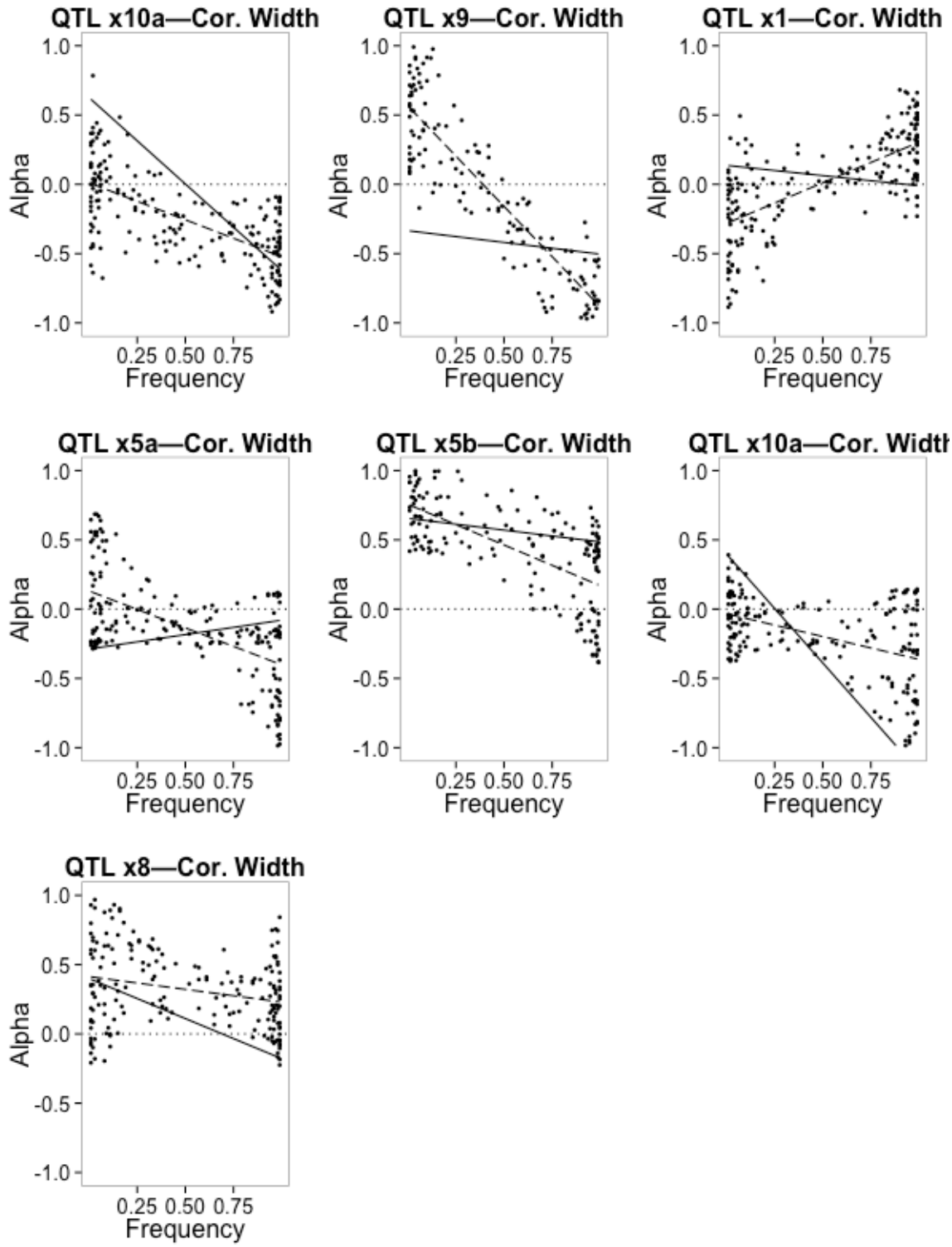
QTL x10a—Cor. Width
QTL x9—Cor. Width
QTL x1—Cor. Width
QTL x5a—Cor. Width
QTL x5b—Cor. Width
QTL x10a—Cor. Width
QTL x8—Cor. Width
Alpha
Frequency
1.0
0.5
0.0
-0.5
-1.0
0.25 0.50 0.75

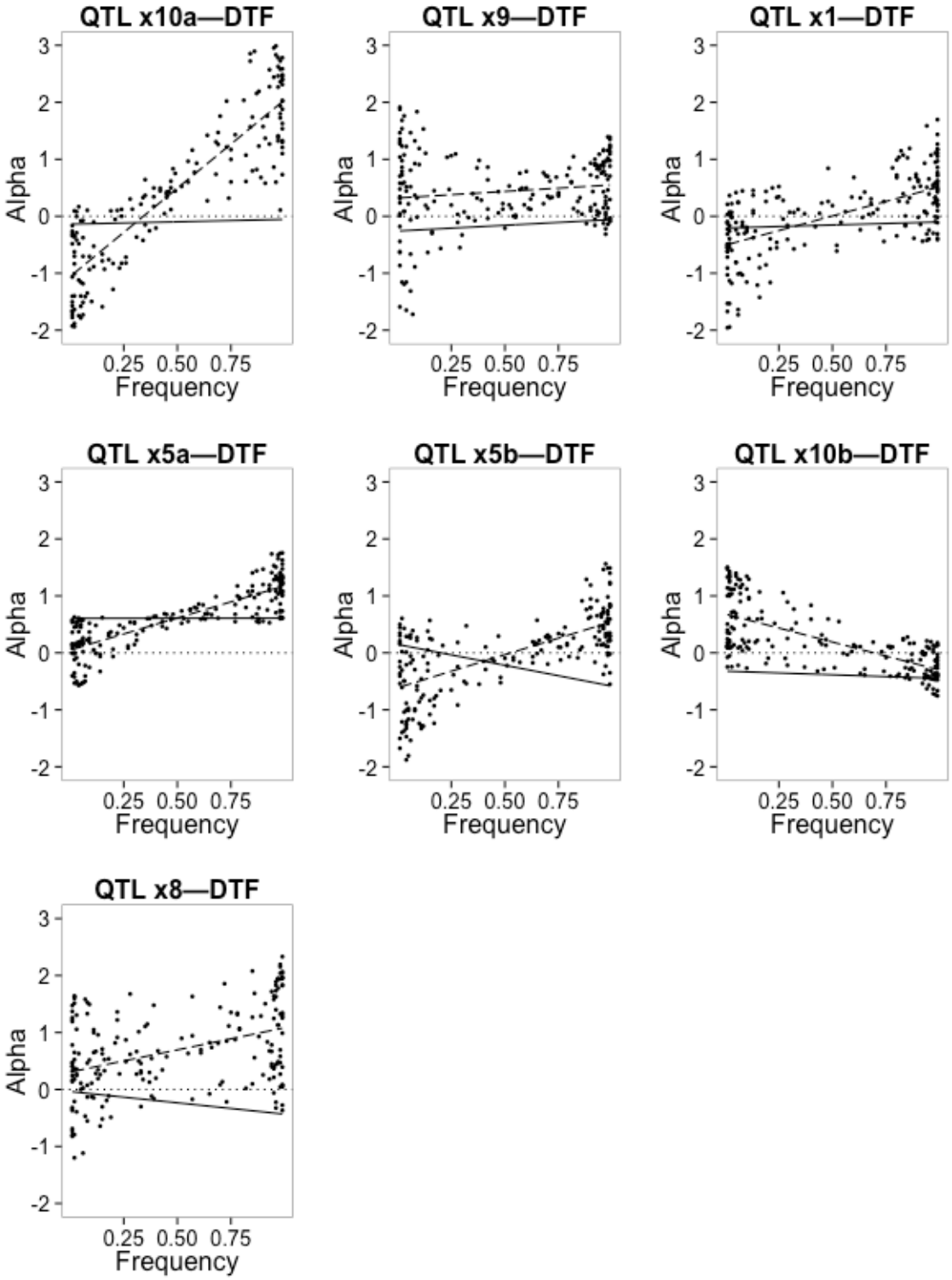
QTL x10a—DTF
QTL x9—DTF
QTL x1—DTF
QTL x5a—DTF
QTL x5b—DTF
QTL x10b—DTF
QTL x8—DTF
Alpha
Frequency
3
2
1
0
-1
-2
0.25 0.50 0.75

Appendix 9— Distributions for corrected additive genetic variance for the U-shaped distribution of allele frequencies.

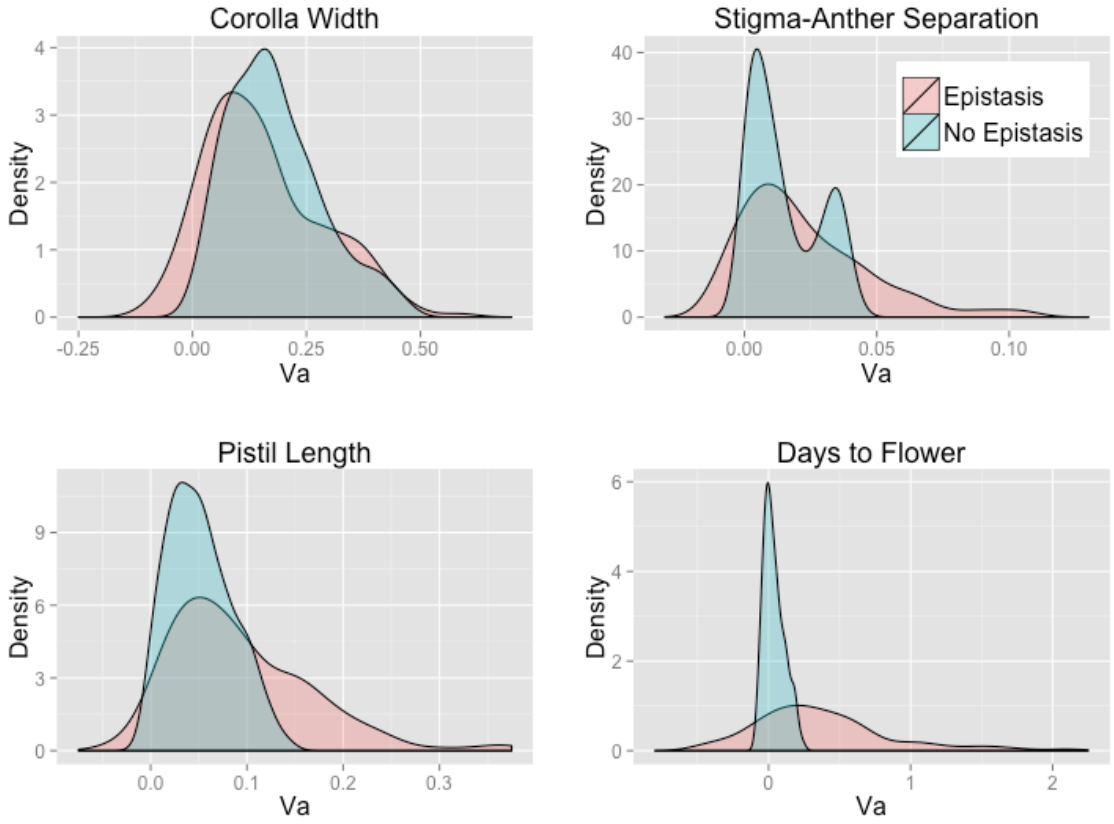

Appendix 10—Distributions for corrected genetic variance for the Uniform distribution of allele frequencies.

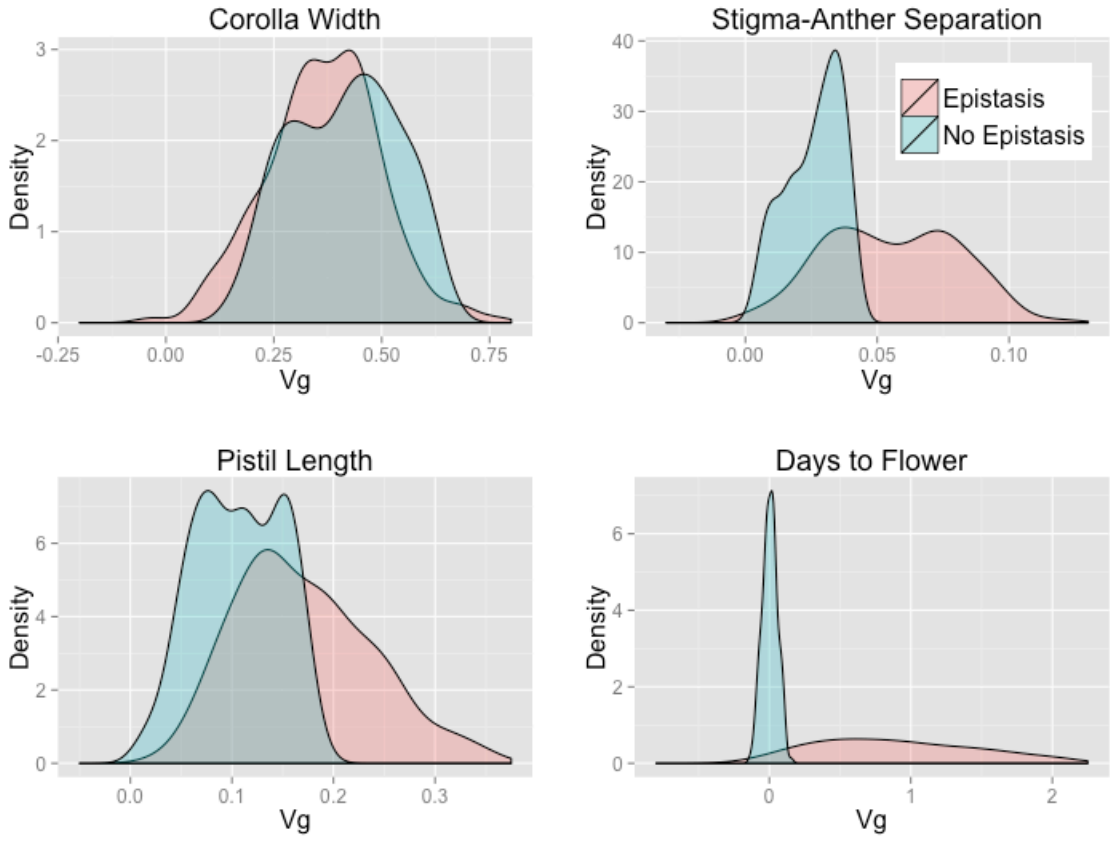

Appendix 11— Distributions for corrected genetic variance for the U-shaped distribution of allele frequencies.

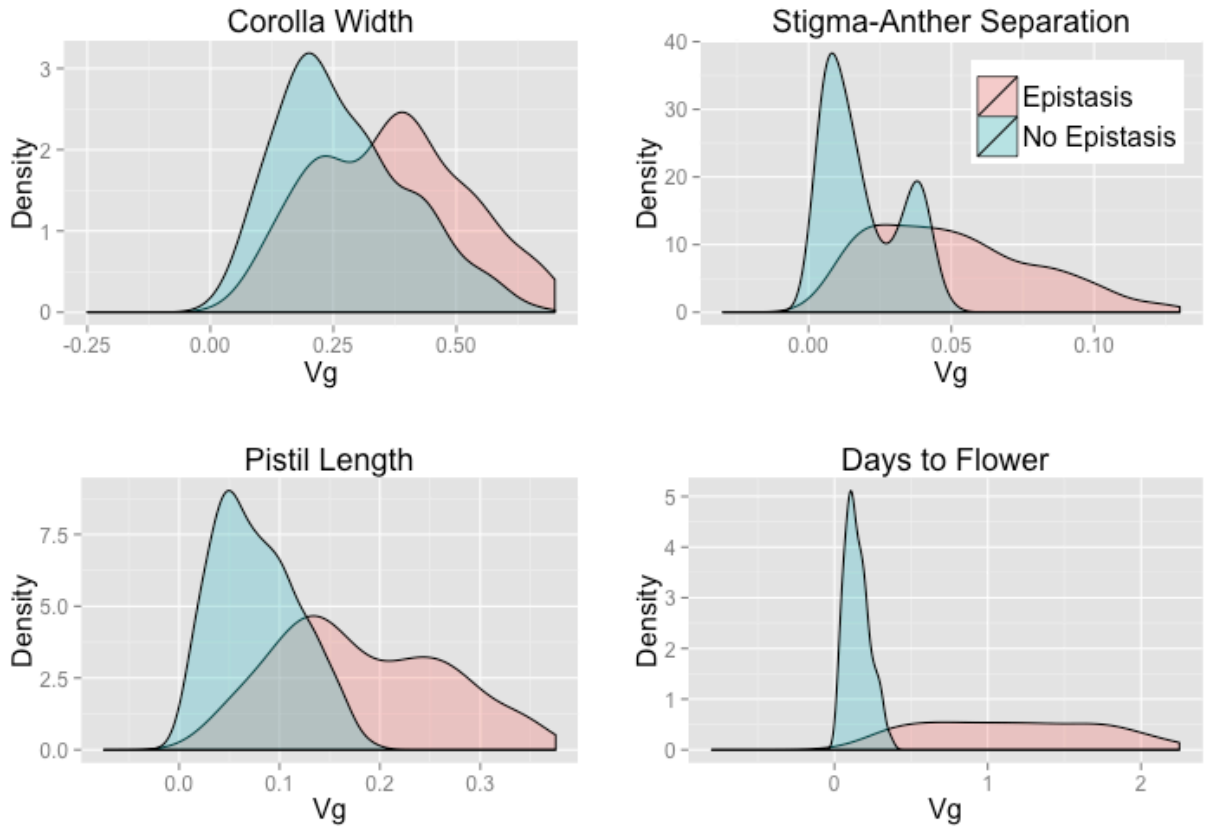

Appendix 12—Distributions for uncorrected genetic variance for the Uniform distribution of allele frequencies.

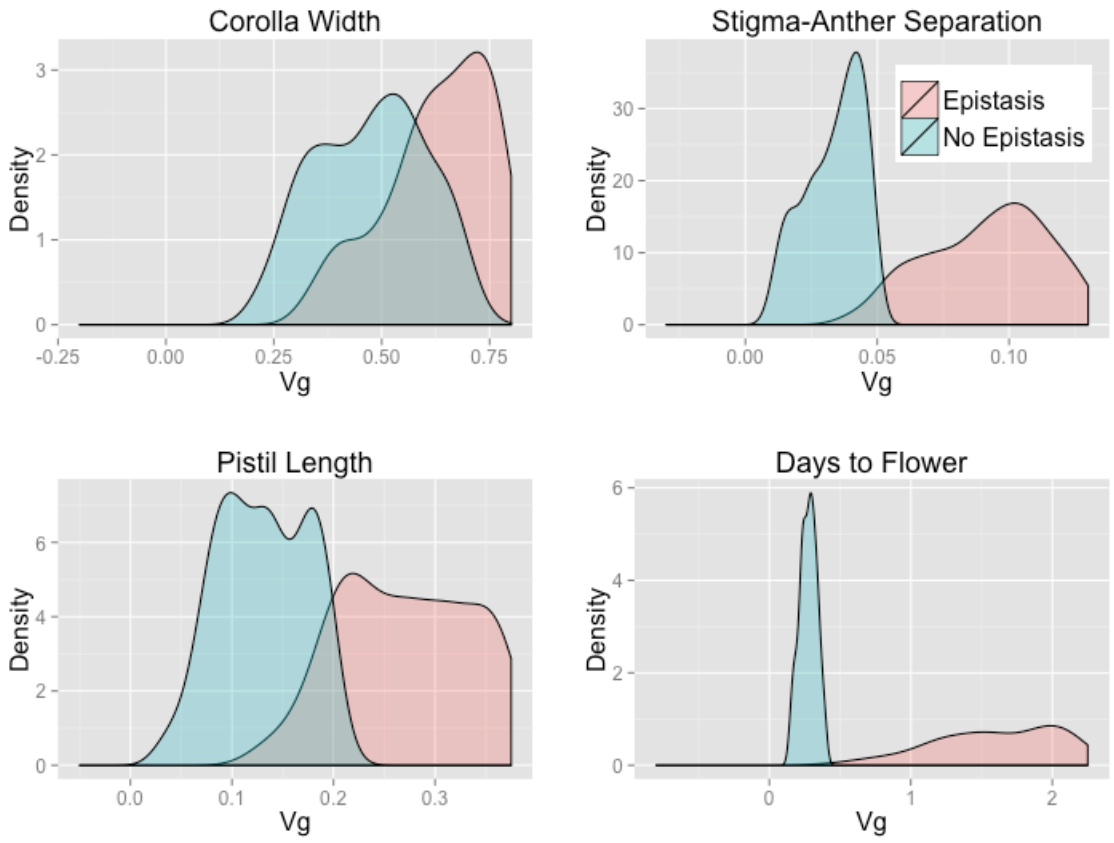

Appendix 13—Distributions for uncorrected genetic variance for the U-shaped distribution of allele frequencies.

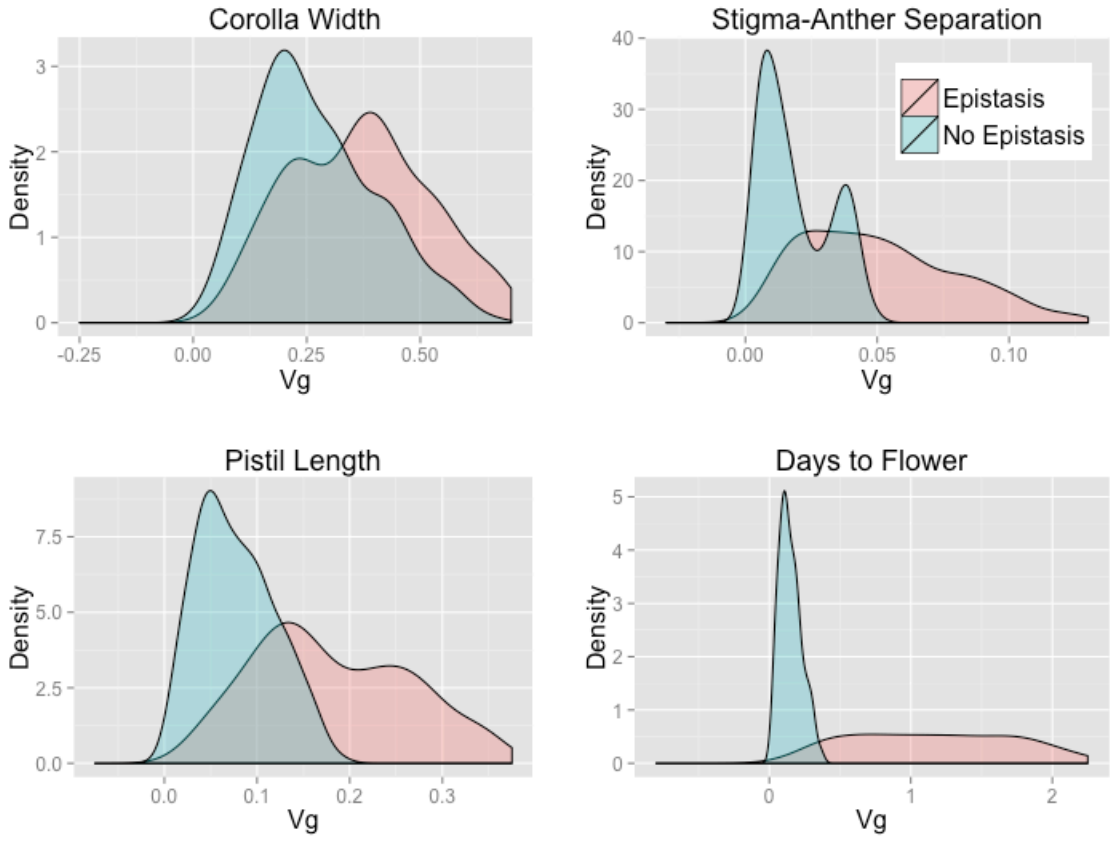

Appendix 14—Distributions for uncorrected additive genetic variance for the Uniform distribution of allele frequencies.

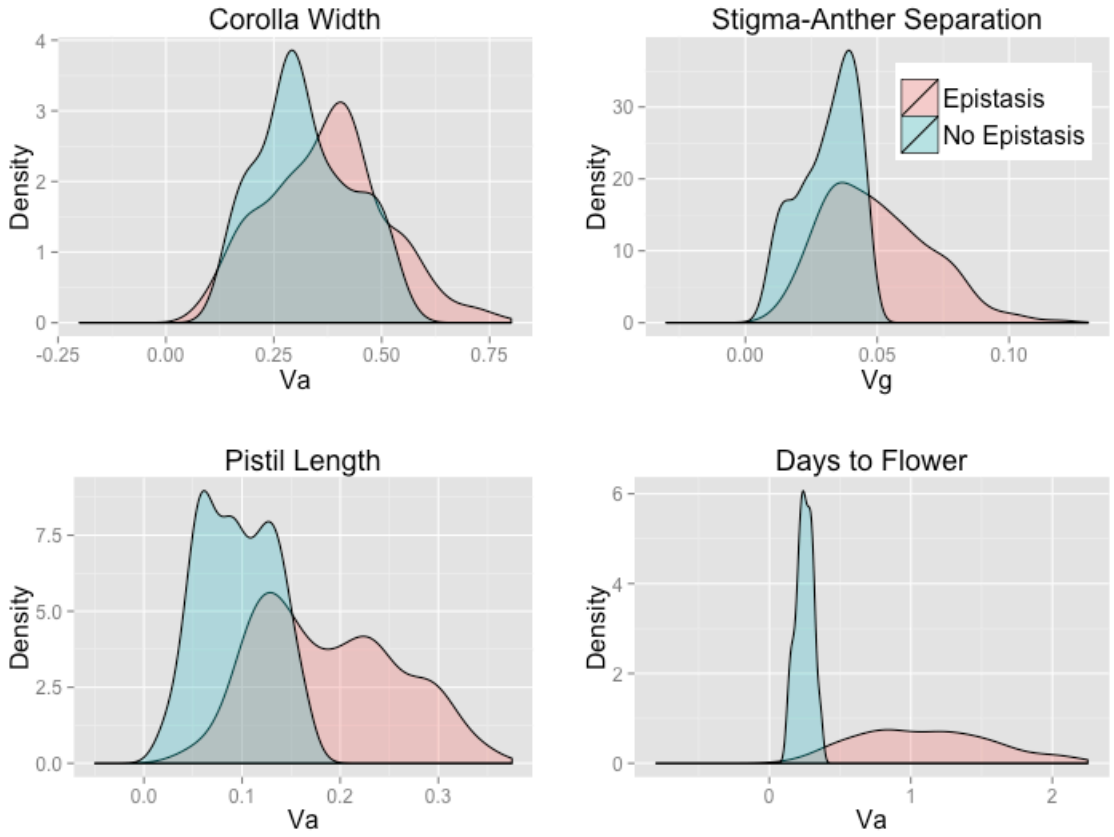

Appendix 15—Distributions for uncorrected additive genetic variance for the U-shaped distribution of allele frequencies.

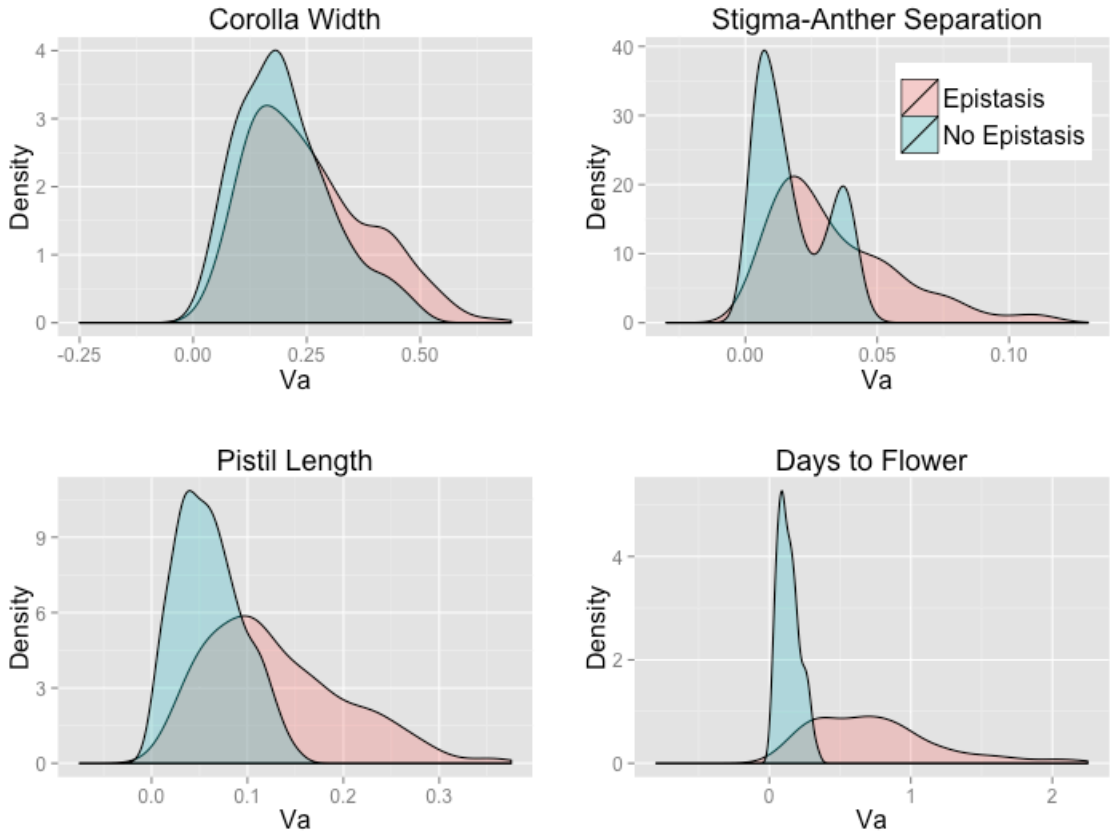

Appendix 16—Distributions for additive genetic variances calculated with and without bias-correction for the bias-correction simulations. The black arrows indicate the 'true' value predicted using the effects from which data was simulated.

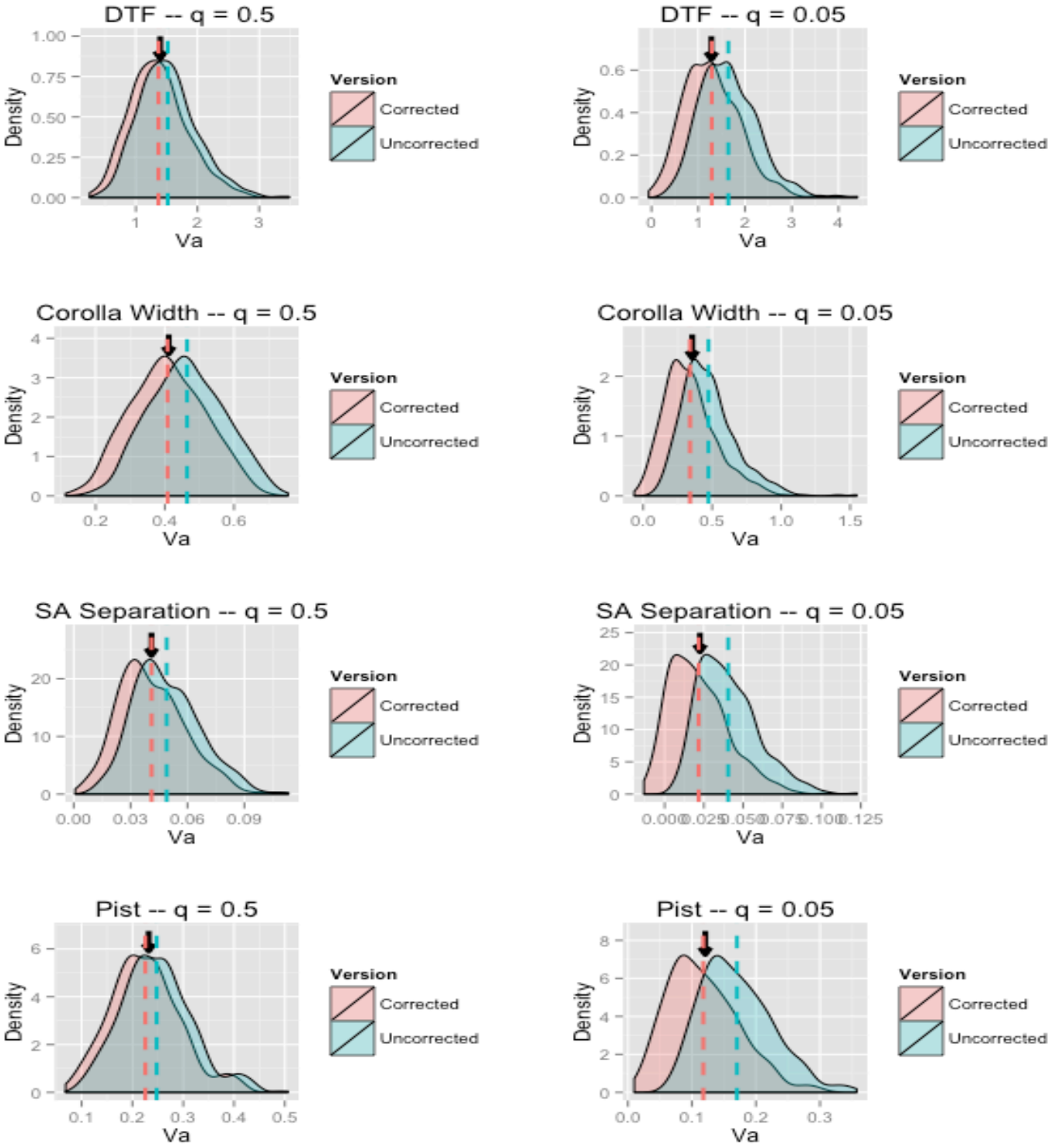

Appendix 17—Distributions for genetic variances calculated with and without bias-correction for the bias-correction simulations. The black arrows indicate the 'true' value predicted using the effects from which data was simulated.

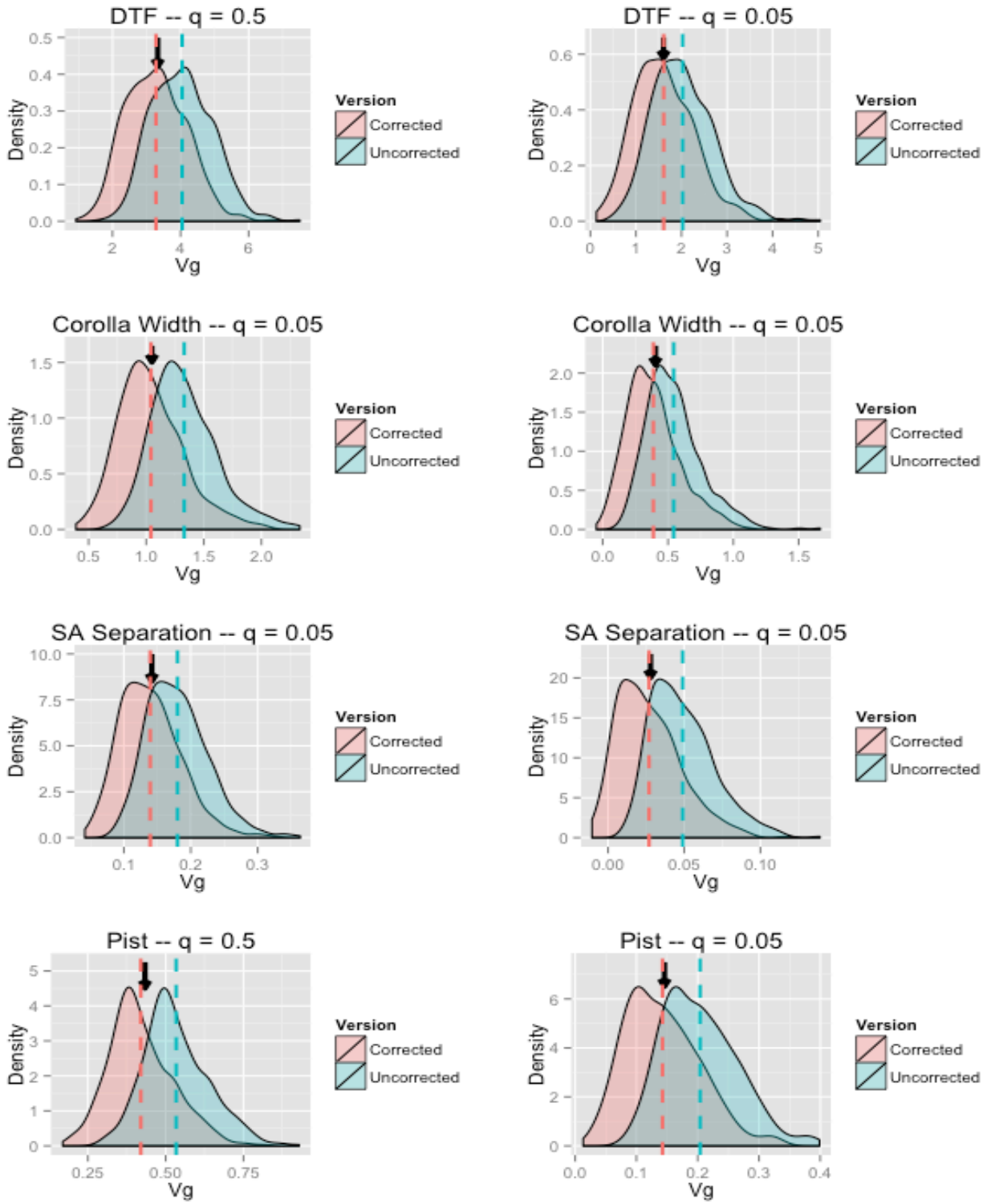

Appendix 18—Summary of linear model for greenhouse data. Models were fit similarly to that of the field data, except for the Year and Flat variables. Instead, "cohort" was included as a random variable.

Trait	Term	Chi-squared	DF	P-value
Days to Flower	QTL1	5.4307	2	0.06618
Days to Flower	QTL2	1.5088	2	0.47029
Days to Flower	QTL1:QTL2	12.4536	4	0.01428
Internode Length	QTL1	10.9378	2	0.004216
Internode Length	QTL2	2.0664	2	0.355858
Internode Length	QTL1:QTL2	7.502	4	0.111623
Pedicle Length	QTL1	0.3495	2	0.8397
Pedicle Length	QTL2	0.0765	2	0.9625
Pedicle Length	QTL1:QTL2	1.4785	4	0.8304
Pistil Length	QTL1	25.651	2	2.69E-06
Pistil Length	QTL2	29.956	2	3.13E-07
Pistil Length	QTL1:QTL2	37.278	4	1.58E-07
Corolla Width	QTL1	13.757	2	0.00103
Corolla Width	QTL2	41.951	2	7.77E-10
Corolla Width	QTL1:QTL2	16.185	4	0.00278

It should be noted that there are some slight discrepancies between these results and those reported for this QTL pair in Chapter 1. This is due to differences in how the models were specified to test for epistasis as well as due to differences in the data that was used in each study.

Appendix 19—Trait histograms from field study

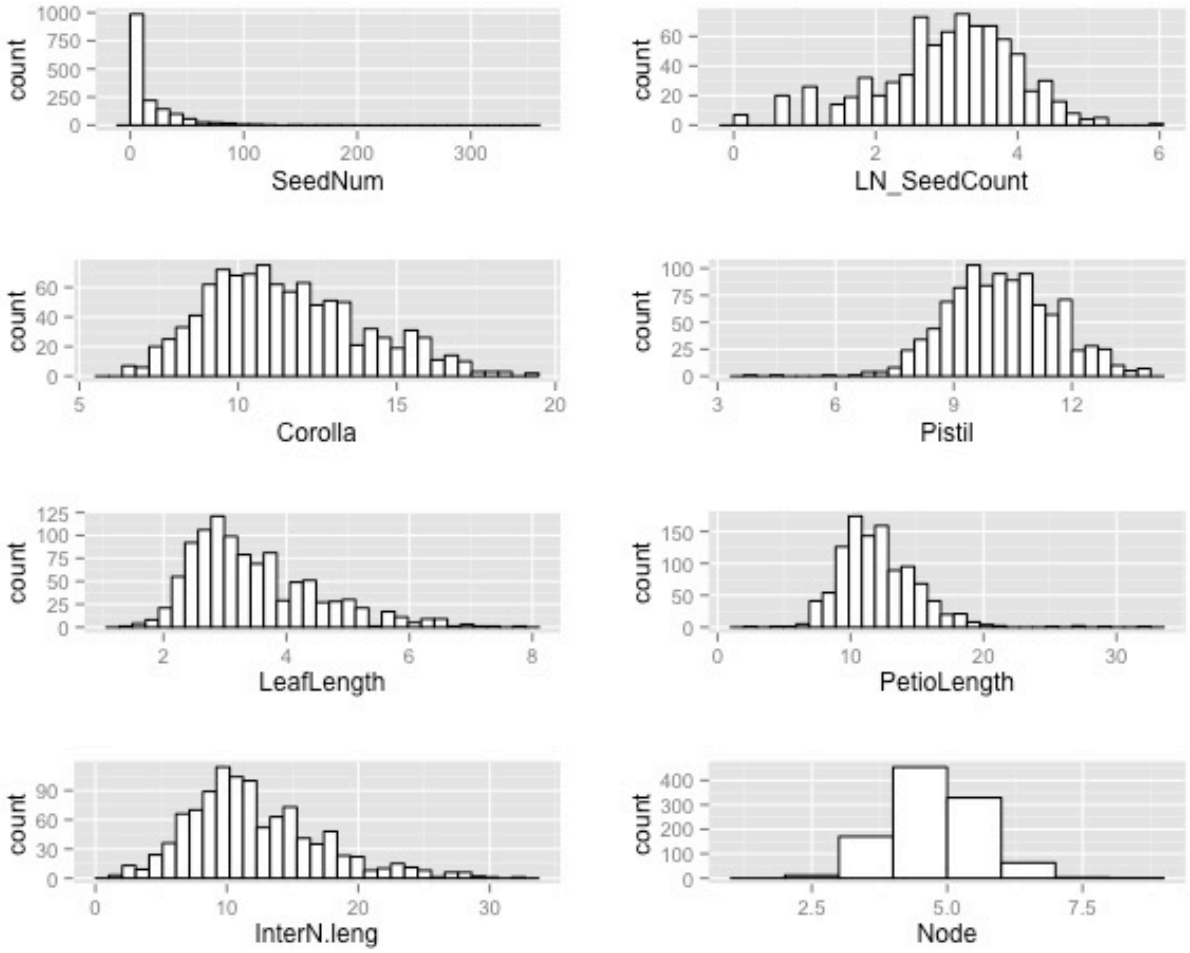

Appendix 20—Poisson regression fit using glmer() with family="Poisson" and 'Flat' specified as a random effect. Response variable was untransformed seed count for all plants, including those that failed to set seed (zero values). P-values were determined using the Anova() function from the 'car' package and specifying type III sums of squares.

	Chisq	Df	Pr(>Chisq)
(Intercept)	225.15	1	<0.00001
QTL1	216.169	2	<0.00001
QTL2	77.655	2	<0.00001
Year	13.148	1	0.0002878
QTL1:QTL2	147.962	4	<0.00001

Appendix 21—Summary of linear models investigating the effect of field versus greenhouse conditions on genetic effects. A significant interaction of one or both QTL with 'Env' indicates a significant dependency of genetic effects on growing environment. Cohort, which includes the effect of the different years of the field study, was specified as a random variable.

Term	Chi-Square	DF	P-value	Term	Chi-Square	DF	P-value
	Days to Flower				Pistil Length		
QTL1	32.389	2	9.26E-08	QTL1	0.1498	2	0.9278256
QTL2	3.5919	2	0.1659707	QTL2	2.9463	2	0.2292074
Env	377.1847	1	<2.20E-16	Env	21.2921	1	3.94E-06
QTL1:QTL2	22.1687	4	0.0001855	QTL1:QTL2	3.031	4	0.5526566
QTL1:Env	11.7379	2	**0.0028259**	QTL1:Env	9.4835	2	**0.0087234**
QTL2:Env	2.9668	2	0.2268606	QTL2:Env	23.5033	2	**7.88E-06**
QTL1:QTL2:Env	3.4862	4	0.4799803	QTL1:QTL2:Env	19.4889	4	**0.0006298**
	Internode Length				Corolla Width		
QTL1	19.4493	2	5.98E-05	QTL1	4.3114	2	0.11582
QTL2	2.1468	2	0.341838	QTL2	1.3858	2	0.50011
Env	0.6157	1	0.432645	Env	20.5311	1	5.87E-06
QTL1:QTL2	17.3818	4	0.001629	QTL1:QTL2	3.81	4	0.43233
QTL1:Env	11.5745	2	**0.003066**	QTL1:Env	4.909	2	0.08591
QTL2:Env	1.4474	2	0.484966	QTL2:Env	25.6336	2	**2.72E-06**
QTL1:QTL2:Env	4.9565	4	0.291785	QTL1:QTL2:Env	5.9607	4	0.2021
	Pedicle Length						
QTL1	9.6948	2	0.0078488				
QTL2	3.8602	2	0.1451304				
Env	7.0144	1	0.0080858				
QTL1:QTL2	21.431	4	0.0002601				
QTL1:Env	2.08	2	0.3534502				
QTL2:Env	0.2774	2	0.8704724				
QTL1:QTL2:Env	3.9362	4	0.414707				

Appendix 22—Genotypic means in field (including each year separately as well as the average across years) and greenhouse conditions. Error bars are ± 1 Standard Error.

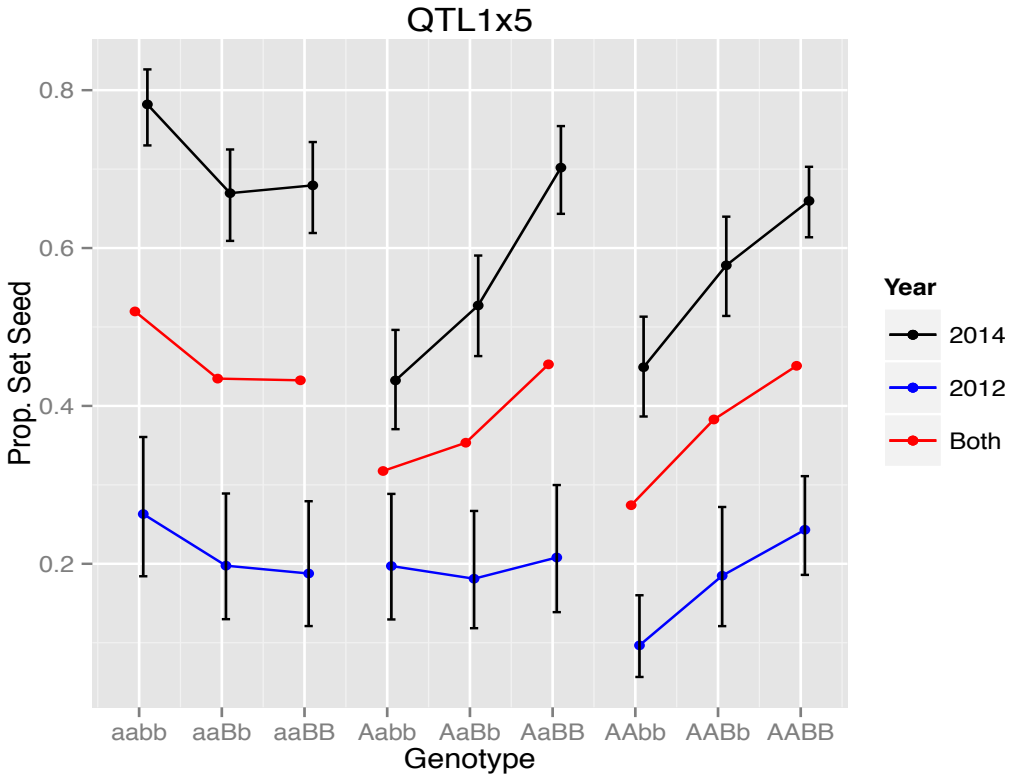

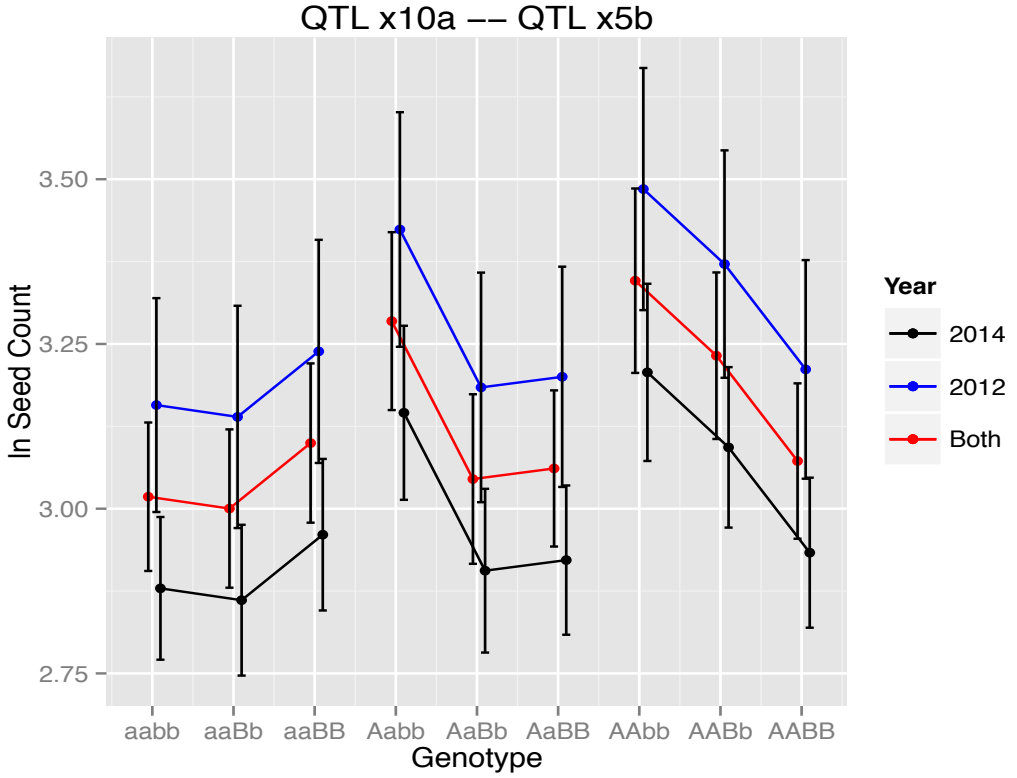

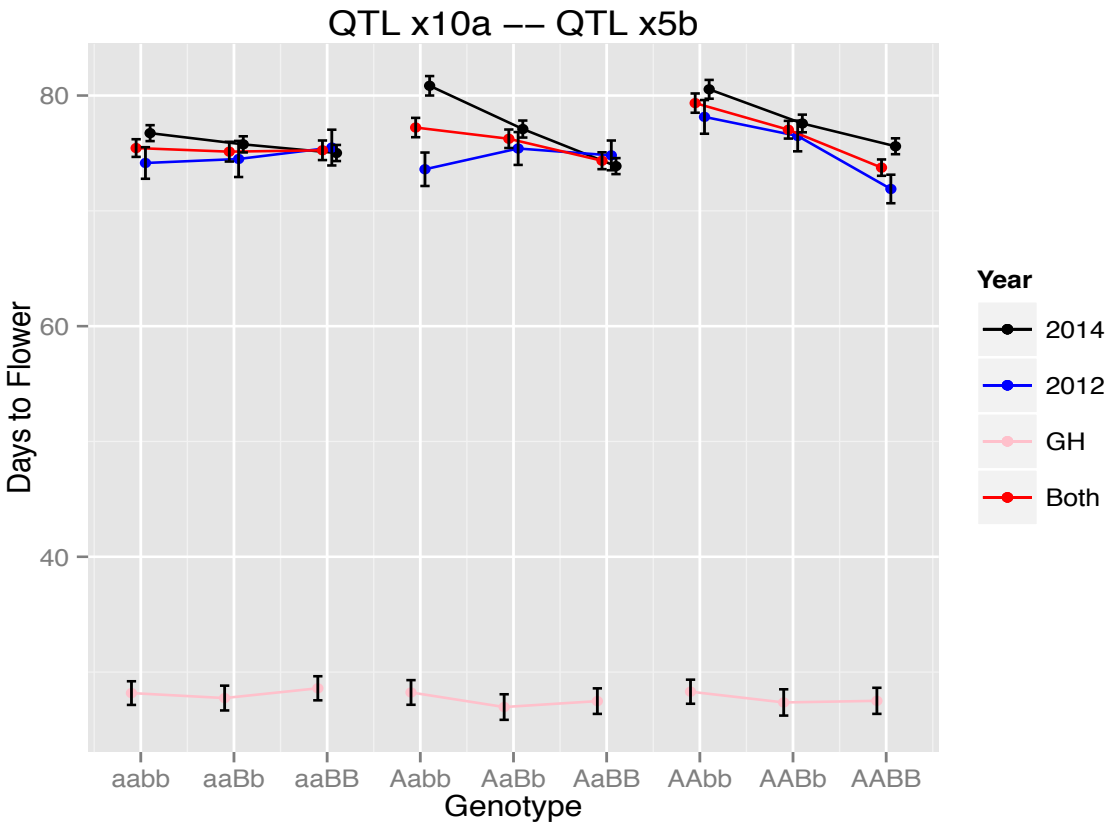
QTL x10a –– QTL x5b
Days to Flower
80
60
40
aabb
aaBb
aaBB
Aabb
AaBb
AaBB
AAbb
AABb
AABB
Genotype
Year
2014
2012
GH
Both

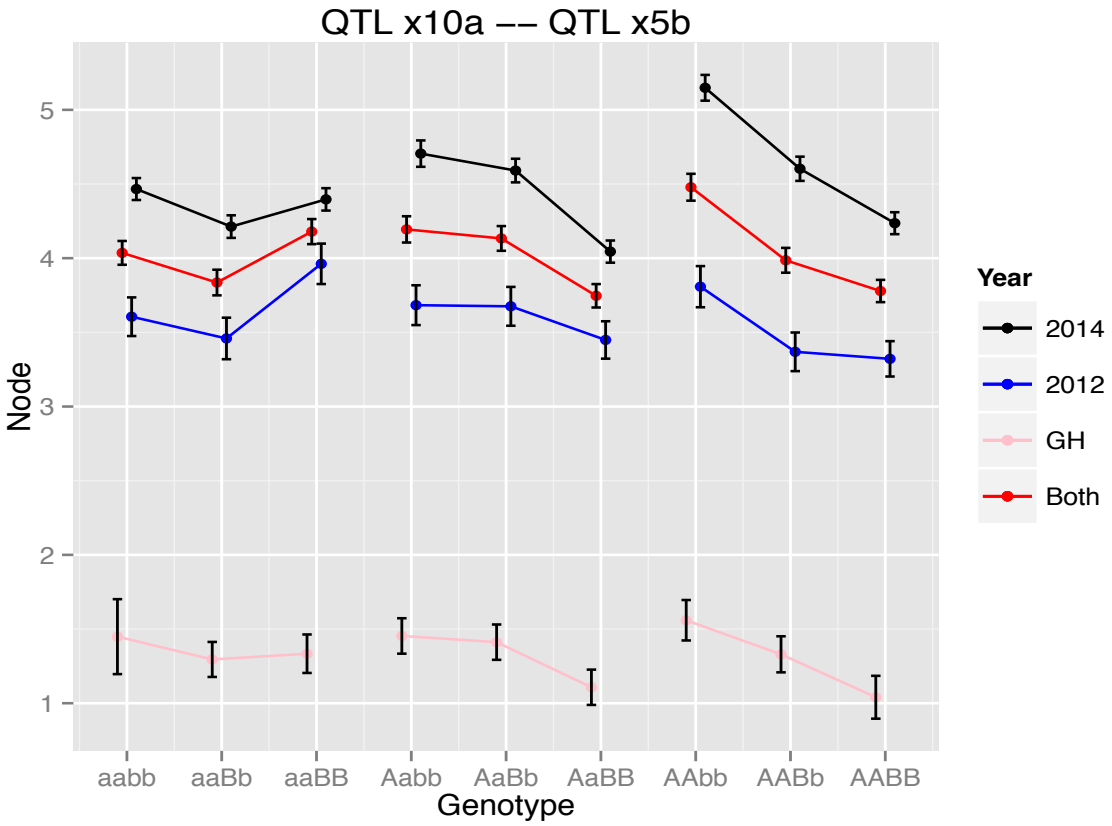
QTL x10a –– QTL x5b
Node
5
4
3
2
1
aabb
aaBb
aaBB
Aabb
AaBb
AaBB
AAbb
AABb
AABB
Genotype
Year
2014
2012
GH
Both

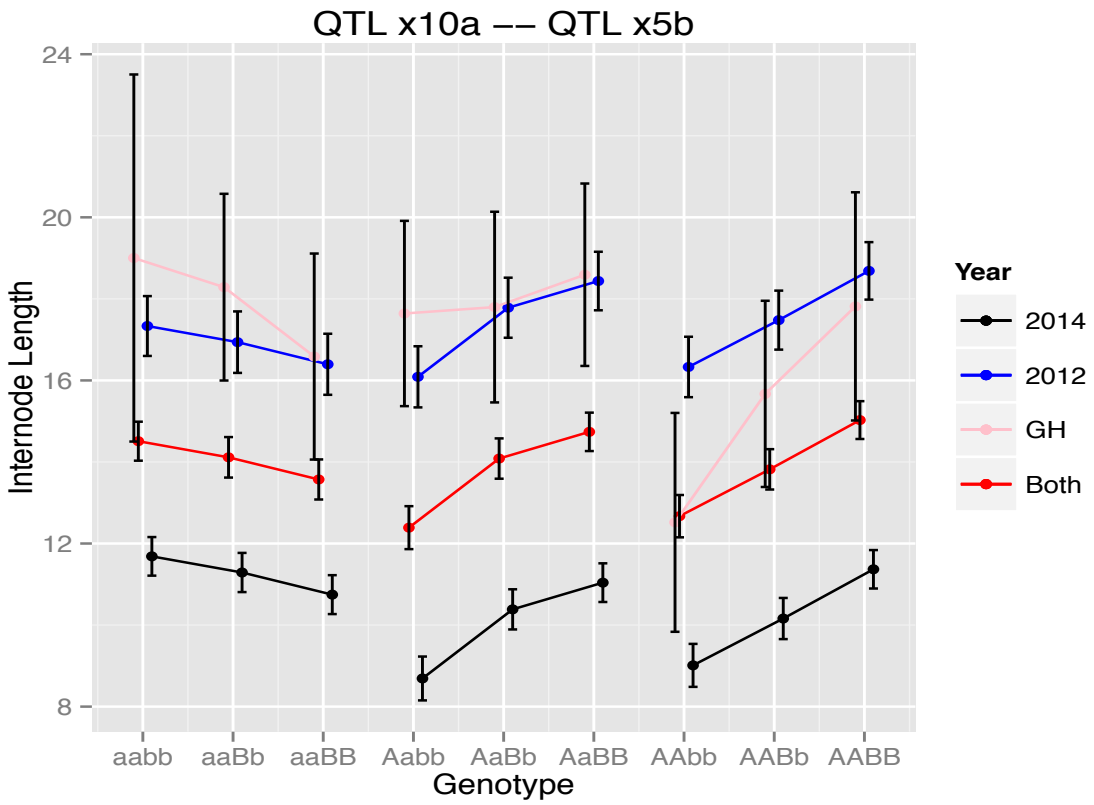
QTL x10a –– QTL x5b
Internode Length
24
20
16
12
8
aabb
aaBb
aaBB
Aabb
AaBb
AaBB
AAbb
AABb
AABB
Genotype
Year
2014
2012
GH
Both

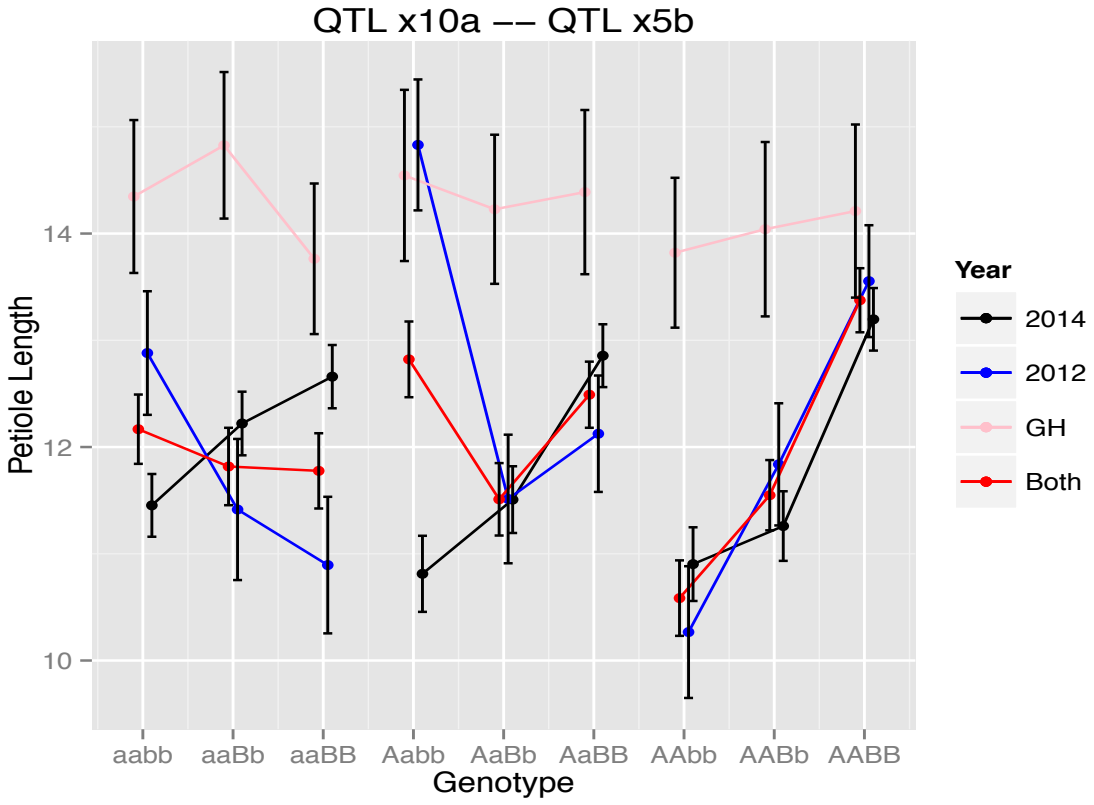
QTL x10a –– QTL x5b
Petiole Length
14
12
10
aabb
aaBb
aaBB
Aabb
AaBb
AaBB
AAbb
AABb
AABB
Genotype
Year
2014
2012
GH
Both

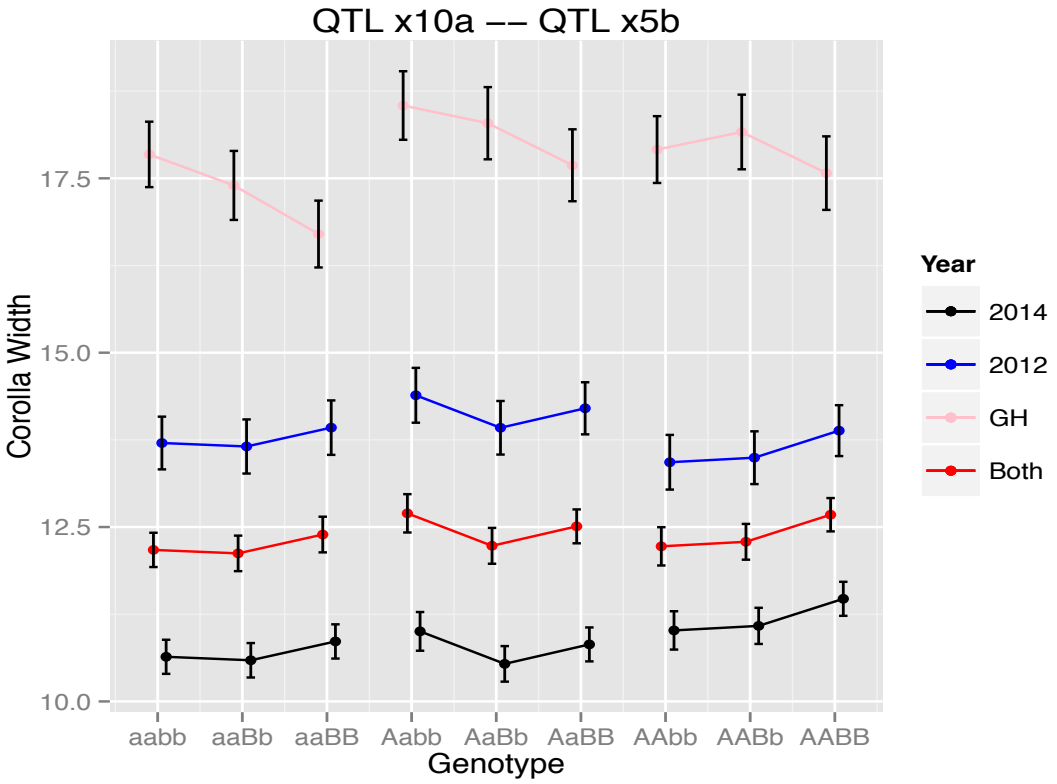
QTL x10a –– QTL x5b
Corolla Width
17.5
15.0
12.5
10.0
aabb
aaBb
aaBB
Aabb
AaBb
AaBB
AAbb
AABb
AABB
Genotype
Year
2014
2012
GH
Both

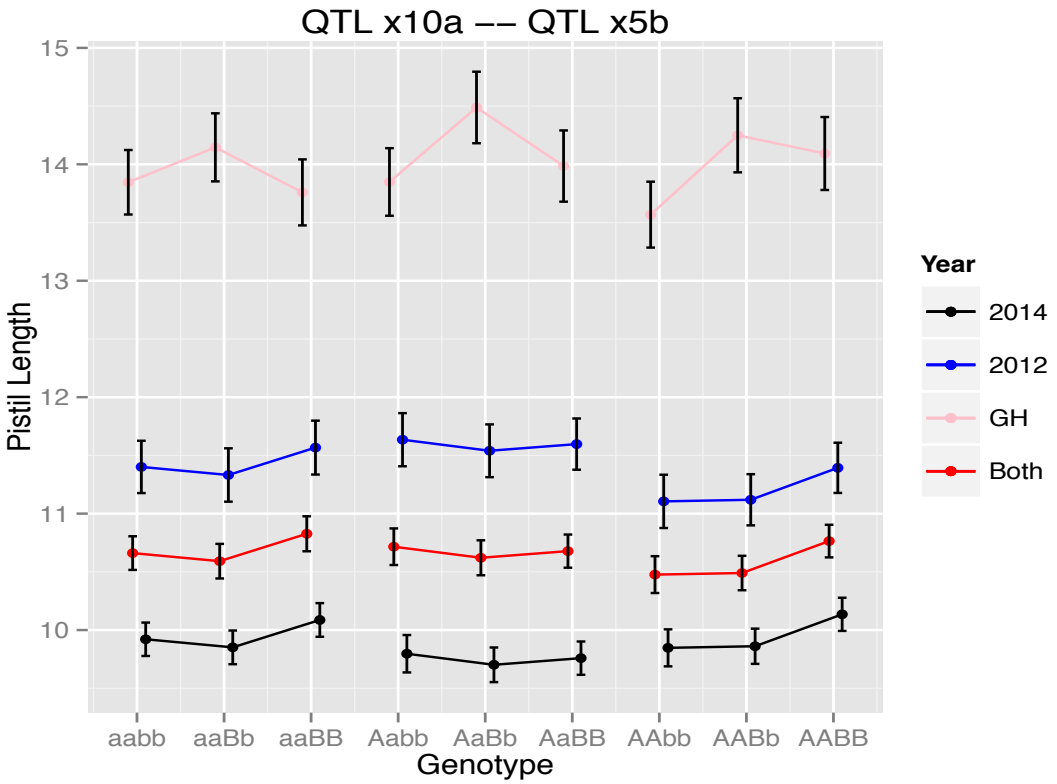
QTL x10a –– QTL x5b
Pistil Length
15
14
13
12
11
10
aabb
aaBb
aaBB
Aabb
AaBb
AaBB
AAbb
AABb
AABB
Genotype
Year
2014
2012
GH
Both

Appendix 23—Summary of tests for genome scan. Prop.sig is the proportion of tested sites that are deemed significant in each test.

Test	P-cutoff for FDR 0.1	NumSig	NumTests	Prop.sig
OmniY	0.000112267	6249	5565379	0.001122835
OmniP	0.060793629	3449927	5674805	0.607937541
OmniB	0.000159407	10985	6888629	0.001594657
IM Y	2.85E-05	1105	3880525	0.000284755
IM B	1.87E-05	909	4828660	0.000188251
IM Y*B	4.42E-06	154	3458706	4.45253E-05
Q Y	9.49E-05	4030	4237533	0.000951025
Q B	0.000160195	8808	5497820	0.00160209
Q Y*B	6.76E-06	262	3840040	6.82285E-05
BR B	3.47E-07	15	3715897	4.03671E-06

number of sites = 7689713

Appendix 24-- Collection Dates, Mean depth of each library, and library-specific variances.

Pop	Bulk	Year	Collection.Date	MedianDepth	LibPrepVar
BR	Early	2013	June 11 to 17	42	0.02038163
BR	Late	2013	July 3 to 8	38	0.021624611
BR	Early	2014	6-Jun	20	0.025826066
IM	Early	2013	June 21 to 25	40	0.012374074
IM	Late	2013	July 13 to 18	59	0.013591486
IM	Early	2014	14-Jun	49	0.014762537
IM	Late	2014	16-Jul	50	0.02189802
Q	Early	2013	June 17 to 25	45	0.014286642
Q	Late	2013	19-Jul	37	0.0145339
Q	Early	2014	9-Jun	49	0.015992555
Q	Late	2014	14-Jul	48	0.027969425

Appendix 25—Enriched Gene Ontology terms for the test of allele frequency divergence among populations.

GO-ID	Term
GO:0009056	catabolic process
GO:0009653	anatomical structure morphogenesis
GO:0009791	post-embryonic development
GO:0030154	cell differentiation
GO:0006629	lipid metabolic process
GO:0016043	cellular component organization
GO:0019748	secondary metabolic process
GO:0000003	reproduction
GO:0005829	cytosol
GO:0006520	cellular amino acid metabolic process
GO:0009719	response to endogenous stimulus
GO:0005975	carbohydrate metabolic process
GO:0005654	nucleoplasm
GO:0003700	transcription factor activity, sequence-specific DNA binding
GO:0005794	Golgi apparatus
GO:0005886	plasma membrane
GO:0009628	response to abiotic stimulus
GO:0009856	pollination
GO:0003682	chromatin binding

GO:0008219 cell death

Appendix 26-- Venn diagrams depicting whether sites are polymorphic in one or more of the populations. Left: sites deemed significant for a test of either bulk, year, or population. Right: sites deemed not significant. Sites that are not polymorphic in any population are fixed for alt in one or two of the populations